11-16-2007

Characterization of Putative Magnesium Transport systems in yeast

Andrew James Franklin
University of Missouri-St. Louis, ajfck4@umsl.edu

Characterization of Putative Magnesium Transport systems in yeast

by

Andrew J. Franklin
B. A., Microbiology, Southern Illinois University- Carbondale, 2000

A THESIS

Submitted to the Graduate School of the

UNIVERSITY OF MISSOURI- ST. LOUIS
In partial Fulfillment of the Requirements for the Degree

MASTER OF SCIENCE

in

Biology
with an emphasis in Molecular and Cellular Biology

December, 2007

Advisory Committee

Colin MacDiarmid Ph. D.
Chairperson

Wendy Olivas Ph. D.
Marc Spingola Ph. D.

Abstract

Magnesium (Mg^{2+}) is essential for all life, and is utilized for many important biological processes. All cells must maintain an appropriate concentration of Mg^{2+} in the cytosol and within organelles in order to maintain key biological processes such as transcription and translation. Despite the fundamental importance of Mg^{2+} homeostasis, relatively little is known about homeostasis in eukaryotic cells. The goal of this work was to identify membrane transport systems that may be involved in the active transport of Mg^{2+}, using *Saccharomyces cerevisiae* as a model organism. Although a variety of Mg^{2+} influx systems have been described, proteins mediating active transport of Mg^{2+} (which are essential to prevent the overaccumulation of cytosolic Mg^{2+}) have not been identified from any organism. In yeast, a vacuolar Mg^{2+}/H^{+} exchange activity has been described, but the molecular identify of this protein is not known. To try and identify this activity, a candidate gene approach was used. Four yeast genes of unknown function (*PER1*, *YNL321w*, *YDL206w*, and *YJR106w*) were screened for phenotypic effects on Mg^{2+} homeostasis when overexpressed or deleted. *PER1* encodes a membrane protein that is essential for growth in high Mg^{2+} concentrations. *YNL321w*, *YDL206w*, and *YJR106w* are members of the CaCA (calcium/cation antiporter) superfamily, members of which transport a variety of divalent metal cations via a cation/proton exhange mechanism. Experiments to determine the function of Per1 showed that overexpression of this gene did not affect the Mg^{2+} content of yeast, but the *per1* mutation did reduce Mg^{2+} content. However, information communicated from another research group indicated that this effect was not specific to Mg^{2+}. In addition, Per1 was subsequently identified by another research group as an ER protein mediating a step in the pathway for

glycosylphosphatidylinositol (GPI) anchor synthesis. Of the three remaining candidate proteins, only one (Ynl321w) produced a significant increase in intracellular Mg^{2+} content when overexpressed. However, the *ynl321w* deletion mutation did not alter Mg^{2+} accumulation, Mg^{2+} tolerance, or tolerance to a range of other potentially toxic cations. Combining the *ynl321w* mutation with knockout mutations in the other two CaCA proteins also did not affect metal tolerance, indicating that these proteins do not have a redundant function. However, the *ynl321w* mutant did show a slight sensitivity to a high Ca^{2+} concentration (700 mM). As a result of this, I screened for other Ca^{2+} related phenotypes in *ynl321w* mutants, alone and when combined with other mutations that disrupt Ca^{2+} homeostasis. I observed that when combined with *ynl321w, vcx1* and *pmc1* mutations displayed synthetic Ca^{2+} sensitivity phenotypes. Measurement of cellular Ca^{2+} content with AAS showed that the *ynl321w* mutation was associated with an increase in Ca^{2+} content, and that this effect that was still observed in *vcx1* or *pmc1* backgrounds, indicating it was independent of vacuolar Ca^{2+} storage. Thus, these findings suggest a role for Ynl321w in Ca^{2+} secretion from the cell via the secretory pathway or plasma membrane. Localization studies using fluorescence microscopy and sucrose gradient fractionation showed that Ynl321wp to be localized to the ER membrane. As a consequence of these observations, I propose that Ynl321w may perform a similar function to Pmr1p, a P-type ATPase that transports Ca^{2+} and Mn^{2+} into the Golgi (and eventually, releases the ion to the external environment). Therefore, I renamed the Ynl321w protein Ecx1 (for ER calcium exchanger). The identification of Ecx1 is the first described example of a CaCA protein participating in Ca^{2+} homeostasis within the secretory pathway. Although the work did not provide insight into the molecular

mechanisms of Mg^{2+}, it did identify a factor in Ca^{2+} homeostasis.

Acknowledgments

First, I would like to thank my mentor Dr. Colin MacDiarmid for his guidance with my research and advice in writing this thesis. Additionally, I would also like to thank my thesis committee members Dr. Wendy Olivas and Dr. Marc Spingola for their time. Also, I would like to thank the MacDiarmid lab members for their helpfulness, advice, and encouragement, in particular Nilambari Pisat and Charlie Jackson. I would also like to thank Kendal Hirshi for yeast strains. Finally, I would like to thank my wife, Tracy, for her patience while writing this thesis.

Table of Contents

Chapter 1 Introduction

The divalent cation magnesium (Mg^{2+}) is essential for all life, and is utilized for many important biological processes [reviewed in (Rude, 2000)]. Mg^{2+} is a cofactor and structural stabilizer for many proteins [reviewed in (Sreedhara and Cowan, 2002)] and nucleic acids [reviewed in (Sreedhara and Cowan, 2002)]. All cells must maintain an appropriate concentration of Mg^{2+} in the cytosol and within organelles to maintain key biological processes such as transcription and translation (Sreedhara and Cowan, 2002). Suboptimal or abnormally high concentrations of Mg^{2+} can inhibit these essential biological functions. Thus, biological systems must maintain free ionized Mg^{2+} (Mg^{2+} that is not bound to proteins ligands or small molecules) within a narrow concentration range.

Surprisingly, despite the fundamental importance of Mg^{2+} homeostasis, relatively little is known about the molecular basis of Mg^{2+} homeostasis in eukaryotes. For other biologically important cations, this regulation is primarily mediated by specific transport systems in the plasma and organelle membranes of living cells. Many key questions about Mg^{2+} homeostasis, such as how cells respond to changes to environmental or intracellular [Mg^{2+}], remain unanswered. Although a variety of Mg^{2+} influx systems have been described, proteins mediating active transport of Mg^{2+} (which is essential to prevent the over-accumulation of Mg^{2+} within the cytosol) have yet to be identified from any eukaryotic organism. Studies of transport systems have been the first step in understanding the mechanisms of ion homeostasis in eukaryotes. Thus, research into the molecular identity of Mg^{2+} transporters is of fundamental importance.

This thesis describes my research into several putative membrane transport systems that may be involved in the active transport of Mg^{2+}. I used the model eukaryotic organism *Saccharomyces cerevisiae* (Bakers' yeast) to investigate the role of these genes in magnesium homeostasis. The first part of this introduction describes the role of Mg^{2+} in biology, and the known mechanisms of homeostasis. As my results will illustrate, as a consequence of my early observations, the focus of my work began to shift from magnesium to the regulation of other metal ions. For this reason, in addition to describing the state of knowledge of magnesium transport and homeostasis in eukaryotes, the introductory section will also provide a general summary of metal homeostasis and cation transporters, in particular focusing on calcium homeostasis.

1.1 Mg^{2+} in biology

Mg^{2+} is distinguished from other biologically important metal cations by its relatively small ionic radius and consequent high charge density, and its relatively high affinity for water molecules and other oxygen-containing ligands [reviewed in (Wolf and Cittadini, 2003; Wolf et al., 2003)]. As a consequence of these properties, Mg^{2+} interacts strongly with phosphate in biological systems. All enzymes that transfer phosphate from ATP require Mg^{2+}-activated ATP for function [reviewed in (Barbagallo et al., 2003; Wolf and Cittadini, 2003; Wolf et al., 2003)]. RNA and DNA polymerases require Mg^{2+} as a cofactor to mediate nucleotidyl and phosphoryl transfer [reviewed in (Wolf and Cittadini, 2003)]. Other enzymes that require Mg^{2+} for their function include kinases, enolase (and other enzymes of glycolysis), adenylate cyclase, and nucleases [reviewed in (Barbagallo et al., 2003; Sreedhara and Cowan, 2002; Wolf and Cittadini, 2003)]. Mg^{2+} also interacts with nucleic acids to stabilize base pairing and other interactions [(Heus and Pardi, 1991) and reviewed in (Sreedhara and Cowan, 2002)], and affects the physiology of other ions by modulating the activity of ion channels (Perez-Vazquez et al., 2003; Tang et al., 2000; Wei et al., 2002). A consequence of the high charge density on Mg^{2+} ions is the large water shell that surrounds the ions in solution. Hydrated Mg^{2+} ions are much larger than the naked ion, and the water shell requires a large input of energy to remove. Nevertheless, most Mg^{2+} in cells is bound to small molecules or protein ligands: less than 1% is free ionized Mg^{2+} in the cytoplasm (Millart et al., 1995).

1.1.1 Magnesium and human health

Acute magnesium deficiency can occur as the consequence of a severely Mg^{2+}-deficient diet, various genetic disorders of magnesium homeostasis, or as a secondary

effect of major illnesses (e.g., bacterial or viral infections and kidney diseases) or certain drugs (e.g. diuretics and alcohol) (Meij et al., 2002; Tahara and Nishizawa, 2007; Tong and Rude, 2005). Symptoms of acute Mg^{2+} deficiency include muscle spasms (tetany) and neurological symptoms. Research has shown that Mg^{2+} supplements can have a therapeutic effect for people with Mg^{2+} deficiency symptoms [(Kawano et al., 1998) and reviewed in (Gums, 2004)]. Due to the efficiency of magnesium homeostasis in healthy patients, the occurrence of such acute magnesium deficiency is relatively rare. However, there is increasing concern about the occurrence of low-grade Mg^{2+} deficiency contributing to the longer-term development of various pathological conditions. In developed countries, processing of foods has greatly decreased the average dietary intake of Mg^{2+} [reviewed in (Kimura, 2007)]. There is evidence that the majority of people in developed countries do not consume the recommended daily allowance of Mg^{2+} (Kimura, 2007). Sub-acute Mg^{2+} deficiency has been associated with the development of many diseases, including cardiovascular disorders and diabetes [reviewed in (Barbagallo et al., 2003; Gums, 2004; McGuigan et al., 2002)].

1.1.2 Magnesium and agriculture

One important role of Mg^{2+} in plants is as a co-factor in chlorophyll. Mg^{2+} ions are thus essential for photosynthesis and primary production, and Mg^{2+} deficiency can negatively impact agricultural yield. The primary symptoms of deficiency are leaf yellowing (chlorosis), initially of the older leaves. In more severe cases, the older leaves will die (Hermans and Verbruggen, 2005). Mg^{2+} deficiency is commonly encountered in plants, particularly when grown in acidic soils. Since Mg^{2+} is very soluble, it is rapidly leached from acidic soils in regions with high rainfall. Acidic soils make up the majority

of arable land in tropical regions, and are also found in many locations in the USA (Altura and Altura, 1996). Mg^{2+} deficiency can also be exacerbated as a consequence of aluminum toxicity, which is also promoted by acidic soils. Al^{3+} ions retard growth of the root system and have a general inhibitory effect on nutrient uptake. In addition, Al^{3+} ions may directly prevent Mg^{2+} accumulation by blocking the transport systems responsible for uptake (Delhaize and Ryan, 1995; Kochian, 1995). Mg^{2+} can be supplemented to alleviate deficiency, although this strategy may not be economically viable, particularly in developing nations.

1.2 Physiology of cation transport

The tight regulation of metal cation concentrations in the cytosol and organelles of living cells is accomplished by the action of specific transport proteins, which allow processes of influx, efflux, and sequestration to occur [reviewed in (Nelson, 1999)]. The transport of cations can be classified as passive or active. Passive transport via ion-specific channels is driven by the electrochemical gradients of these ions. Due to the action of ATP-dependent proton or Na^{+} pumps in the plasma membrane, the cytosol is negatively charged relative to the external environment. This charge difference provides a major driving force for the influx of cations. In addition, the lumen of organelles such as mitochondria and chloroplasts are negatively charged relative to the cytosol, as a consequence of the proton gradient generated by oxidative phosphorylation or photosynthesis within these organelles. In contrast, endosomal compartments such as the yeast vacuole are positively charged relative to the cytosol, as ATP-dependent proton pumps generate a proton concentration gradient over the membranes of these compartments.

For these reasons, in contrast to passive influx, efflux of most cations from the cytosol into the vacuole or over the plasma membrane requires energy input. This energy is provided by systems which directly use the energy from ATP hydrolysis to pump cations (primary active transport systems), or which take advantage of the energy stored in ion gradients to drive the exchange of ions over the membrane (secondary active transport systems).

1.3 Identification and characterization of cation transporters

In general, the low expression of membrane transport proteins and their relative hydrophobicity has hindered their identification by biochemical methods. Genetic methods to identify novel strains with altered homeostasis have proven to be very useful in understanding ion homeostasis. For example, genetic screens have been used to identify mutants with altered expression of nutrient-regulated genes (Persson et al., 2003), altered growth under nutrient-deficient conditions (Dancis et al., 1994), or tolerance to an excess of toxic cations (Conklin et al., 1993). Due to the facile genetics of these organisms and the availability of complete genome sequences, bacterial and yeast systems have proven to be very useful for these studies. These studies have revealed many different families of cation transporters with members in higher eukaryotes (Hanikenne et al., 2005; Maser et al., 2001; Nelson, 1999). The members of each family diverge significantly in sequence and even in structure, but share recognizable conserved sequence motifs and perform similar functions in species ranging from bacteria to humans. Some genomes contain several members of the same gene family: these orthologous proteins are often adapted to perform specific roles under differing environmental conditions or in different cellular compartments. Thus, studies in microbes

have been instrumental in identifying novel transporters and related proteins from more complex organisms.

1.4 Yeast as a model for analysis of eukaryotic cation homeostasis

Yeast is an excellent model organism to study metal ion transport in eukaryotes (Perego and Howell, 1997). As discussed below, Baker's yeast was the organism from which the first Mg^{2+} transporter was identified, and Mg^{2+} homeostasis is still best understood in this organism. Yeast can be propagated as haploid strains to determine the phenotype of recessive alleles, or they can be mated to form diploids in order to study allelic interactions. As a consequence of the ability to efficiently perform homologous recombination, the yeast genome can be easily manipulated: genes can be modified *in situ* or eliminated from the genome, and mating or transformation can rapidly generate strains with multiple mutations. Genes can also be introduced on plasmids, which replicate independently of the chromosome. Plasmids with different replication origins allow us to vary gene copy number, providing a simple way to alter the level of gene expression. Genes discovered in yeast often have homologs with conserved functions in higher eukaryotes, and in some cases the function of these proteins can be determined and studied in the yeast system. In addition, yeast has proven to be an excellent system for biochemical analysis of transporters and other enzymes. Since proteins with conserved motifs can have similar functions, putative metal cation transporters may be identified by the use of search algorithms such as BLAST, using a known transporter as a query sequence. Putative transporter genes can then be screened for metal homeostasis-related phenotypes when the protein is overexpressed or deleted, such as metal tolerance or sensitivity and changes in metal content (using a "candidate gene" approach to the

reverse genetic analysis of putative transporters). For these and other reasons, yeast was selected to perform the research described in this thesis.

1.5 Mg^{2+} transport systems

1.5.1 Mg^{2+} transport systems in prokaryotes

The best characterized Mg^{2+} transporters in bacteria and Archaea are members of the CorA family, named after the first identified protein in this family, CorA (Cobalt resistance), isolated from *Salmonella typhimurium* (Hmiel et al., 1986). Mutants in this gene were isolated by their tolerance to toxic environmental levels of cobalt, as this protein also transports other divalent metal cations (Co^{2+} and possibly Ni^{2+}) with low affinity (Gibson et al., 1991). CorA also mediates the efflux of Mg^{2+} when high extracellular concentrations of Mg^{2+} are present (Snavely et al., 1989). In contrast to CorA, the MgtA and MgtB transport systems are ATPases that are involved in the influx of Mg^{2+} in low extracellular concentrations of Mg^{2+} (Snavely et al., 1989). These transporters are regulated by the PhoP/PhoQ two-component sensory system, which monitors the availability of extracellular Mg^{2+} (Tao et al., 1998). The PhoQ protein acts as a sensor to monitor the extracellular Mg^{2+} concentration, and in the presence of low (μM) concentrations it phosphorylates the PhoP protein. Phosphorylated PhoP activates transcription of many genes, including MgtA and MgtB. In some bacteria, a fourth protein (MgtE) is also involved in Mg^{2+} uptake. MgtE was originally discovered by screening a genomic library screen from *Bacillus firmus* OF4 for clones that could restore the ability of a *corA*, *mgtA*, and *mgtB* triple mutant to grow in minimal media without supplemental Mg^{2+} (Smith and Maguire, 1995). However, it is not clear at this time if Mg^{2+} transport is the primary function of this protein, as it has been shown to transport a

variety of metal cations (Mg^{2+}, Ni^{2+}, Zn^{2+}, and Co^{2+}) with the highest affinities for Mg^{2+} and Co^{2+} (Smith and Maguire, 1995). The crystal structure of a bacterial MgtE protein was recently solved (Hattori et al., 2007), which should provide many insights into the function of these important proteins. Eukaryotic homologs of MgtE exist in vertebrates and appear to mediate Mg^{2+} influx (Sahni et al., 2007), although their physiological function is still unclear.

1.5.2 Mg^{2+} transport systems in eukaryotes

1.5.2.1 CorA family

Genetic studies in yeast identified the first eukaryotic Mg^{2+} transporter (Alr1p), named for its resistance to high concentrations of Al^{3+} (MacDiarmid and Gardner, 1998). Alr1p is a plasma membrane protein that is distantly related to the bacterial CorA protein. The Alr1 protein forms a Mg^{2+} channel located on the plasma membrane, which allows the entry of Mg^{2+} to the cytoplasm [reviewed in (Gardner, 2003)]. Alr1p is required for growth at normal Mg^{2+} concentrations (4 mM) (MacDiarmid and Gardner, 1998) and deletion of the gene reduces cellular Mg^{2+} content (Da Costa et al., 2007; Graschopf et al., 2001). Overexpression of the bacterial CorA protein in an *alr1* mutant partly restored growth (Graschopf et al., 2001), indicating functional conservation of CorA and Alr1. It was previously demonstrated that Mg^{2+} influx in yeast occurs through a high capacity transport

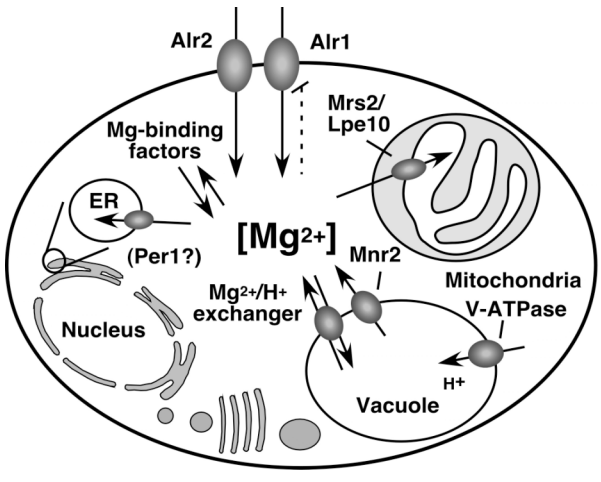

Figure 1 Mg^{2+} homeostasis in yeast.

system that can also accumulate Mn^{2+}, Co^{2+}, Ni^{2+}, and Zn^{2+} ions with low affinity (Conklin et al., 1993; Fuhrmann and Rothstein, 1968; MacDiarmid and Gardner, 1998; Okorokov et al., 1977). This observation suggests that Alr1 can transport other divalent cations in addition to Mg^{2+}. This idea is supported by studies showing an increase in sensitivity to and transport of Co^{2+}, as well increased sensitivity to other divalent cations as a consequence of Alr1 overexpression (MacDiarmid and Gardner, 1998). Evidence has shown that Mg^{2+} influx by Alr1 is driven by the electrochemical gradient, as demonstrated by using the patch-clamp method to measure whole-cell ion currents in a wild type and an *alr1 alr2* strain that overexpressed *ALR1* (Liu et al., 2002). The overexpressing strain demonstrated a five-fold increase in current compared to the wild type in a bathing solution containing 50 mM Mg^{2+}. Interestingly, when the pipette solution contained mostly Mg^{2+}, an outward current was also detected in the overexpressing strain: this observation suggests that when external Mg^{2+} concentrations are high, Alr1p may also participate in Mg^{2+} efflux, revealing another functional similarity to CorA.

A closely related ortholog of Alr1, Alr2, has also been shown to be involved in the uptake of Mg^{2+} in yeast (MacDiarmid and Gardner, 1998; Wachek et al., 2006). In experiments to measure low-affinity divalent cation uptake via the Alr proteins using the isotope $^{57}Co^{2+}$, an *alr2* mutant did not show a noticeable reduction in Co^{2+} uptake compared to wild type, but an *alr1 alr2* double mutant showed a reduction compared to an *alr1* single mutant. This observation suggested that the Alr2 protein could also contribute to divalent cation uptake (including, presumably, Mg^{2+} uptake), but that it plays a role secondary to Alr1 in this process. Recent work in this laboratory to determine

the Mg^{2+} content of *alr1* and *alr2* mutants supports this interpretation (N. Pisat, personal communication). *ALR2* overexpression suppressed the Mg^{2+}-dependent phenotype of an *alr1* mutant (MacDiarmid and Gardner, 1998), indicating that this protein is capable of mediating sufficient Mg^{2+} uptake to support maximal growth. This and other observation lead to the proposal that the relatively low expression of Alr2 may explain its low activity (MacDiarmid and Gardner, 1998). However, the Alr2 protein also displays an altered sequence to Alr1 in the extracellular domain, a change which may contribute to its low activity (Wachek et al., 2006). It has recently been shown that Alr1 and Alr2 can interact and form homo and hetero-oligomers (Wachek et al., 2006), although the functional significance of this interaction is unknown.

More recently, two other CorA transporters were identified in yeast. Mrs2p and Lpe10p are located on the inner mitochondrial membrane, and are both essential for the influx of Mg^{2+} into the mitochondrial matrix (Gregan et al., 2001a; Kolisek et al., 2003). Mitochondrial Mg^{2+} is essential for group II intron splicing in yeast (Gregan et al., 2001b). Overexpression of either of the Mrs2 or Lpe10 proteins leads to an increase in the accumulation of Mg^{2+} by mitochondria (Gregan et al., 2001a; Kolisek et al., 2003), whereas reduced concentrations of Mg^{2+} were seen in the absence of these proteins (Gregan et al., 2001a; Kolisek et al., 2003). Recently, single channel patch-clamp experiments have shown that Mrs2p is highly selective for Mg^{2+} as opposed to other cations (Ca^{2+}, Mn^{2+}, Co^{2+}) (Schindl et al., 2007), although the channel was also observed to be permeable to Ni^{2+} to a smaller extent. The requirement of both Mrs2p and Lpe10p for the influx of Mg^{2+} into mitochondria, suggests that they interact to form a hetero-oligomer. The function of these proteins is conserved in eukaryotes from yeast to

humans. In fact, the human gene that encodes the hsaMrs2 protein can suppress the *mrs2* mutation when expressed in yeast (Zsurka et al., 2001).

1.5.2.2 Biochemistry of Mg^{2+} active transport systems

Mg^{2+} transport by the CorA family of the proteins is driven by the charge difference over either the plasma membrane or the inner mitochondrial membrane. Transport of cations out of these compartments is important for maintaining the appropriate concentration, and these processes require energy input, via a mechanism for the active transport of this ion. Thus far, active transport systems for Mg^{2+} have only been identified in bacteria (the Mgt systems), which are responsible for the movement of Mg^{2+} ions into (rather than out of) the cell (Snavely et al., 1989). The Mgt proteins are likely to contribute to Mg^{2+} uptake under conditions of extreme deficiency (*e.g.*, the survival of pathogenic phagocytosed bacteria is dependent on these systems) (Garcia-del Portillo et al., 1992). It is currently unclear what proteins are responsible for the efflux of Mg^{2+} from the cytosol in eukaryotes. One study provided evidence that Mg^{2+} may be sequestered into vacuoles or the secretory pathway via a Mg^{2+}/H^{+} exchange mechanism (Borrelly et al., 2001). Similar systems are known to play a role in the maintenance of cytosolic Mg^{2+} homeostasis in higher eukaryotes (*e.g.*, a Na^{+}/Mg^{2+} antiport system is present in the plasma membranes of a variety of cell types) (Ferreira et al., 2004; Gonzalez-Serratos and Rasgado-Flores, 1990; Ikari et al., 2003; Picado et al., 1994; Wisdom et al., 1996). However, despite the widespread occurrence of these systems in eukaryotes, and their demonstrated importance for homeostasis, definitive evidence implicating a specific protein from any organism in Mg^{2+}/H^{+} (or Mg^{2+}/Na^{+}) exchange has yet to be reported.

1.6 Ca^{2+} transport in yeast

Calcium (Ca^{2+}) is similar to Mg^{2+} in many aspects: both are alkali metals that are relatively "hard" divalent cations (i.e., they prefer to associate with oxygen-containing ligands). Thus, Ca^{2+} and Mg^{2+} transport systems might be expected to be similar in structure and function. Ca^{2+} transport has been very well studied in yeast, and many calcium transport proteins have been identified. High affinity uptake of Ca^{2+} from the environment is mediated by the Cch1 and Mid1 proteins, which interact to form a channel in the plasma membrane (Fischer et al., 1997; Iida et al., 1994). Excess Ca^{2+} entering the cell is sequestered in the vacuole. Pmc1p is a primary Ca^{2+} pump (related to P-type ATPases) located in the vacuole membrane (Marchi et al., 1999), which removes Ca^{2+} from the cytosol (Cunningham and Fink, 1994; Marchi et al., 1999). The inactivation of this protein causes a reduction in Ca^{2+} tolerance as a consequence of reduced vacuolar storage. Another important transport system in the vacuole is the Vcx1 protein, a Ca^{2+}/H^{+} exchanger (Pozos et al., 1996). Vcx1 is a member of the CaCA (calcium/cation exchanger) family, examples of which are found in all phylogenic groups (Hanikenne et al., 2005; Maser et al., 2001). The human Ca^{2+}/Na^{+} exchanger was the first member of this family to be identified at the molecular level (Nicoll et al., 1990). CaCA family proteins contain 10 to 14 putative transmembrane domains, and contain two or more repeats of a conserved domain (the α-repeat) (Philipson and Nicoll, 2000). Calcium transport via CaCA proteins is driven by exchange with protons (in yeast and plants) or Na^{+} ions (in animal cells) (Philipson et al., 2002), and is thus dependent on the primary ATPase enzymes required to generate proton and Na^{+} concentration gradients.

Another mechanism for removal of Ca^{2+} from the cytosol in yeast is via sequestration in the secretory pathway. The ER and Golgi require Ca^{2+} and Mn^{2+} for

glycosylation of proteins and other biochemical functions (Durr et al., 1998). Transport of Ca^{2+} into the Golgi is mediated by the Pmr1 protein, a P-type ATPase related to Pmc1. Spf1, also a P-type ATPase, performs a similar function for the ER. In addition to their role in supplying Ca^{2+} and Mn^{2+} to these organelles, the Pmr1, Spf1 and Pmc1 are high affinity Ca^{2+} pumps that maintain the low levels of cytosolic Ca^{2+} required for signal transduction processes. Studies have shown that *pmr1* and *spf1* deletion mutants are sensitive to Ca^{2+} (Cronin et al., 2002), and combining the *pmr1* and *spf1* mutations resulted in an even greater sensitivity. *pmr1* mutants display an increase in intracellular Ca^{2+} content (presumably as a consequence of reduced Ca^{2+} efflux via the secretory pathway); in contrast, the *spf1* mutation had little effect on Ca^{2+} content in isolation, but there was a synergistic increase in the Ca^{2+} content of the *pmr1 spf1* double mutant (Cronin et al., 2002).

1.7 Aims of this research

The facile genetics and molecular tools available for yeast make this organism ideal for studying the molecular components that maintain Mg^{2+} homeostasis. As has been demonstrated for other metal ions, it is possible to characterize novel genes via phenotypes produced by overexpression from multicopy plasmids, as well as by inactivating gene function. It is also possible to systematically examine genes of unknown function for those with features suggesting that they may perform a particular function of interest. The goal of the work described here was to identify and characterize a yeast gene encoding the Mg^{2+}/H^{+} exchange activity in the vacuole membrane. The importance of this work is that if successful, it would represent the first molecular

identification of a protein capable of the active efflux of Mg^{2+} ions. The specific aims of this work are as follows:

1) To determine the role of the Per1 protein, a candidate Mg^{2+} transporter, in Mg^{2+} homeostasis. In a previous screen, Per1 was shown to be required for tolerance to high Mg^{2+} concentrations, implicating this protein in Mg^{2+} storage.

2) To determine if any yet uncharacterized members of the CaCA gene family in yeast play a role in the sequestration of Mg^{2+} in the vacuolar compartment. The vacuolar Mg^{2+}/H^{+} exchanger may be related in sequence to CaCA proteins that transport other divalent cations, such as the vacuolar Ca^{2+}/H^{+} exchanger Vcx1p. Strains lacking or overexpressing each candidate gene will be screened for Mg^{2+} related phenotypes, including changes in Mg^{2+} content, as well as resistance to excess Mg^{2+} and other cations.

3) If the above aims are unsuccessful in identifying a candidate for a Mg^{2+} transporter in the vacuole, I will determine if these genes play a role in the homeostasis of other divalent cations.

Chapter 2: Materials and Methods

2.1 Yeast and bacterial strains

2.1.1 Saccharomyces cerevisiae strains

Yeast strains used or generated in this work are detailed in **Table 2.1**.

Table 2.1 Yeast strains

Strain	Genetic background	Genotype	Source/ref
DY1457	W303	*MATα ade6 can1-100^{oc} his3-11,15 leu2-3,112 trp1-1 ura3-52*	David Eide
DY1456	W303	*MATa ade6 can1-100^{oc} his3-11,15 leu2-3,112 trp1-1 ura3-52*	David Eide
DY1514	W303	*MATa/α ade2/+ ade6/+ can1-100^{oc}/- his3-11,15/- leu2-3,112/- trp1-1/- ura3-52/-*	David Eide
BY4743	S288C	*MATa/α his3Δ1/- leu2Δ0/- met15Δ0/+ lys2Δ0/+ ura3Δ0/-*	Open Biosystems[1]
BY4741	S288C	*MATa his3Δ1 leu2Δ0 met15Δ0 ura3Δ0*	Open Biosystems[1]
YNL321wΔ	S288C	*MATa/α his3Δ1/- leu2Δ0/- met15Δ0/+ lys2Δ0/+ ura3Δ0/- ynl321w::KAN^{R}/-*	Open Biosystems[1]
YDL206wΔ	S288C	*MATa/α his3Δ1/- leu2Δ0/- met15Δ0/+ lys2Δ0/+ ura3Δ0/ -ydl206w::KAN^{R}/-*	Open Biosystems [1]
YJR106wΔ	S288C	*MATa/α his3Δ1/- leu2Δ0/- met15Δ0/+ lys2Δ0/+ ura3Δ0/- yjr106w::KAN^{R}/-*	Open Biosystems[1]
YCR044cΔ	S288C	*MATa/α his3Δ1/- leu2Δ0/- met15Δ0/+ lys2Δ0/+ ura3Δ0/- ycr044c::KAN^{R}/-*	Open Biosystems[1]
B31	W303	*MATα ade2-1 can1-100 his3-11,15 leu2-3, 112 trp1-1 ura3-1 mall0 ena1Δ::HIS3::ena4Δ nha1Δ::LEU2*	Kendal Hirschi[2]
WX1	W303	*MATα ade2-1 can1-100 his3-11,15 leu2-3,112 trp1-1 ura3-1 mall0 nhx1::TRP1*	Kendal Hirschi[2]
SEY6210	SEY6210	*MATα ura3-52 leu2-3 his3Δ200, trp1-Δ901 lys2-800 suc2-Δ9*	David Bedwell[3]
YDB224	SEY6210	*MATα ura3-52 leu2-3 his3Δ200, trp1-Δ901 lys2-800 suc2-Δ9 pmc1::TRP1*	David Bedwell[3]
YDB225	SEY6210	*MATα ura3-52 leu2-3 his3Δ200, trp1-Δ901 lys2-800 suc2-Δ9 vcx1::URA3*	David Bedwell[3]
YDB254	SEY6210	*MATa ura3-52 leu2-3 his3Δ200, trp1-Δ901 lys2-800 suc2-Δ9 pmc1::TRP1 vcx1::URA3*	David Bedwell[3]
AJF01	W303	*MATα, ade6 can1-100^{oc} his3-11,15 leu2-3,112 trp1-1 ura3-52 ynl321w::KAN^{R}*	This study
AJF02	W303	*MATa ade6 can1-100^{oc} his3-11,15 leu2-3,112 trp1-1 ura3-52 ynl321w::LEU2*	This study
AJF03	W303	*MATα ade6 can1-100^{oc} his3-11,15 leu2-3,112 trp1-1 ura3-52 ydl206w::KAN^{R}*	This study
AJF04	W303	*MATα ade6 can1-100^{oc} his3-11,15 leu2-3,112 trp1-1 ura3-52 yjr106w::KAN^{R}*	This study
AJF05	W303	*MATa ade6 can1-100^{oc} his3-11,15 leu2-3,112 trp1-1 ura3-52 ynl321w::LEU2 ydl206w::KAN^{R}*	This study

AJF06	W303	*MATa ade6 can1-100^{oc} his3-11,15 leu2-3,112 trp1-1 ura3-52 ynl321w::LEU2 yjr106w::KAN^{R}*	This study
AJF07	W303	*ade6 can1-100^{oc} his3-11,15 leu2-3,112 trp1-1 ura3-52 ynl321w::LEU2 ydl206w::KAN^{R} yjr106w::KAN^{R}*	This study
AJF08	W303/ SEY6210	*leu2-3,112 ura3-52 his3 trp1*	This study*
AJF09	W303/ SEY6210	*leu2-3,112 ura3-52 his3 trp1 ynl321w::KAN^{R}*	This study*
AJF10	W303/ SEY6210	*leu2-3,112 ura3-52 his3 trp1 vcx1::URA3*	This study*
AJF11	W303/ SEY6210	*leu2-3,112 ura3-52 his3 trp1 pmc1::TRP1*	This study*
AJF12	W303/ SEY6210	*leu2-3,112 ura3-52 his3 trp1 vcx1::URA3 pmc1::TRP1*	This study*
AJF13	W303/ SEY6210	*leu2-3,112 ura3-52 his3 trp1 ynl321w::KAN^{R} vcx1::URA3*	This study*
AJF14	W303/ SEY6210	*leu2-3,112 ura3-52 his3 trp1 ynl321w::KAN^{R} pmc1::TRP1*	This study*
AJF15	W303/ SEY6210	*leu2-3,112 ura3-52 his3 trp1 ynl321w::KAN^{R} vcx1::URA3 pmc1::TRP1*	This study*
AJF16	W303	*ade6 can1-100^{oc} his3-11,15 leu2-3,112 trp1-1 ura3-52 nhx1::TRP1 ynl321w::LEU2*	This study

[1](Winzeler et al., 1999), [2](Banuelos et al., 1998), [3](Miseta et al., 1999).
*Complete genotypes of these strains were not determined: they carry either the *his3-Δ200* or *his3-11,15* allele, and the *trp1-Δ901* or *trp1-1* allele. In addition, they may possess the additional markers *lys2-801, suc2-Δ9, ade6,* and *can1-100^{oc}*.

2.1.2 Bacterial strains

E. coli DH10β^{TM} [genotype F^{-} *mcr*A Δ(*mrr-hsd*RMS-*mcrBC*) ϕ80*lacZ*ΔM15 *ΔlacX*74 *rec*A1 *end*A1 *ara*D139 Δ(*ara, leu*)7697 *gal*U *gal*K λ- *rps*L *nup*G] was used for transformation by electroporation and for preparation of plasmid DNA.

2.2 Commonly used solutions

All percentages are weight/volume unless otherwise stated.

TE buffer: 10 mM Tris-Cl pH 7.5, 1 mM Na-EDTA.

Antibiotics: Ampicillin (Fisher Scientific) was included in LB medium to select ampicillin resistant *E. coli*. After the medium was autoclaved and cooled to 50° C, a filter-sterilized solution of ampicillin was added to give a final concentration of 100 mg/L. To

select for the *KAN*^{R} marker in yeast strains, Geneticin (G418, Invitrogen) was included in YPD at a concentration of 150 mg/L.

Bacterial growth media: **LB**: (Luria-Bertani broth) 1% tryptone, 0.5% yeast extract, 172 mM NaCl. A commercial preparation of LB broth (Fisher) was obtained as a pre-mixed powder: 20 g powder was dissolved in 1 L deionized water and autoclaved. As a gelling agent for plates, agar (Difco) was added before autoclaving to a final concentration of 1.5%. **SOB:** 2% Tryptone, 0.5% Yeast extract, 10 mM NaCl, 2.5 mM KCl, 10 mM $MgCl_2$, and 10 mM $MgSO_4$, pH 7.0. **SOC**: SOB with 20 mM glucose.

Zymolyase 20T: Zymolyase 20T (Seikagaku, Tokyo) was dissolved in 50% glycerol/50 mM KPO_4 pH 7.4, at a concentration of 110 U/ml, and stored at -20.

2.3 Preparation of reagents

2.3.1 Tris-saturated phenol

One hundred g of solid phenol (Sigma) was mixed with 100 ml of 50 mM Tris-Cl pH 8.0, and allowed to stand at RT until the phenol liquefied. The layer of Tris was removed with a pipette, the phenol layer mixed with an equal volume of fresh Tris solution, and the mixture left for 20 min to separate the phases. This procedure was repeated twice more until the pH of the solution was between 7 and 8. Tris-saturated phenol was stored in the dark at 4° C.

2.3.2 Phenol/chloroform/isoamyl-alcohol (PCA)

Chloroform (96 ml) was mixed with 4 ml of isoamyl-alcohol in a glass measuring cylinder. The mixture was divided into 10 ml aliquots, and 10 ml of phenol and 10 ml 50 mM Tris-Cl pH 8 was added to each. The aliquots were stored at -20 until required.

2.3.3 Taq polymerase

Thermus aquaticus (Taq) DNA polymerase was prepared essentially as previously described by (Pluthero, 1993). DH10β *E. coli* cells were transformed with the plasmid pTTQ18, which contains the gene for Taq polymerase under the control of a synthetic *tac* promoter and the *Lac*I repressor. One liter of LB+Amp medium was inoculated with 0.5 ml of an overnight culture of this strain, and grown to an A_{600} of 0.8 at 37° C. Transcription of the Taq polymerase gene was induced with the addition of 10 ml of 1.25% IPTG, and the cells were grown for 12 hours at 37° C with agitation. After induction, the cells were collected (3,000x g/10 min) and washed with 100 ml Buffer A (50 mM Tris pH 7.9, 50 mM Dextrose, 1 mM EDTA). The cells were resuspended in 50 ml Buffer A and transferred to a 250 ml flask. Lysozyme (250 mg) was added and the cells were incubated at room temperature for 15 min. Buffer B (10 mM Tris pH 7.9, 50 mM KCl, 1 mM EDTA, 1 mM PMSF, 0.5% Tween-20, 0.5% Nonidet P40) (50 ml) was added and the cell solution was incubated for 1 hour in a 75° C water bath to denature all other proteins. These conditions do not inactivate Taq polymerase, as it is a thermostable protein. The solution was transferred to centrifuge tubes and centrifuged (12,000x g/10 min). The supernatant was transferred to a fresh 250 ml flask and 30 g of powdered ammonium sulfate was added with stirring. The solution was transferred to a new centrifuge tube and collected by centrifugation (12,000x g/10 min). The pellet was resuspended in 20 ml of Buffer A, transferred to a dialysis bag, and dialyzed for 24 hours in 2 changes of 1 L storage buffer (50 mM Tris pH 7.9, 50 mM KCl, 0.1 mM EDTA, 1 mM DTT, 0.5 mM PMSF, 50% Glycerol) at 4° C. The concentrated protein solution was removed from the dialysis bag, aliquoted into microfuge tubes, and stored at -80° C.

Approximate activity of the Taq solution was determined via comparison with a commercial preparation of Taq of known activity (iTaq, Bio-Rad).

2.4 Yeast Growth Media

2.4.1 Complex yeast media

Yeast cells were routinely grown in YPD (Yeast extract, Peptone, Dextrose) medium containing 1% Yeast extract (Fisher Scientific), 2% Peptone (Fisher), and 0.1 M glucose or glycerol. To gel plates, agar was added to a final concentration of 1.5%.

2.4.2 Synthetic media

2.4.2.1 SD and SC minimal media

Yeast were routinely grown in synthetic dextrose (SD) media in order to maintain plasmids or test for the presence of selectable markers. SD media contained 6.7% Yeast Nitrogen Base (YNB) without amino acids (Q-Biogene), a carbon source (2% glucose or 3% glycerol), 0.01% Adenine, 0.01% Uracil, 0.01% L-Tryptophan, 0.01% L-Leucine, 0.01% L-Lysine-HCl, 0.01% L-Histidine-HCl, and 0.01% L-Methionine. Nutrients were omitted as necessary for selection. To maintain selection of *URA3*-expressing plasmids during routine growth, a simpler medium (SC) was used that contained 6.7% YNB, 0.01% Casamino acids (Difco), 0.01% Adenine, 0.01% Tryptophan, and 0.1 M glucose.

2.4.2.2 Low Magnesium Medium (LMM)

LMM was used for experiments in which the amount of available Mg^{2+} in synthetic medium needed to be precisely controlled. For routine preparation of LMM, a commercial YNB mix without amino acids and divalent cations was used (Q-Biogene). YNB was prepared as normal from this mix, except that divalent cations were added to concentrations of 0.5 mM $CaCl_2$, 5 μM $CuCl_2$, 5 μM $FeSO_4$, 5 μM $MnCl_2$, and 5 μM

$ZnCl_2$. The final medium was identical to normal YNB except for the absence of Mg^{2+}. To avoid background contamination with environmental Mg^{2+}, the medium was filter sterilized into sterile polycarbonate flasks that had been washed using Citronox metal-free acidic detergent (Alconox). Analysis with AAS indicated that Mg^{2+} was undetectable in this medium.

For some applications, LMM was assembled from simple inorganic and organic components. Sterile solutions of major salts (10x concentration), trace elements (1000x), and vitamins (1000x) were prepared and mixed to assemble the final medium. The composition of these solutions was as follows:

10x Major salts: 400 mM NH_4SO_3, 50 mM KCl, 20 mM NaCl, 1 mM $CaCl_2$, 1 mM KH_2PO_4).

1000x Trace elements: 0.2 mM $CuSO_4$, 2.5 mM $MnSO_4$, 10 mM H_3BO_3, 0.5 mM KI 1 mM Na_2MoO_4, 1.5 mM $ZnSO_4$, 1 mM $FeCl_3$.

1000x Vitamins: 0.0002% Folic acid, 0.04% Niacin, 0.0002% Biotin, 0.04% Calcium Pantothenate, 0.02% Riboflavin, 0.02% p-Aminobenzoic acid, 0.04% Pyridoxine Hydrochloride, 0.04% Thiamine Hydrochloride.

Major salts and trace element solutions were autoclaved, and the vitamin solution was filter sterilized to avoid hydrolysis of heat-sensitive components. Sterile solutions of carbon sources, amino acids and bases were added as needed at the same concentrations used for standard SD medium. After assembling the sterile Mg-free medium, sterile $MgCl_2$ solutions were added to give the appropriate concentration of this element for the experiment performed.

2.4.2.3 Low sulfate medium

In order to prevent Ca^{2+} and Zn^{2+} from precipitating when included at high concentrations in synthetic medium, a low-sulfate medium was used. This medium included 1.7% YNB without ammonium sulfate, dextrose, and zinc (Q-Biogene), 2 μM $ZnCl_2$ and 75 mM NH_4Cl. Carbon sources, amino acids and organic bases were also added as required.

2.4.2.4 Low pH phosphate-buffered medium

To determine tolerance to low pH conditions, a synthetic minimal medium was prepared as previously described (Nass et al., 1997). The medium contained 10 mM arginine, 8 mM phosphoric acid, 1 mM KCl, 0.2 mM $CaCl_2$, 2 mM $MgSO_4$, 2% glucose, and trace minerals and vitamins. The pH was adjusted to the required value using phosphoric acid.

2.4 Sporulation and Spore Isolation

For strains of the easily sporulated W303 genetic background, the following method of sporulation was used. Sterile YPD medium (5 ml) was inoculated with a single colony of a diploid strain and grown to saturation. Cells were collected by centrifugation (2,000x g/5 min) and washed twice with 5 ml sterile deionized water. 5 ml of Spo medium 1 (1% yeast extract, 10% potassium acetate, 0.05% glucose, 0.01% adenine, 0.005% arginine, 0.005% histidine, 0.005% leucine, 0.005% lysine, 0.005% methionine, 0.025% phenylalanine, 0.001% tryptophan, and 0.01% uracil) was inoculated with 100 μl of the washed cell sample, and the culture was incubated at 30° C with agitation (260 RPM) for 3-7 days. Sporulation was verified by observation with a light microscope.

To sporulate strains of the genetic background S288C (for example, the BY

strains obtained from Research Genetics), strains were patched to YPD plates and grown for 1 day at 30° C, then replica plated to freshly made GNA presporulation plates (5% glucose, 3% Difco nutrient broth, 1% Difco yeast extract, 2% Bacto agar) and incubated for 1 day at 30° C. This process was repeated with a fresh GNA presporulation plate, and the resulting cells were scraped off the plate and transferred to 2 ml supplemented liquid sporulation medium (1% potassium acetate, 0.005% zinc acetate, 0.002% uracil, 0.004% histidine, 0.004% leucine). The suspensions were incubated on a roller wheel for 5 days at RT, then 3 days at 30° C. Sporulation was monitored via microscopy.

To isolate purified spore suspensions, sporulated cultures were washed twice with 5 ml of sterile deionized water and suspended in softening buffer (10 mM dithiothreitol, 100 mM Tris-SO_4 pH 9.4) to a final A_{600} of 5.0. Each sample was incubated at 30° C for 10 min with agitation, then collected by centrifugation (2,000x g/5 min) and resuspended in spheroplasting buffer (2.1 M sorbitol, 10 mM potassium phosphate, pH 7.2) to give a final A_{600} of 25. Zymolyase 20T (Seikagaku, Tokyo) was added at a concentration of 1 U/A_{600} unit of cells, and the suspension incubated at 30° C with agitation for 1 hour. The suspension was washed once with 4 ml of 0.5% Triton X-100 and resuspended in 1 ml of 0.5% Triton X-100. The suspension was then sonicated until only single spores remained (no tetrads or intact diploid cells), as determined by microscopic examination. Dilutions of each spore sample were plated onto YPD plates, allowed to grow for 2-3 days at 30° C, and replica plated to selective media to determine genotype of each spore clone.

2.5 Oligonucleotides

All oligonucleotides were obtained from Sigma-Genosys. Oligonucleotide sequences were selected using the ApE sequence editing software, and tested *in silicio*

prior to synthesis, using the Amplify 3X software.

Table 2.2 Oligonucleotides used in this study

Name	Sequence 5'-3'	Description/purpose
YNL321wF	CGTTGTAAAACGACGGCCAGTGAATTC GAGCTATGTAATAGCGTGCGACG	*YNL321w* (Forward) for cloning into pFL vectors
YNL321wR	GACCATGATTACGCCAAGCTTGCATGC CTGCACAGTGCAATTGACGGAGA	*YNL321w* (Reverse) for cloning into pFL vector series
YDL206wF	CGTTGTAAAACGACGGCCAGTGAATTC GAGCTAATATGTGGGTGCTGCGA	*YDL206w* (F) for cloning into pFL vector series
YDL206wR	GACCATGATTACGCCAAGCTTGCATGC CTGCAGAAGATTCCATGGCGTGT	*YDL206w* (R) for cloning into pFL vector series
ECM27-5	CGTTGTAAAACGACGGCCAGTGAATTC GAGCTGCTGGTGGCTTTATGGCT	*YJR106w* (F) for cloning into pFL vector series
ECM27-3	GACCATGATTACGCCAAGCTTGCATGC CTGCAAAAGTCTGGCAGGCATCA	*YJR106w* (R) for cloning into pFL vector series
Per1-5	CGTTGTAAAACGACGGCCAGTGAATTC GAGCTCCACGCGTAATGTTTTCC	*YCR044c* (F) for cloning into pFL vector series
Per1-3	GACCATGATTACGCCAAGCTTGCATGC CTGCAGGAAGCATCAAGTGGAGC	*YCR044c* (R) for cloning into pFL vector series
YNL3xHA-tag	TAGCCCGCATAGTCAGGAACATCGTAT GGGTACTCCGAAAGAGCTCCCTG	*YNL321w* primer (R) with homology to the HA epitope at the 5' end.
5'leu2	TTTAGAGCACCACCGCACATGGACAGA CCTGGAGCAGATCTGGTACTTTG	*LEU2* (F) with 5' *YNL321w* homology
3'leu2	ATTAGTATGCAGCAATTCTACAATTGGG TGACGCCAGCAGATCTATTACA	*LEU2* (R) with 5' *YNL321w* homology
YNL321w test1	GACAGCATCAACACAGGA	To verify correct insertion of *ynl321w::LEU2* marker (F)
YNL321w test2	TTGATGTGAGCTTGGTCG	To verify correct insertion of *ynl321w::LEU2* marker (R)
5' universal FP	TATTGTTGTAGGATTCTACTTCCAGGGA GCTCTTTCGGAGGACGGTGCTGGTTTAA TT	Universal primer (F) for generation of YNL321w-fluorescent protein fusions
3' universal FP	ATTGGTAGGTATCCAGGTGAAAAGCGG GGACAGTTGCTTTCCACTAGTGGATCTG ATA	Universal primer (R) for generation of YNL321w-fluorescent protein fusions

2.6 Plasmids

Plasmids used in this work are listed in **Table 2.3**.

Table 2.3 Plasmids used or generated during this study

Plasmid	Yeast selectable marker	Insert/description	Reference
pFL38	*URA3*	Low copy shuttle vector	1
pFL44-S	*URA3*	Multiple copy shuttle vector	1
pFL46-S	*LEU2*	Multiple copy shuttle vector	1
YEpZRC1-HA	*URA3*	*ZRC1* with C-terminal triple HA tag	2
YCpZRC1-HA	*URA3*	*ZRC1* with C-terminal triple HA tag	2
pKT211	*SpHIS5*	YFP and *SpHIS5* cassette	3
pTTQ18	none	*Taq* DNA Polymerase	4
pFL38YNL	*URA3*	YNL321w genomic clone	This study
pFL38YNLHA	*URA3*	YNL321w tagged with triple HA at C-terminus	This study
pFL44YNL	*URA3*	YNL321w genomic clone	This study
pFL44YNLHA	*URA3*	YNL321w tagged with triple HA at C-terminus	This study
pFL44YDL	*URA3*	*YDL206w* genomic clone	This study
pFL44ECM27	*URA3*	*ECM27* genomic clone	This study
pFL44PER1	*URA3*	*PER1* genomic clone	This study
211YNL44	*URA3, SpHIS5*	*YNL321w*-YFP C-terminal fusion via *SpHIS5* insertion.	This study
211YNL38	*URA3, SpHIS5*	*YNL321w*-YFP C-terminal fusion via *SpHIS5* insertion.	This study
ynl321w::LEU2	*URA3*	Alternative *LEU2* knockout allele of *YNL321w*	This study

References: [1](Bonneaud et al., 1991), [2](MacDiarmid et al., 2002), [3](Sheff and Thorn, 2004) [4](Stark, 1987).

2.7 Plasmid construction by homologous recombination

Plasmids in this study were constructed by utilizing homologous recombination in yeast (Hua et al., 1997; Ma et al., 1987). This method provided a very accurate, versatile and reliable method of constructing yeast shuttle vectors. In general, a WT yeast strain was co-transformed with a mixture of linearized DNA of a yeast shuttle vector, and a PCR product with termini homologous to the vector (**Figure 2.3**). The PCR products were generated using oligonucleotides that included 32 bp of sequence at the 5' end, and were thus homologous to two regions of the vector separated by a restriction site or sites. Amplification of a PCR product from genomic DNA or plasmid templates using such primers generated a DNA fragment capable of mediating gap repair of the linearized vector. After transformation, cells that successfully recombined the two fragments expressed the *URA3* gene associated with the plasmid (or an alternative selectable marker), enabling selection for recombinant clones. Control transformations were

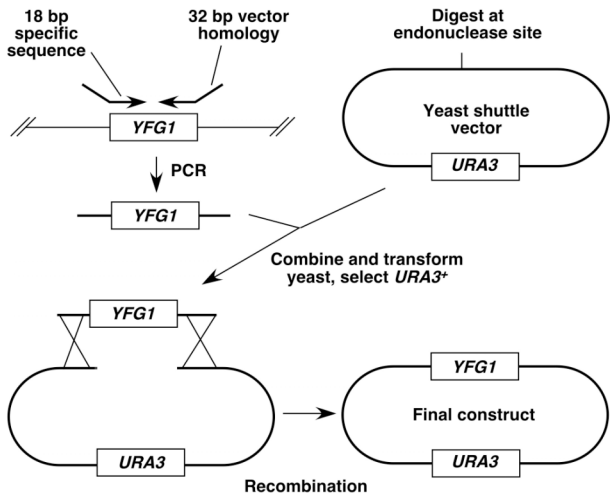

Figure 2.1 Construction of yeast shuttle vectors using homologous recombination. In general, yeast plasmids were constructed by generating a PCR product using two 50-mer oligonucleotide primers. The primers included 18 bases of homology to the gene of interest (*YGF1*, Your Favorite Gene 1) at the 3' end, and 32 bases of homology to the target vector at the 5' end. The vector DNA was cleaved with a restriction enzyme, and the PCR product and vector were used to transform a *ura3*$^{-}$ strain to *URA3*$^{+}$.

performed using the vector fragment alone to enable an estimation of the success of the experiment by comparison of transformation frequency. To verify the structure of the new plasmids, plasmid DNA was extracted from yeast strains and transferred to *E. coli* by electroporation, followed by purification via standard methods. Correct construction of the new plasmids was verified by restriction digestion or sequencing. Specific details of the construction of the various plasmids used in this work are given below.

2.7.1 Multicopy overexpression vectors

To generate constructs for gene overexpression, three CaCA genes (*YNL321w*, *YDL206w*, and *YJR106w)* and the *PER1* gene were amplified with the appropriate oligonucleotides (for example, *YNL321w* was amplified with *YNL321wF* and *YNL321wR*, **Table 2.2**). The resulting products included homology to the polylinker of the yeast vector pFL44-S, which contains the replication origin of the 2μ yeast vector (Bonneaud et al., 1991). pFL44 was linearized by digestion with *Bam*HI and *Hin*dIII restriction enzymes, and a mixture of the vector and PCR product was used to transform DY1457 (**Figure 2.1**). Recombinant plasmids were rescued from yeast and the identity of the

insert verified by restriction digestion. pFL38YNL is a low-copy version of the pFL44YNL plasmid with the identical insert, and was constructed by combining the PCR product with the pFL38 vector after digestion with the same enzymes.

pFL38YNLHA and pFL44YNLHA are low and high copy vectors containing the YNL321w gene fused to a triple repeat of the HA epitope: they were constructed by first amplifying the *YNL321w* gene from genomic DNA of the DY1457 strain using the YNL321wF and YNL3xHA-tag oligonucleotides. The YEpZRC1-HA and YCpZRC1-HA vectors (MacDiarmid et al., 2002) were cleaved with the restriction enzymes *Bam*HI and *Bst*XI to linearize the vector within the insert of the *ZRC1* gene. This PCR product was inserted into the cut vector via homologous recombination. In the resulting plasmids, the *ZRC1* gene was replaced with *YNL321w* so that the HA tag was fused to the *YNL321w* C-terminus. Correct fusion to the HA epitope tag was verified by restriction digestion and DNA sequencing.

The 211YNL44 and 211YNL38 vectors are derivatives of pFL44YNL and pFL38YNL in which the C-terminus of Ynl321w was fused to the YFP protein sequence derived from the pKT211 vector **(Table 2.3)**. The pKT vectors contain promotorless coding sequences for fluorescent proteins, cloned next to a selectable marker for yeast (the KAN^R gene, which confers resistance to Geneticin, or the *HIS5* gene from *S. pombe,* which complements the *his3* mutation in *S. cerevisiae*) (Sheff and Thorn, 2004). Two oligonucleotides (5’ and 3' universal FP) were designed to allow amplification of the YFP and selectable marker combination and include homology to sequences flanking the unique *Sac*I restriction site at the 3' end of the Ynl321w coding sequence. To fuse YFP to the Ynl321w ORF, the pFL44YNL plasmid was digested with *Sac*I, and the PCR product

and vector were recombined in yeast as described previously. Correct insertion of the PCR product was ensured by selection for the expression of the novel *SpHIS5* marker as well as *URA3* in the yeast clones, and verified by restriction digestion after plasmid rescue through *E. coli*.

The *ynl321w::LEU2* plasmid is a derivative of pFL44YNL in which part of the *YNL321w* coding sequence is replaced with the *LEU2* gene. To construct this plasmid, a PCR product including the *LEU2* gene was amplified from genomic DNA using the 5'leu2 and 3' leu2 oligonucleotides. pFL44YNL was digested with *Bam*HI and *Bst*XI, and DY1457 was co-transformed with the cut vector and PCR product. Strains expressing both *URA3* and *LEU2* were selected from the transformation, and the plasmid was rescued through *E. coli* and verified by digestion with restriction enzymes. To delete *YNL321w* from the genome, the insert of *ynl321w::LEU2* was excised by digestion with *Eco*RI and *Sac*I, gel purified, and used to transform WT yeast to *LEU2*$^+$. Correct insertion of the new allele was verified by amplifying the correct product from yeast genomic DNA, using the YNL321w test1 and YNL321w test2 oligonucleotides.

2.8 DNA Isolation and Purification

2.8.1 Plasmid Isolation and Purification from E. coli

2.8.1.1 Plasmid purification from E. coli for routine use

Plasmid DNA was routinely isolated using a modification of a previously described protocol (Sambrook et al., 1989). Single colonies of *E. coli* were used to inoculate 5 ml LB containing the appropriate antibiotic, and cultures incubated overnight at 37° C. Cells were collected by centrifugation (5000 x g/10 min at 4° C), and the cell pellet resuspended in 200 µl Solution I (25 mM Tris-Cl pH 8.0, 10 mM EDTA, 50 mM

glucose); 400 μl of Solution II (0.2 N NaOH, 1% SDS) was then added and the suspension gently mixed until it cleared, indicating complete lysis. 300 μl of ice cold Solution III (3 M potassium acetate, adjusted to pH 4.8 with glacial acetic acid) was then added, and the mixture was agitated gently until a precipitate was observed. The mixture was then chilled on ice for 20 min. The white precipitate of genomic DNA and other contaminates were separated by centrifugation (12,000x g/10 min at 4° C). The supernatant was recovered and transferred to a new tube, and the plasmid DNA was precipitated by the addition of 1 volume isopropanol (600 μl), and collected by centrifugation (12,000x g/10 min). The supernatant was discarded, and the pellet was washed with 1 ml 80% ethanol, dried under vacuum for 10 min in a Speed-Vac, and dissolved in 0.3 ml TE. To degrade residual RNA, 2 μl of 1 mg/ml RNase A (Fisher Scientific) was added and the solution was incubated at 65° C for 15 min. PCA (0.3 ml) was then added, and the mixture was vortexed for 30 s, then centrifuged (12,000x g/5 min) to separate the phases. The aqueous layer was recovered and transferred to a new tube. One volume of isopropanol and 1/10 volume of 3 M sodium acetate pH 5.2 was added to precipitate the DNA. The mixture was allowed to incubate at room temperature for at least 15 min. The DNA was collected by centrifugation, washed once with 80% ethanol, dried, and redissolved in 50 μl sterile deionized water for storage at -20°C. This protocol was scaled appropriately when larger yields were required.

2.8.1.2 Plasmid Isolation and Purification for Sequencing

Plasmid DNA intended for sequencing reactions was purified using a Wizard Plus SV Miniprep kit (Promega) according to the manufacturers instructions.

2.8.2 Genomic and plasmid DNA isolation from Yeast

Cultures of yeast (5 ml) were grown to saturation at 30° C in synthetic medium (SC). Cells were collected by centrifugation (2,000x *g*/5 min), washed with 5 ml of sterile water, and resuspended in 1 ml of sterile deionized water. The suspension was transferred to a 1.5 ml microfuge tube and centrifuged for 1 minute to collect the cells. The cells were resuspended in 200 μl of genomic DNA buffer (2% Triton X-100, 1% SDS, 0.1 M NaCl, 1 mM EDTA, 1 mM Tris pH 8.0), and 200 μl of PCA was added, followed by 0.3 g of glass beads (425-600 mesh size, Sigma). The cells were broken by vortexing for 10 min at 4°C. TE buffer (200 μl) was then added and the mixture was centrifuged at high speed (12,000x g/5 min) in a microfuge. The aqueous layer was transferred to a new microfuge tube, and 1 ml of isopropanol and 140 μl of 3 M sodium acetate were added. The mixture was left at room temperature for at least 1 hour to allow precipitation, then centrifuged at high speed (12,000x g/10 min) to collect the DNA. The supernatant was removed and the pellet was washed twice with 70% ethanol (1 ml). The ethanol was removed, and the pellet was dried in a Speed-Vac (Savant). The pellet was dissolved in 200 μl TE and 1 μl of 10 mg/ml of RNase A was added, followed by incubation at 65° C for 15 min to degrade RNA. The sample was then extracted with an equal volume of PCA and the aqueous layer transferred to a new tube. The DNA was precipitated by addition of 1 volume isopropanol and 1/10 volume 3M NaOAc, collected by centrifugation, washed twice with 70% ethanol, and dissolved in 50 μl of sterile deionized water. The same protocol was used for the isolation of plasmid DNA from yeast, with the exception that cells were grown in a medium suitable for retention of plasmids (usually SC medium without uracil).

2.9 Polymerase Chain Reaction

PCR reactions performed for analytical purposes utilized Taq polymerase prepared in this laboratory (see above). Standard reactions contained 20 mM Tris-HCl pH 8.4, 50 mM KCl, 0.5 mM $MgCl_2$, 0.2 mM of each dNTP, 1 μM of each primer, 1-2 units of Taq DNA polymerase, and approximately 1 ng of plasmid or 100 ng of genomic DNA template, in a total volume of 50 μl. Reactions were carried out in a MyCycler thermal cycler (Bio-Rad). Reactions consisted of a 30 second denaturing step at 94° C, a 30 second annealing step at the relevant temperature, and extension at 72° C for 1 minute per kb of the expected product. PCR products suitable for cloning were obtained using the Easy-A High Fidelity DNA Polymerase (Stratagene) or Platinum Taq DNA Polymerase High Fidelity (Invitrogen) with the included buffer, according to the manufacturers instructions. For subsequent manipulations, PCR products were purified using a Wizard-SV Gel and PCR Clean up system (Promega) according to the manufacture's instructions, or precipitated via the addition of 3 M NaOAc and isopropanol as described previously.

2.10 Restriction endonuclease digestion

Plasmid DNA was digested by incubation in the appropriate NEB (New England Biolabs) buffer according to manufacture's recommendations (usually 5 U of enzyme per μg DNA at 37° C for 3 hours).

2.11 Bacterial and yeast transformation procedures

2.11.1 Transformation of E. coli using electroporation

2.11.1.1 Preparation of electrocompetent cells

A single colony of DH10β was used to inoculate 25 ml of LB, and the culture was grown to saturation overnight at 37° C with agitation (260 RPM). 1 L of LB media pre-

warmed at 37° C was inoculated with 10 ml of the overnight culture and incubated at 37° C with agitation. In some cases, 1% glucose was added to aid growth. Cells were grown to an A_{600} of 0.6 and quickly chilled in an ice water bath. During subsequent manipulations, all solutions were chilled to 0° C, and the cells were stored on ice. The cells were centrifuged in a pre-chilled rotor using a Sorvall RC5B Plus refrigerated centrifuge (5000g/10 min at 4° C). The media was discarded and the cells gently resuspended in 50 ml sterile deionized water. A 450 ml volume of sterile deionized water was added and the cells were collected as described above. This wash process was repeated 4 times with 500 ml volumes, once with a 200 ml volume, and once with a 50 ml volume. The cells were then washed twice with 50 ml of sterile 10% glycerol, and resuspended in a volume of 10% glycerol sufficient to contain the cells (about 2 ml). Aliquots of cells (100 μl) were distributed into sterile 1.5 ml microfuge tubes, frozen on a dry ice/ethanol bath, and stored at -80°C. Transformation efficiency was determined by electroporation with 10 pg of pUC19 DNA, as described below.

2.11.1.2 Electroporation of competent cells

An aliquot of cells (25 μl) was thawed on wet ice, mixed with plasmid (1 ng) or yeast genomic DNA (100 ng), and immediately transferred to an ice-cold electroporation cuvette with an electrode gap width of 1 mm. The cuvette was subjected to a voltage pulse of 1.8 kV using an Eppendorf Electroporater model 2510. SOC media (1 ml) was immediately mixed with the cells, and the suspension incubated with shaking for 1 hour at 37°C. Transformed cells were plated onto LB+Amp plates and incubated at 37°C overnight.

2.11.2 Yeast Transformation

Yeast strains were transformed with plasmids using a modification of a published protocol (Schiestl and Gietz, 1989). YPD media (50 ml) was inoculated with 2 ml of a saturated overnight culture of yeast, and the culture incubated at 30° C with shaking until it reached log phase (A_{600} of 0.5-0.7). The cells were collected by centrifugation (2,000x g/5 min in a Beckman GPR centrifuge) and washed with sterile deionized water (40 ml). The pellet was resuspended in 1 ml of TE/LiOAc buffer (0.1 M LiOAc, 0.01 M Tris-Cl pH 7.5, 1 mM EDTA), transferred to a sterile 1.5 ml microfuge tube, and centrifuged as before. The cells were resuspended in the minimal volume of TE/LiOAc buffer required (approximately 1/3 of the pellet volume), and distributed into 50 μl aliquots. Salmon sperm carrier DNA was prepared as follows: 200 mg of genomic DNA (Type III from Salmon Testes, Sigma D1626) was added to 100 ml of TE buffer and dispersed by repeatedly drawing into a 10 ml pipette. The solution was agitated on a magnetic stirrer until dissolved, dispersed into 0.5 ml aliquots and stored at -20. Before use, an aliquot of carrier DNA was boiled for 10 min and immediately cooled on ice. Ten μl of carrier DNA was added to each 50 μl aliquot of cells, and immediately mixed in to prevent gelling of the DNA. Plasmid DNA (1 μl) was then added to the cells, followed by 300 μl of 40% PEG/TE/LiOAc buffer (40% Polyethylene glycol, 0.1 M Lithium Acetate, 0.01 M Tris-Cl pH 7.5, 1 mM Na-EDTA). The mixture was incubated at 30° C for 30 min, then subjected to a 15 minute heat shock at 42°C. The cells were collected by centrifugation at low speed (2,000x g/2 min), washed once with 1 ml of deionized water, and resuspended in 0.5 ml of deionized water. Aliquots of each transformation were plated onto selective medium and incubated for 2-3 days at 30° C.

2.12 Protein extraction and manipulation

2.12.1 Protein Extraction using TCA

To isolate total protein from yeast, 5-10 ml overnight cultures were grown to log phase (A_{600} 0.5-1.0) in the appropriate medium. The cells were pelleted by centrifugation (2,000x *g*/5 min) and washed once with 10 mM Na_2EDTA (5 ml). Cell pellets were resuspended in 1 ml of 10 mM Na_2EDTA, transferred to a 1.5 ml microfuge tube, and collected by centrifugation. The cells were resuspended in 400 µl cold extraction buffer (10% TCA, 20 mM Tris pH 8.0, 50 mM ammonium acetate, 2 mM Na_2EDTA, 2 mM PMSF) and placed on ice. After the addition of 3 g of glass beads (Sigma), the tube was vortexed at 4° C for 10 min. The glass beads were allowed to settle, and the buffer suspension containing lysed cells were removed. Another aliquot of extraction buffer (200 µl) was added to the glass beads, the mixture was briefly vortexed, and the supernatant was removed. The supernatant recovered at each step was pooled and centrifuged at high speed (12,000x g/5 min) at 4°C. The supernatant was discarded and the pellet (containing broken cells and precipitated protein) was resuspended in protein buffer (100 mM Tris-base, 3% SDS, 1 mM PMSF) and boiled for 5 min. The insoluble debris was removed by high-speed centrifugation (12,000g/5 min) and the supernatant (containing the protein) was retained and stored at -80° C. Protein content was assayed by using a DC protein assay kit (Bio-Rad) according the manufactures instructions. Colorometric reactions were quantified using an EL_X800 Universal Microplate Reader at a wavelength of 750 nm. Absorbance was converted to concentration by use of a standard curve generated from a BSA standard.

2.12.2 SDS-Polyacrylamide gel electrophoresis (PAGE)

SDS-PAGE was used to separate proteins by molecular weight prior to Western blotting. The resolving gel was composed of 375 mM Tris-Cl pH 8.8, 0.1% SDS, 10% acrylamide mix (29.2 acrylamide:0.8 bis-acrylamide (Fisher)**,** 0.1% ammonium persulfate, and 0.1% TEMED. The stacking gel layer was composed of 125 mM Tris-Cl pH 6.8, 4.5% acrylamide mix, 0.1% SDS, 0.1% ammonium persulfate, and 0.1% TEMED. Generally, 10 μg of protein was boiled in loading buffer (25 mM Tris-Cl pH 6.8, 2% SDS, 5% glycerol, 5% β-mercaptoethanol, 0.01% bromophenol blue) prior to loading. Electrophoresis was performed at 200V for approximately 30 min in a Mini-PROTEAN III gel rig (Bio-Rad laboratories), using a Tris-glycine buffer system (25 mM Tris-base, 20 mM glycine, 0.1% SDS). To visualize proteins when required, gels were stained with Coomassie Brilliant Blue R250 (Sigma). The gel was immersed in an aqueous solution of 0.025% Coomassie blue, 40% methanol and 7% acetic acid, and incubated until the gel was no longer visible in the stain. The gel was then destained for 30 min-2 h in the same solution lacking dye.

2.12.3 Electroblotting and immunodetection of proteins

Proteins contained in PAGE gels were blotted to Hybond-N nitrocellulose membranes (Amersham Biosciences) by electrophoretic wet transfer, using a Mini Trans-Blot Electrophoretic Transfer Cell (Bio-Rad). A gel and membrane sandwich was assembled, inserted in an electrode module, and immersed in a tank containing transfer buffer (50 mM Tris-base, 380 mM Glycine, 0.1% SDS, and 20% methanol). Transfer was performed at 63V for 3 hours, with the entire transfer cell placed on ice to prevent overheating.

To detect proteins transferred to nitrocellulose membranes, the membranes were rinsed twice in TBST buffer (50 mM Tris-Cl pH 8.0, 150 mM NaCl, 0.05% Tween 20) and incubated in blocking buffer (1% fat free dried milk in TBST) overnight to prevent non-specific antibody binding. The membranes were washed in TBST with gentle agitation (twice for 10 seconds each, once for 20 min, and then twice for 5 min each). Primary antibodies (obtained from Molecular Probes or Abcam) were added to 10 ml of blocking buffer at the appropriate concentrations, added to the membranes, and incubated with gentle agitation for 2 hours at room temperature. The previous washing procedure was repeated, and then a secondary antibody coupled to horseradish peroxidase (Pierce) was added and incubated for 2 hours at room temperature. The antibodies were then removed, and the membranes washed with TBST as described above. To detect horseradish peroxidase activity, the ECL (Enhanced Chemiluminescence) detection system (Pierce) was used according to the manufacturers instructions. Light emission was detected using BioMax scientific imaging film (Kodak), developed and fixed with GBX developer and fixer (Kodak).

2.13 Sucrose gradient fractionation of yeast organelles

To localize intracellular proteins in yeast, sucrose gradient fractionation of organelles was performed. Yeast cultures (200-300 ml) were grown to log phase in an appropriate minimal medium. The cells were collected via centrifugation, washed twice with sterile deionized water (25 ml), and resuspended in 10 ml of sorbitol buffer (10 mM potassium phosphate buffer pH 7.4, 1.2 M sorbitol) containing 10 mM DTT (added fresh). By measurement of the A_{600} of a dilution of the cells, the total number of A_{600} units of cells was determined. Zymolyase 20T (Seikagaku, Tokyo) was then added to the cells

in the ratio of 1 U/A_{600} unit, and the mixture was incubated for 1 hour at 30° C in a shaker with gentle agitation (100 RPM). To remove the Zymolyase, the spheroplasts were washed twice in 25 ml of ice-cold sorbitol buffer: to avoid breakage, spheroplasts were gently resuspended in a small volume of buffer by gently drawing up and down with a 5 ml autopipette, then collected by centrifugation in a Beckman GPR centrifuge (2,000x g/5 min). After the last wash, all residual supernatant was removed with a pipette, and the cells were resuspended in 2 ml of ice-cold lysis buffer (10 mM Tris-Cl pH 7.6, 2 mM $MgCl_2$, 10% sucrose, 10 mM DTT). The suspension was homogenized using 20 strokes of a 5 ml Dounce homogenizer, and the extent of cell lysis was checked with the use of a light microscope. If lysis was incomplete, a one third volume of glass beads (Sigma) was added to the mixture, and the tube was vortexed at full speed for 30 seconds. The lysate was spun at low speed at 4° C (200x g/3 min) to pellet any unbroken cells and nuclei, and the upper layer containing the free organelles was removed. One ml of the organelle suspension was loaded on top of a 20-60% continuous sucrose gradient (from top to bottom). Depending on the experiment, two gradient systems were used: a buffer with 2 mM $MgCl_2$ (10 mM Tris-Cl pH 7.6, 10 mM DTT), and another that contained the same buffer, except the $MgCl_2$ was replaced with 1 mM EDTA. The gradients were generated from 20% and 60% sucrose + buffer solutions using a gradient maker. After loading the organelles, the gradients were centrifuged at 95,000x *g* for 2 hours at 4° C in an OTD70B Ultracentrifuge (Sorvall) using the AH629 rotor. Fractions (1 ml) were collected drip-wise by puncturing the bottom of the ultracentrifuge tube with a needle. An equal volume of each fraction was then separated by SDS-PAGE and subjected to immunoblotting to detect marker proteins associated with each fraction. When required to increase

sensitivity, the proteins were concentrated from the fractions using TCA precipitation. An equal volume of a 20% solution of ice-cold trichloroacetic acid (TCA) was added to the fraction and the mixture placed on ice for 2-3 hours, then centrifuged at high speed (16,000x g/30 min) at 4° C to collect the protein. The pellet was washed once with cold acetone (200 μl) to remove residual TCA, then dried in a vacuum chamber. Samples were resuspended in 100 μl of protein buffer (Tris-base, 3% SDS, 1 mM PMSF) and boiled for 5 min in a water bath. Prior to TCA precipitation, dense fractions (>30% sucrose) were diluted 4-fold with gradient buffer lacking sucrose, to enable collection of the precipitates by centrifugation.

2.14 Immunofluorescence

Indirect immunofluorescence was used to detect protein location in whole yeast cells via fluorescence microscopy. Yeast cells expressing epitope-tagged proteins were grown in selective medium (25 ml) to an A_{600} of approximately 1.0. The cells were collected by centrifugation (2,000x g/5 min), washed twice with 10 ml of 1x PBS (140 mM NaCl, 2.7 mM KCl, 10 mM Na_2PHO_4, 2 mM NaH_2PO_4), and fixed by addition of 1 ml of 37% w/w formaldehyde, followed by incubation for 2 hours at 30° C with agitation (260 RPM). Fixed cells were washed twice with ice-cold Solution A (100 mM $KHPO_4$ pH 7.0, 1.2 M sorbitol) and resuspended in 2 ml of Solution A containing 10 mM DTT (added from a 1 M solution). The A_{600} was determined, and a solution of Zymolyase 20T was added at a ratio of 2 U/A_{600} unit of cells to digest the cell wall. The cells were incubated for 2 hours at 30° C with gentle agitation (100 RPM), then collected by centrifugation (200x *g*/5 min), washed twice with Solution A (10 ml), resuspended in cold methanol (-20°C), and stored for 1 hour at -20°C. This step permeabilized the cell

membrane, allowing subsequent entry of antibodies. The cells were washed twice with 5 ml cold PBS and resuspended in 100 μl cold PBS. To promote adherence of the yeast cells, microscope slides with paint wells (Fluorescent Antibody Rite-On Slides, Fisher) were treated with poly-L-lysine (PLL) by the application of 40 μl of 0.1% PLL (Sigma) to the well of the slide for 10 min. The excess PLL was removed (leaving a layer on the slide), and the slides were allowed to air dry. The slides were washed with deionized water, the excess PLL was removed by gently scrubbing with a wet Kimwipe, and the slides were allowed to dry. To affix cells to the slides, 50 μl of cells were applied to the well of the slide, and the slide was placed on a wet Kimwipe inside a Petri plate. The slides were then left at 4° C for 1 hour to allow the cells to adhere, then washed twice with 1x PBS to remove unbound cells. The slides were covered with blocking buffer (1x PBS, 5% non-fat dried milk, 0.1% Tween-20) and incubated overnight at room temperature. An appropriate concentration of the primary antibody in blocking buffer was added to the well and the slides were incubated at room temperature for 1 hour. The slides were washed 5 times with 1x PBS containing 1% Tween-20 with gentle agitation for 10 min in a slide bath. This procedure was repeated with the appropriate fluorescently labeled secondary antibody, except that the incubation was performed in a slide bath that was masked with aluminum foil to prevent bleaching of the fluorescent dye. After the last wash, 1 drop (20 μl) of Mowiol solution was added to the slide, and a cover slip was placed over the well. (To prepare Mowiol solution, 2.4 g Mowiol [Calbiochem] was added to 6 g glycerol, 12 ml 0.2 M Tris-Cl pH 8.5, and 6 ml H_2O; the mixture was heated until the Mowiol dissolved, then stored in 1 ml aliquots at -20° C.) Slides were allowed to harden during storage overnight at 4° C. For fluorescence microscopy, slides were viewed

with an Olympus 1X70 microscope using a Chroma 41028 filter set and a Cool Snap Mono HQ camera (Roper Scientific). Images were captured using QED *in vivo* software (Media Cybernetics) and manipulated with Adobe Photoshop (Adobe).

2.15 Atomic Absorbance Spectroscopy (AAS)

To determine the elemental content of yeast cells, AAS was performed as described below. Yeast cells were grown to log phase in selective medium with a range of metal ion concentrations. Cells were collected by centrifugation, then washed twice in 200 ml 1 mM Na_2-EDTA pH 8.0 to remove externally bound divalent cations, and twice with deionized water to remove the EDTA. For cells grown in supplemental Na^+, an extra wash with 50 mM KCl was performed after the EDTA washes to remove any externally bound Na^+. The final cell pellet was resuspended in 1 ml of purified water, and the A_{600} of 1:20 dilutions of each sample was recorded. After measurement of cell density, 1 ml of each undiluted suspension was transferred to 13 ml glass tubes, mixed with 1 ml of concentrated nitric acid, and digested by overnight incubation at 95° C.

For magnesium and calcium measurements, 2 ml of 1x La buffer (10 mM LaCl, 240 mM HCl) was added to each digest, and each sample was then adjusted to a total volume of 4 ml with purified water (to adjust for evaporation during the digest). By binding P, La^{3+} ions act as a "releasing agent", preventing its interaction with divalent metal cations: this interaction can lead to an underestimation of the Mg^{2+} and Ca^{2+} concentration. Samples were diluted 5-fold in 0.5x LaCl Buffer before measurement.

For determination of Na^+ content, 2 ml of 1x KCl buffer (25 mM KCl, 240 mM HCl) was added to each digest, and each sample was adjusted to a total volume of 4 ml with purified water. Before measurement, samples were diluted 10-fold in 0.5x KCl

Buffer.

Ion concentration was measured using an Atomic Absorbance Spectrophotometer (GBC 904AA) according to the manufacture's recommendations. The instrument was calibrated using a set of $MgCl_2$, $CaCl_2$, or NaCl solutions of known concentration (0 - 60 μM $MgCl_2$, 0 - 50 μM $CaCl_2$, and 0 - 25 μM NaCl). To convert the concentrations to values of cation mass/cell, the concentration was multiplied by the dilution factor and volume of the digested cells to obtain the total cation content of the sample, which was then divided by the number of cells in the suspension. The absorbance values of each sample were converted into cell number using a standard curve, which was generated as described below. The cell density (A_{600}) of a culture of actively growing yeast cells was measured using an EL_X800 Microplate Reader (Bio-Tek). Serial dilutions of the culture were plated on YPD medium to determine the number of viable cells in the suspension. A standard curve was then generated relating the number of viable cells to the A_{600} of each dilution. The curve was linear up to an A_{600} of 1.0, indicating good accuracy over this range.

Chapter 3: Results

3.1 *YCR044c*/*PER1* encodes a putative Mg^{2+} transporter

My interest was to identify novel membrane proteins capable of actively transporting Mg from the cytosol to other compartments. The first possible candidate for such a transporter examined was the Per1 protein, which was of interest because it had previously been implicated in ion homeostasis. Per1p was identified in a screen for mutations that suppressed the manganese sensitivity of a *cdc1* mutant (*cos16*) (Paidhungat and Garrett, 1998). Although the mechanism of this suppression was unclear, the phenotype implicated this protein in the regulation of divalent cation homeostasis. For three reasons, I suspected that Per1 might also be involved in Mg^{2+} homeostasis: first, Per1 encodes an apparent membrane protein with several transmembrane domains; second, an early study indicated that Per1 was located in the vacuole membrane, and third, mutants lacking the Ycr044cp/Per1p protein were sensitive to high Mg^{2+} concentrations (Paidhungat and Garrett, 1998). These observations suggested that Per1 was required for the regulation of cytosolic Mg^{2+} concentration, perhaps via the sequestration of Mg^{2+} in the vacuole. An alternative explanation for the Mg sensitivity of *per1* strains might be that Per1 is required for vacuolar function or formation. However, unlike mutations that compromise vacuolar function (e.g. *pep3*, *pep5*, and *vps4*), *per1* displayed normal tolerance to excess Na^{+}, Li^{+}, Ca^{2+}, Mn^{2+}, Ni^{2+} and Zn^{2+} ions [(Paidhungat and Garrett, 1998) and data not shown]. In addition, I observed no gross morphological changes in *per1* vacuoles indicative of a major defect in vacuole formation or maintenance (data not shown).

While this work was in progress, a large-scale survey of protein location in yeast

(Huh et al., 2003) showed that a Per1-green fluorescent protein (GFP) fusion was located in the ER membrane. I obtained the yeast strain used and determined that the Per1-GFP fusion was functional, as the strain did not display the inability to utilize non-fermentable carbon sources (a "petite" phenotype) that is associated with this mutation (Steinmetz et al., 2002) (data not shown). This location for Per1 suggested that the protein may play a role in ER function, perhaps by mediating the supply of Mg^{2+} to the lumen. If so, I reasoned that the phenotypes of the *per1* mutant might be a consequence of a decreased supply of Mg^{2+} to the ER, and that increasing the Mg^{2+} supply to the cell might suppress these phenotypes. To test this prediction, I examined the effect of Mg^{2+} on the petite phenotype of the *per1* mutant and observed that it was conditional on Mg^{2+} availability; a small but significant increase in growth was observed when the YPGly medium was supplemented with 5-10 mM extra Mg^{2+} (**Figure 3.1A**), although this effect was eliminated at higher Mg^{2+} concentrations (where the Mg^{2+} sensitivity of *per1* was observed). In addition to partial suppression of this petite phenotype by Mg^{2+}, *per1* also showed Mg^{2+}-dependent phenotypes in glucose-containing medium. Cells of *per1* grown under deficient conditions (5 μM Mg^{2+}) had a reduced growth rate (data not shown), and displayed an aberrant morphology; in Mg^{2+}-deficient conditions, *per1* daughter cells failed to completely separate after cell

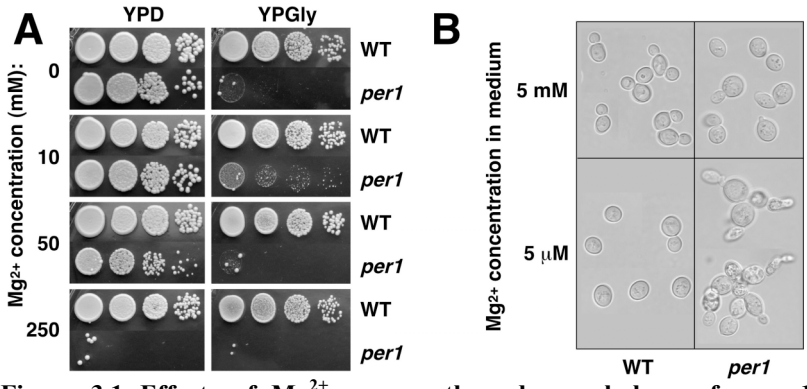

Figure 3.1 Effects of Mg^{2+} on growth and morphology of a *per1* mutant. A: Effect of Mg^{2+} and carbon source on growth of *per1* on YPD (2% glucose) and YPGly (3% glycerol). **B:** WT and *per1* mutant strains were grown for 12 hours in synthetic medium with 5 μM or 5 mM Mg^{2+} as indicated, and examined with bright field illumination.

division and had a filamentous shape (**Figure 3.1B**). Hence, the *per1* mutant exhibited both an increased requirement for Mg^{2+} and Mg^{2+}-sensitivity phenotypes, further implicating this gene in Mg^{2+} homeostasis. The Mg^{2+}-dependent phenotypes are consistent with the *per1* mutation blocking the supply of Mg^{2+} to some essential compartment, and the ER location of Per1 suggests that this compartment may be the one affected.

To further analyze the effect of Per1 on Mg^{2+} homeostasis, I examined the effect of altered Per1 expression on the Mg^{2+} content of yeast cells. If Per1 was required for the intracellular storage of Mg^{2+}, I reasoned that the deletion of this gene might affect Mg^{2+} content by reducing vacuolar storage. To determine if this was the case, I measured Mg^{2+} accumulation in WT and *per1* mutant cells grown with a range of Mg^{2+} concentrations, from deficient (<100 μM) to excess. Cell samples were digested with acid and Mg^{2+} content measured with atomic absorption spectroscopy (AAS). Notably, *per1* mutant cells showed a significant decrease in intracellular Mg^{2+} content at all concentrations tested (**Figure 3.2A**). This observation suggested that Per1 might contribute to the intracellular storage of Mg^{2+}. However, subsequent experiments did not support this hypothesis. If Per1 was responsible for Mg^{2+} storage in the vacuole, the overexpression of *PER1* from a multicopy plasmid (pFL44) in a WT strain would be expected to increase cellular Mg^{2+} content. However, when I constructed a multicopy version of *PER1* and introduced this into a WT strain, no significant change in intracellular Mg^{2+} content was observed (**Figure 3.2B**).

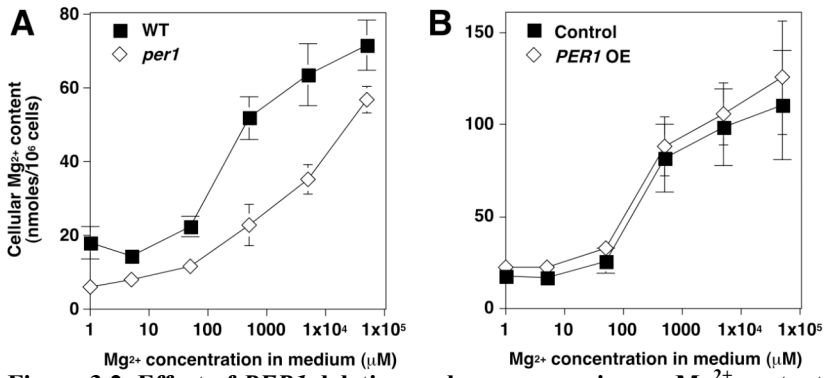

Figure 3.2. Effect of *PER1* deletion and overexpression on Mg^{2+} content. Mg^{2+} content of WT (BY4743) and *per1* (YCR044cΔ) mutant strains (**A**) or Control (DY1457/pFL44-S) and *PER1* overexpressing (DY1457/pFL44PER1) strains (**B**) was assayed with AAS after growth in medium with the indicated Mg^{2+} concentration. Data points indicate the mean of four (for **A**) or five (for **B**) independent experiments, error bars indicate 95% confidence limits.

The above results seem to provide indirect support for the hypothesis that Per1 is a Mg^{2+} transporter with effects on homeostasis: however, my results do not seem consistent with a role in supplying Mg^{2+} to the ER. The alternative explanation, that Per1 is a transporter active in a different compartment to the ER, seems unlikely: a recent study also showed Per1-GFP to be located in the ER membrane (Fujita et al., 2006), and the UPR-related phenotypes of the mutant strain (Ng et al., 2000) also implicates this protein in ER function. One explanation for the Mg^{2+}-related phenotypes of *per1* mutants may be that this protein is responsible for some very general aspect of ion homeostasis: for example, the maintenance of cell membrane integrity. As discussed further in the final section of this chapter**,** recent results from other research groups communicated or published during this work support this idea by providing strong evidence for a general role of Per1 in protein processing and GPI anchor synthesis (Fujita et al., 2006). Since the focus of this work was on identifying Mg^{2+} transporters, when this information became available, I shifted my attention to other proteins that might prove to be better candidates.

3.2 Identification of new members of the calcium/cation exchanger family

As discussed in **Chapter 1**, a Mg^{2+}/H^+ exchanger activity is present in membranes of the yeast secretory pathway and vacuole, but the molecular identity of this protein has yet to be determined. Members of the calcium/cation antiporter (CaCA) superfamily transport a variety of divalent metal cations, using the energy stored in the H^+ or Na^+ gradients generated by primary ATPase pumps (Maser et al., 2001; Shigaki and Hirschi, 2006). It is possible that an uncharacterized member of this group could be responsible for Mg^{2+}/H^+ exchange activity. At the start of this work, I identified three yeast proteins of unknown function (Ynl321wp, Ydl206w, and Yjr106w) that were weakly related to the previously characterized Ca^{2+}/H^+ exchanger Vcx1p (Maser et al., 2001). All three proteins contain a conserved motif (PFAM motif PF01699.12) also found in Ca^{2+}/H^+ exchangers [the α-repeats, reviewed in (Philipson and Nicoll, 2000)]. This motif is repeated at least twice in all CaCA proteins; a region of poorly conserved sequence, which varies widely in length, normally separates the repeats. All three novel yeast proteins share this general structure (**Figure 3.3A**). Using the computer program *ClustalX* (Thompson et al., 1997), I generated an alignment of the most C-terminal conserved motif in previously characterized or closely related calcium exchangers (including yeast, *Arabidopsis*, rat and mouse examples) (**Figure 3.3B**). The alignment shows significant conservation between these proteins and the yeast proteins, concentrated in the regions that include the α-repeats. Thus, all three of these proteins are members of the CaCA superfamily, as previously reported for *YNL321w* and *YDL206w* (Maser et al., 2001).

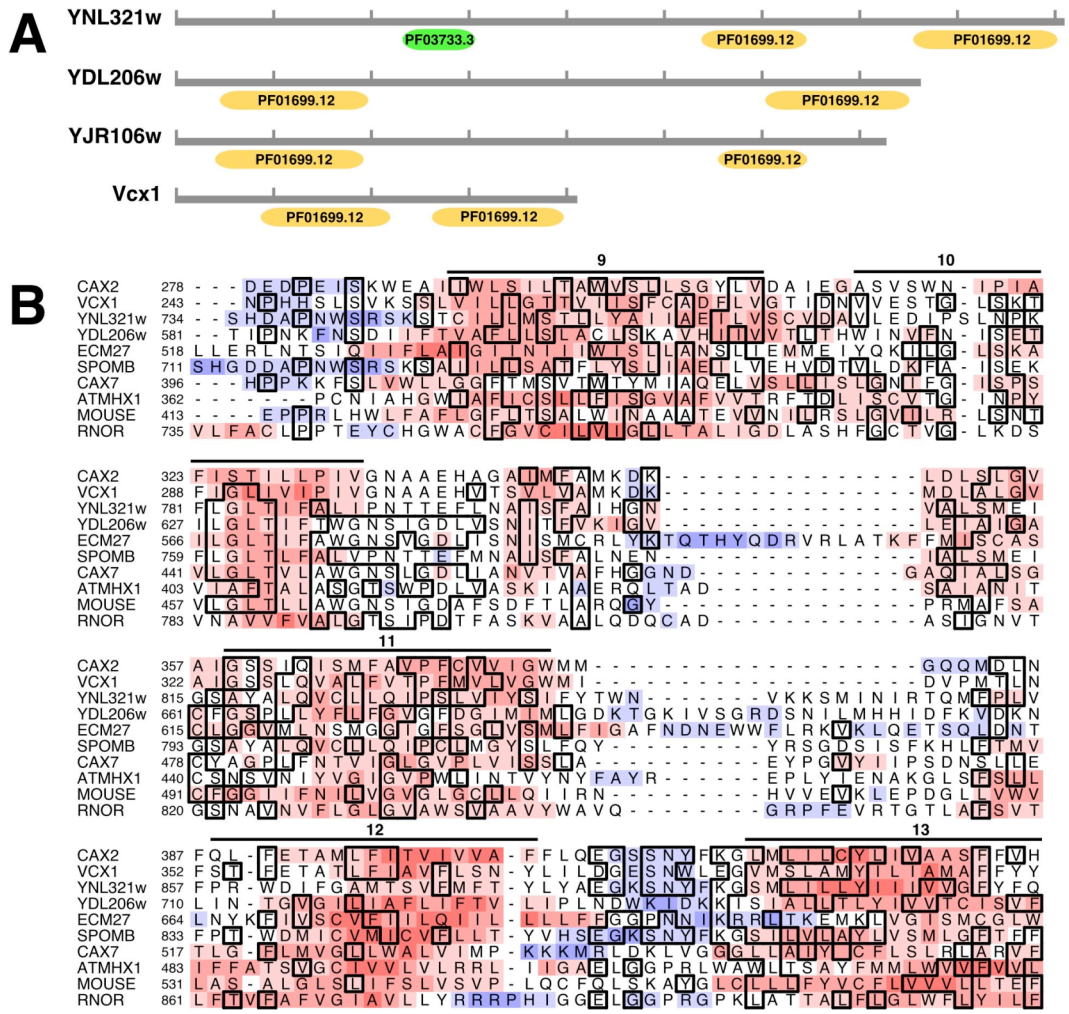

Figure 3.3 Structure and sequence of CaCA family members. A: Comparison of Vcx1 and related yeast proteins, showing the location of the PF01699.12 domains characteristic of Ca^{2+}/Na^{+} and Ca^{2+}/H^{+} exchangers, as well as a domain of unknown function (PF03733.3) unique to Ynl321w. Each tick on the lines indicates 100 residues. **B:** Sequence alignment of the most C-terminal conserved domains (Pfam 01699.12) of several CaCA family members. Proteins closely related to Vcx1 and the yeast CaCA proteins were identified using Blast and aligned using the program ClustalX (Thompson et al., 1997). GenBank accession numbers for each of the sequences shown are: CAX2, *A. thaliana* NP566452; spombe - *S. pombe* CAB86468; Mouse, *M. musculus* Slc24a6 protein; CAX7, *A. thaliana* NP197288; Rnor, *R. norvegicus* NP511174; Atmhx1, *A. thaliana* NP566105. Residues identical in three or more sequences are boxed. Color shading indicates relative hydrophobicity at each residue (red = hydrophobic, blue = hydrophilic), as calculated with a window size of 7 residues and displayed using the program Seqview (Riek et al., 1995). Putative transmembrane domains are indicated, based on the extent of the hydrophobic regions (numbered lines).

One of the novel CaCA proteins, Ynl321w, differed somewhat in structure and sequence from the other two proteins. Ynl321w is a member of the CAX (cation exchanger) subfamily of the CaCA group (Shigaki and Hirschi, 2006), which also

includes Vcx1. The most well characterized members of this subfamily are calcium/proton exchangers, found predominantly in the endosomal compartments of fungi and plant cells (*e.g.* Vcx1) (Shigaki and Hirschi, 2006). **Figure 3.4A** shows a Kyte-Doolittle hydropathy plot of Ynl321w, showing the relative positions of thirteen regions of hydrophobic sequence that probably function as transmembrane domains (numbered 1-13). Most of these domains are found in the PF01699.12 motifs: however, domains 1, 2 and 8 are found only in a small subgroup of CaCA proteins. Members of this group also differ from the bulk of the CaCA superfamily in their possession of an extended N-terminal domain. Blast searches with this region against the non-redundant GenBank database revealed the presence of a conserved motif (positions 238-301, Pfam motif PF03733.3) that is also found in a small family of prokaryotic proteins of unknown function. This motif contains predicted hydrophobic domain 1, perhaps indicating that it forms a transmembrane domain. Alternatively, this region could perform the function of a cleaved leader sequence, analogous to sequences present at the N-termini of many mammalian CaCA proteins (Philipson and Nicoll, 2000). A recent phylogenetic analysis of the CaCA family confirmed these observations of Ynl321w structure, and placed Ynl321w in a separate subgroup of CAX proteins (designated Type II) to reflect the unique features described above (Shigaki and Hirschi, 2006).

The other two yeast proteins (*YDL206w* and *YJR106w*, or *ECM27*) are not members of the CAX subfamily: the above phylogenetic analysis showed that these proteins are most similar to the Arabidopsis CCX1-5 and mammalian NCKX6 proteins (Cai and Lytton, 2004). NCKX6 is believed to be a K^+-dependent Na^+/Ca^{2+} antiporter system, and is the founder member of a new group of proteins termed the Cation Calcium

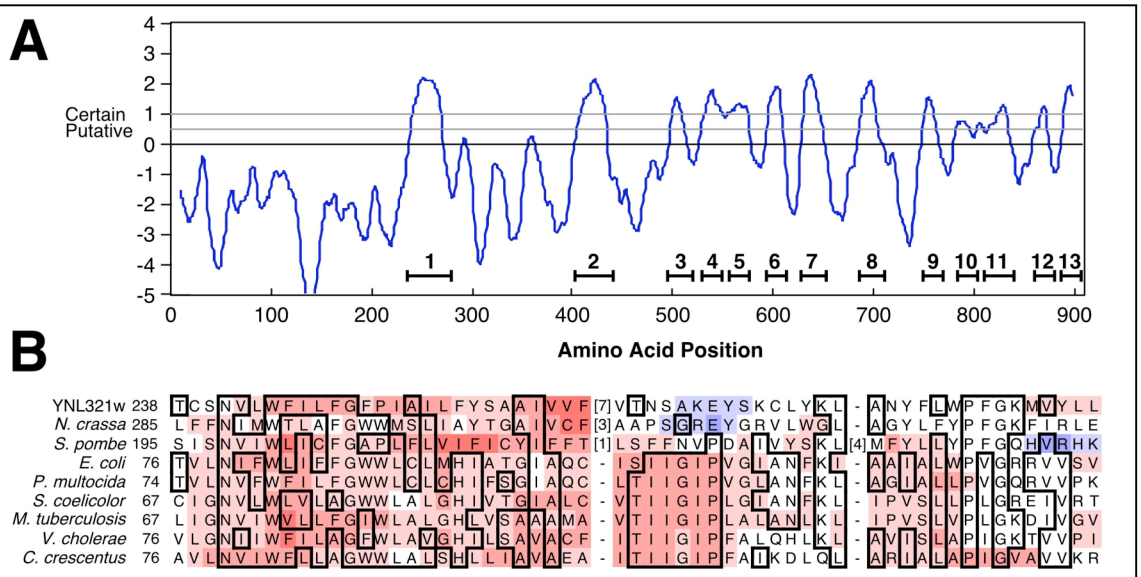

Figure 3.4 Structural features of Ynl321w. A. Hydropathy plot of the YNL321w protein generated using the Kyte-Doolittle algorithm. Positions of putative transmembrane domains are indicated (black bars). "Certain" and "Putative" lines indicate cutoff values for prediction of transmembrane domains. **B:** Sequence alignment of the novel conserved domain found in Ynl321w (Pfam 03733.3) with related hydrophobic domains found in fungal type II CAX proteins, and the most C-terminal Pfam 03733.3 domain, found in many prokaryotic proteins of unknown function. The alignment was generated and displayed as described for **Figure 3.3B.** Genbank accession numbers for the sequences shown are: Ynl321w, gi 11544693; *N. crassa*, gi 7529641; *S. pombe*, gi 2506635; *E. coli*, gi 2506635; *P. multocida*, gi 12720641; *S. coelicolor*, gi 10129706; *M. tuberculosis*, gi 2916929; *V. cholerae*, gi 9658495; and *C. crescentus*, gi 13423598.

eXchanger (CCX) family. As yet, the members of this subfamily of the CaCA group are only poorly characterized.

In summary, the above analysis indicated that the three yeast proteins of unknown function were members of the CaCA superfamily, suggesting that they may play a role in divalent cation transport. Monovalent cation transporters such as the Nhx1 Na^+ transporter are also members of this group, but are separated by a much greater evolutionary distance (Hanikenne et al., 2005; Maser et al., 2001). The yeast proteins did not align well with representative examples of these transporters (*e.g.*, yeast Nhx1 and Nha1, data not shown). Thus, it appears more likely that the three yeast proteins participate in divalent cation homeostasis. Nevertheless, I could not rule out a role for the novel proteins in monovalent cation transport or pH regulation, and this possibility was

examined later in this work.

3.3 Reverse genetic analysis of CaCA gene function

To find phenotypes that might provide evidence for the function of the three CaCA proteins, I analyzed the effects of altered CaCA gene expression in strains either lacking or overexpressing the three genes. Since I was primarily interested in determining if the novel genes were potential Mg^{2+} transporters, I first examined the effect of overexpressing the genes on the Mg^{2+} content of yeast. The rationale for these experiments was that the overexpression of a Mg^{2+} transporter may alter compartmentalization or uptake of Mg^{2+}, generating a difference in the total Mg^{2+} content of the strain. If the transporter was responsible for sequestration in a storage compartment like the vacuole, overexpression might result in a significant increase in total cellular ion content, as has been observed for other vacuolar cation sequestration systems. For example, overexpression of the vacuolar zinc transporter Zrc1 increased Zn^{2+} accumulation (MacDiarmid et al., 2003). However, Mg^{2+} content might also be reduced by CaCA gene overexpression, for example if the transporter mediated efflux from the cell, via the plasma membrane or secretory pathway. CaCA gene overexpression was achieved by cloning the complete coding sequence and regulatory regions of the genes into a multicopy yeast shuttle vector (see **Chapter 2.7.1**). A WT strain was then transformed with the three overexpression constructs and the original control vector. To maximize the possibility of detecting a change in Mg^{2+} content, I supplied the cells with a range of Mg^{2+} concentrations, from deficient (1 μM) to well in excess of normal requirements (conditions in which Mg^{2+} sequestration would be essential for tolerance).

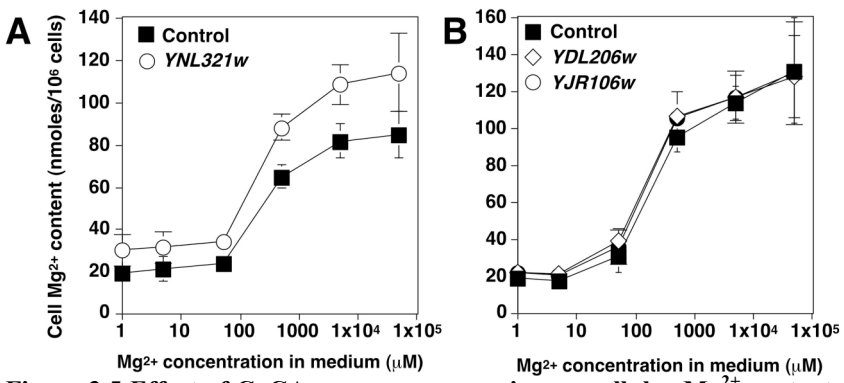

Figure 3.5 Effect of CaCA gene overexpression on cellular Mg^{2+} content. Strains carrying a control or the indicated CaCA gene overexpression vector were grown to log phase in LMM with the indicated Mg^{2+} concentration, and Mg^{2+} content determined using AAS, as described in **Chapter 2**. **A.** Effect of the pFL44YNL overexpression vector (*YNL321w*) vs a control vector (pFL44-S) in DY1457; **B.** Effect of the pFL44YDL (*YDL206w*) and pFL44ECM27 (*YJR106w*) overexpression vectors vs a control (pFL44-S). For **A**, data points display the average of 9 independent replicates; for **B**, data points display the average of three independent replicates. Error bars indicate 95% confidence limits.

The results (**Figure 3.5**) indicated that only one of the three genes, *YNL321w*, caused a significant alteration in cellular Mg^{2+} content: Ynl321w overexpression increased Mg^{2+} content of cells at all concentrations tested, and the difference was highly significant at most concentrations tested (**Figure 3.5A** and data not shown). This increase in Mg^{2+} content suggested that Ynl321w might be involved in the intracellular sequestration of Mg^{2+} in a storage compartment, directing the focus of my subsequent research towards this protein.

3.4 Effect of *YNl321w* overexpression on Ca^{2+} and Na^{+} content

Ynl321w is related to Vcx1, which mediates Ca^{2+} storage in the vacuole, and very weakly related to monovalent cation transporters involved in organelle metal transport. This relationship suggested that Ynl321w might have effects on the homeostasis of other cations in addition to Mg^{2+}. To determine if the effect of *YNL321w* overexpression was specific to Mg^{2+} ions, intracellular concentrations of Ca^{2+} and Na^{+} were determined in a strain overexpressing this gene. As for Mg^{2+}, Ca^{2+} and Na^{+} accumulation was measured after growth of the strains over a range of cation concentrations. As shown in **Figure**

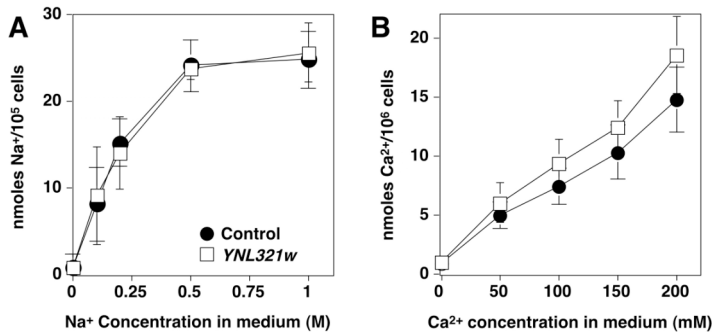

Figure 3.6 Effect of *YNL321w* overexpression on cellular sodium and calcium content. Control and *YNL321w* overexpressing strains (see **Figure 3.5**) were grown in synthetic medium with the indicated concentration of either Na^+ (**A**) or Ca^{2+} (**B**) ions. Ion content of the cells was determined using AAS. For **A**, data points for control or *YNL321w* overexpression indicate the means of 6 or 8 independent experiments respectively. For **B**, data points for control or *YNL321w* overexpression indicate the means of 9 or 12 independent experiments respectively. For all data, error bars indicate 95% confidence limits.

3.6A, overexpression of *YNL321w* had no effect on Na^+ content. There was however a small increase in Ca^{2+} content **(Figure 3.6B)**. Although this increase was not significant at the 95% level, the trend was consistent within the experiment, suggesting that the difference was reproducible. The limitations of the AAS method used may have contributed to the large error observed in these experiments. Despite this uncertainty, the result did hint at a role for *YNL321w* in Ca^{2+} homeostasis: this possibility was examined in more detail later in this work.

3.5 Effect of single CaCA gene deletions on Mg^{2+} accumulation

If the CaCA genes played an important role in Mg^{2+} homeostasis, I expected that eliminating their function would have an effect on the level of Mg^{2+} accumulation by these strains. Accordingly, I tested the effect of deleting each of these genes on Mg^{2+} accumulation (**Figure 3.7**). Deletion mutants in the BY4743 genetic background were obtained from a commercially available collection (Kelly et al., 2001) (**Table 2.1**). I observed no effect of deleting either *YNL321w* (**Figure 3.7A**) or the other two CaCA genes (**Figure 3.7B**) on Mg^{2+} content. Thus, this experiment did not support a significant role for any of these genes in isolation. In particular, since deletion of *YNL321w* did not

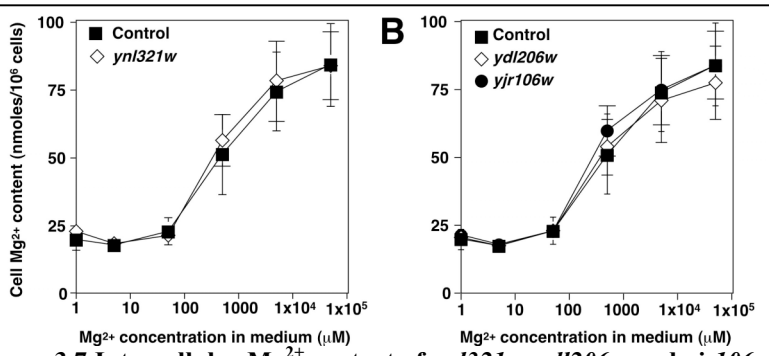

Figure 3.7 Intracellular Mg^{2+} content of *ynl321w, ydl206w* and *yjr106w* deletion mutations. WT (BY4743), YNL321wΔ (**A**), YDL206wΔ, and YJR106wΔ (**B**) strains were grown in LMM with the indicated Mg^{2+} concentrations, and total cellular Mg^{2+} content measured with AAS. Data points are the average of 3 independent experiments, error bars show standard deviation of the mean.

affect either Mg^{2+} tolerance or Mg^{2+} accumulation, I consider it unlikely that this gene is required for intracellular Mg^{2+} storage or efflux in isolation. However, a possibility remained that the three CaCA genes overlapped in function, and that their redundant function masked any effect of their individual deletion.

3.6 Screening for CaCA gene mutant phenotypes

3.6.1 Metal tolerance of single CaCA mutants

Since I observed that the Ynl321w protein was not a major contributor to Mg^{2+} homeostasis, I reasoned that it may be involved in the homeostasis of another cation. Many CaCA proteins have been shown to be required for the removal of various divalent and monovalent ions from the cytosol: this function contributes to the normal regulation of the cytosolic concentration of these cations, and (as a consequence of this) tolerance to excess cations in the environment (for example, Nha1p and Vcx1p, which regulate Na^{+} and Ca^{2+} respectively) (Banuelos et al., 1998; Pozos et al., 1996). If the three novel CaCA proteins were required for homeostasis of cations other than Mg^{2+}, deletion of these genes might be expected to confer altered sensitivity to these cations. To investigate this possibility, I tested the sensitivity of the three CaCA deletion mutants to various metal cations, including Mg^{2+}, Ca^{2+}, Mn^{2+}, Co^{2+}, Ni^{2+}, Zn^{2+}, Na^{+}, and Li^{+} (data not shown).

Wide ranges of cation concentrations were tested, up to levels that inhibited the growth of WT strains (data not shown). In these experiments, I did not observe significant sensitivity of any of the mutants to most of the cations tested, even at very high concentrations (data not shown). However, a slight sensitivity of the *ynl321w* mutant to very high Ca^{2+} (700 mM) was observed (data not shown). Together with our previous observation of increased Ca^{2+} content in strains overexpressing *YNL321w*, this result was further evidence for a role of this protein in Ca^{2+} homeostasis. Again however, I did not observe an effect of any of the mutations on tolerance to high Mg^{2+} concentrations. Very high concentrations of Mg^{2+} ions (>500 mM) inhibited the growth of WT strains, and lower concentrations prevented the growth of mutants lacking V-ATPase activity (data not shown), indicating that an appropriate range of Mg^{2+} concentrations was used to screen for growth phenotypes. Overall, my results indicated that the three CaCA genes were not required for Mg^{2+} tolerance in isolation, and did not reveal a major role in tolerance to any other metal ions tested.

3.6.2 Metal Tolerance of double and triple CaCA mutants

As discussed above, it is possible that the CaCA proteins overlap in function, and that the elimination of each gene in isolation was not sufficient to produce an effect on yeast physiology. For this reason, I decided to construct a set of mutant strains lacking two or all three of the novel CaCA genes, and to screen these strains for new cation tolerance phenotypes. Deletions of had already been constructed as part of the yeast gene deletion collection (Winzeler et al., 1999). To facilitate this process, I wanted to transfer *ynl321w*, *ydl206w* and *yjr106w* knockout alleles marked with KAN^R into the more easily manipulated W303 genetic background. For this reason, I designed PCR primers to

amplify the sequence flanking the deletions, together with the inserted *KAN*^{R} gene, from genomic DNA of the deletion mutants. These PCR products were then used to transform the W303-based DY1456 and DY1457 strains with selection for Geneticin resistance, separately deleting the three genes in these strains. In order to more easily follow the *ynl321w* marker in crosses, a *ynl321w::LEU2* allele was also constructed and introduced into DY1457. The resulting *MATa* single mutant strain (AJF02) was then crossed with the isogenic haploid mutants AJF03 (*ydl206w::KAN*^{R}), and AJF04 (*yjr106w::KAN*^{R}) to obtain double mutants in each case. To obtain the triple mutant strain, I then crossed a *ynl321w::LEU2 ydl206w::KAN*^{R} double mutant (AJF05) with a *ynl321w::LEU2 yjr106w::KAN*^{R} double mutant (AJF06). Spore clones were then screened for specific knockout alleles by using PCR with the oligonucleotides YDL206wF and YDL206wR to detect *ydl206w::KAN*^{R}, or the primers ECM27-5 and ECM27-3 to detect *yjr106w::KAN*^{R}.

The complete set of 7 mutants and an isogenic WT strain was then screened for altered sensitivity to metal cations (Mg^{2+}, Ca^{2+}, Mn^{2+}, Co^{2+}, Ni^{2+}, Zn^{2+}, Na^{+}, and Li^{+}). Tolerance was determined by spot assays using SD medium plates. Again, the only phenotype observed was a slight sensitivity of strains carrying the *ynl321w::LEU2* mutation to 700 mM $CaCl_2$ (data not shown). There was no noticeable increase in Ca^{2+} sensitivity of the double and triple mutants over *ynl321w* alone (data not shown). I concluded that despite their membership of the CaCA family, only one of the three CaCA genes had an effect on metal homeostasis in isolation, and that there was no obvious overlap in function between these three genes. Since I could not identify a reproducible effect of *ydl206w* or *yjr106w* mutation, for the remainder of this work, I focused on trying to understand the function of the Ynl321w protein in cation homeostasis.

3.6.3 Genetic interaction of YNL321w, VCX1 *and* PMC1.

3.6.3.1 Construction of double and triple mutants

Two lines of evidence (the Ca^{2+} content of overexpressing strains, and the Ca^{2+} sensitivity of the deletion mutant) suggested that Ynl321w might be required for calcium homeostasis. To further investigate this possibility, I decided to examine the effect of combining the *ynl321w* mutation with deletions of other genes required for Ca^{2+} homeostasis. The rationale behind this experiment was that in the absence of other mechanisms of Ca^{2+} homeostasis, the effect of the *ynl321w* mutation may be enhanced: double or triple mutant strains may be more sensitive to Ca^{2+}, and may exhibit a difference in Ca^{2+} content, as a consequence of a stronger disruption in homeostasis. Accordingly, I constructed a set of strains combining *ynl321w* with deletion mutations of two known vacuolar calcium transporters, the CAX protein Vcx1p and the P-type ATPase Pmc1p. Vcx1 is a CaCA family member, and Pmc1p is a primary Ca^{2+} pump of the P-type ATPase family (Cunningham and Fink, 1994). Both proteins are believed to participate in the storage of excess Ca^{2+} in the vacuole: loss of both proteins caused a reduction in Ca^{2+} tolerance and intracellular calcium content (Cunningham and Fink, 1996). I decided to examine the interaction of these two genes with *YNL321w* for two reasons: first, Vcx1 is related to Ynl321w, suggesting that these proteins overlap in function; and second, the *vcx1* and *pmc1* mutant phenotypes of altered calcium sensitivity and cellular calcium content are easily assayed. Mutant strains were generated by mating the W303-derived strain YDB254 (*vcx1::URA3 pmc1::TRP1*) (Miseta et al., 1999) with the AJF01 *ynl321w::KAN*^{R} single mutant. Spore clones from the cross were replica-plated to marker test plates (YPD+Geneticin, SC-uracil and SC-trptophan) to determine

which mutations were present. This analysis indicated that all combinations of the three mutations were viable on normal YPD and SD medium, and showed no obvious growth phenotypes in standard media (data not shown). Two sets of eight strains carrying all possible combinations of the three mutations were isolated for study.

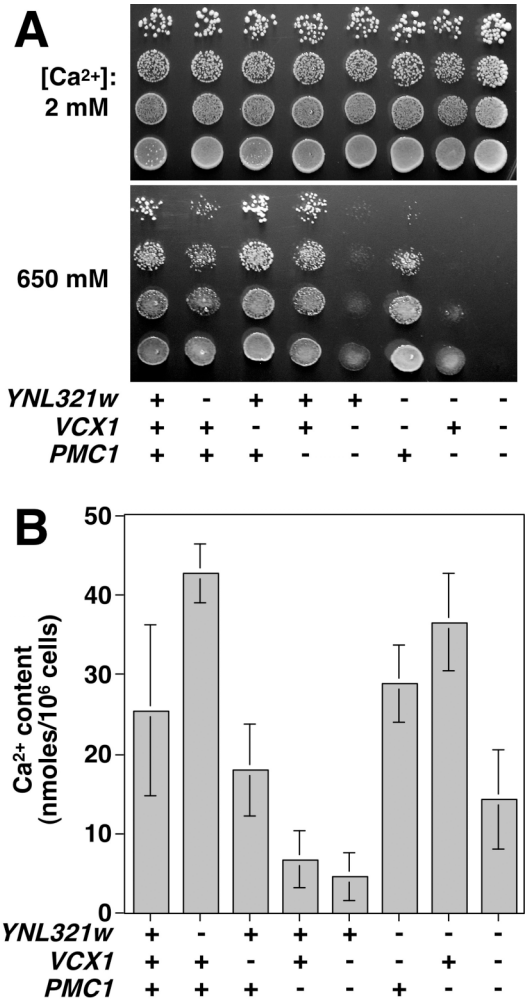

Figure 3.8 Interaction of *ynl321w*, *vcx1* and *pmc1* mutations. A: Ca^{2+} sensitivity of *pmc1*, *vcx1* and *ynl321w* mutants (strains AJF08-AJF15). Serial dilutions of cells (10-fold, bottom-top) were applied to low-sulfate synthetic medium containing the indicated Ca^{2+} concentration. Plates were incubated for three days at 30°C. **B:** Ca^{2+} content of mutants (strains AJF08-AJF15). Strains of the indicated genotypes were grown for 20 hours in low-sulfate synthetic medium containing 400 mM Ca^{2+}. Total cellular Ca^{2+} content was measured with AAS. Error bars represent 95% confidence limits (mean of four independent experiments).

3.6.3.2 Ca^{2+}-related phenotypes of ynl321w, vcx1 *and* pmc1 *mutants*

I compared the Ca^{2+} sensitivity of two sets of the seven possible mutant strains and the WT. As previously observed, *ynl321w* mutants were slightly sensitive to Ca^{2+} ions (**Figure 3.8A**). Despite their well-defined importance for Ca^{2+} homeostasis, inactivation of the other two genes had no reproducible effect on Ca^{2+} tolerance in isolation. However, as previously reported, (Marchi et al., 1999) combining these two mutations strongly reduced tolerance. In addition, combining *vcx1* or *pmc1* mutations with the *ynl321w* deletion caused an increase in Ca^{2+} sensitivity over *ynl321w* alone, with the *pmc1* mutation showing the strongest

effect. These findings are consistent with a role for Ynl321w in removal of excess Ca^{2+} from the cytosol. The observation that Ynl321w appeared to have a stronger effect on tolerance in isolation than either of the other two previously characterized vacuolar transporters suggests this novel protein plays an important role in Ca^{2+} homeostasis.

I then examined the effect of the three mutations on intracellular Ca^{2+} content in the same set of deletion mutants. The strains were grown to log phase in medium supplemented with 400 mM $CaCl_2$, a concentration that did not substantially inhibit the growth of the strains (data not shown). The results are shown in **Figure 3.8B.** Previous studies have shown that *vcx1* and *pmc1* mutations independently reduce intracellular calcium accumulation, and my results agree with these reports: although the difference between *vcx1* and WT strains was not significant, the *pmc1* mutation significantly reduced accumulation in isolation, and the *vcx1 pmc1* double accumulated less than either single mutant, consistent with the overlapping function of these two transporters. Strikingly however, the *ynl321w* mutation was associated with a significant increase in cellular Ca^{2+} content, the opposite effect to that of the *vcx1* and *pmc1* mutations. This effect of the *ynl321w* mutation was seen in all combinations of the mutations that we tested, including the triple mutant strain.

3.7 Preliminary model for Ynl321w function

These results strongly suggest that the Ynl321wp is required for Ca^{2+} homeostasis, but are not consistent with a role in Ca^{2+} sequestration in the vacuole. In contrast, the results strongly suggest that Ynl321w is required for the efflux of Ca^{2+} from the cell. If Ynl321w is directly responsible for Ca^{2+} transport, this model predicts that Ynl321w is located on the plasma membrane and mediates efflux directly across the

plasma membrane, or that it is located in the secretory pathway and loads Ca^{2+} into the lumen of secretory organelles. From the latter location, Ca^{2+} ions could be released to the outside of the cell via the normal process of vesicle transport and exocytosis.

3.8 Determination of Ynl321w subcellular location

3.8.1 Detection of Ynl321w using epifluorescence microscopy

To test the above predictions about Ynl321w location, I constructed a version of Ynl321w fused to three copies of the *HA* (Influenza hemagglutinin) epitope at the C-terminus (**Chapter 2.7.1**), which was inserted in both single copy and multicopy shuttle vectors. Upon construction of these vectors, I utilized the previously described phenotype associated with Ynl321w overexpression (higher Mg accumulation) to determine if the modified version of Ynl321w retained function. The modified Ynl321w protein was expressed in a wild-type yeast strain, and the resulting strain grown over a range of Mg^{2+} concentrations, as previously described (**Figure 3.2**). As positive and negative controls, I included a strain carrying an empty control vector, and a strain overexpressing the untagged Ynl321w. The results (**Figure 3.9A**) indicate that both the tagged and untagged proteins conferred the same phenotype of increased Mg^{2+} accumulation, indicating that the tagged protein was functional.

To determine the subcellular location of YNL321w-HA, I performed a series of immunofluorescence experiments to detect the HA tag. A diploid strain (DY1514) was transformed with pFL44YNLHA or a control (empty) vector. Using whole cells, the epitope-tagged protein was labeled with a fluorescent dye by using an indirect immunofluorescence protocol (see **Chapter 2.12.5**). The labeled cells were examined using epifluorescence microscopy. In most cells of the cultures expressing the tagged

protein, I did not detect Ynl321w-HA: however, a small minority of cells (about 1/100) stained brightly. In these cells, the signal appeared to outline the vacuole membrane, as revealed by Nomarski differential intereference contrast optics (DIC), but additional signal was also present in a compartment adjacent to the vacuole, which based on its location and morphology is most likely the ER/nuclear membrane. No corresponding signal was observed in the negative control cells. Although these results suggest a vacuolar and/or ER location, the absence of signal in most cells suggested that the brightly staining cells did not provide definitive evidence for the normal location of Ynl321w.

To ensure that the immunofluorescence technique was performing adequately, I also included a positive control in these experiments, by staining untagged cells with an antibody to the vacuolar membrane protein Vma1p. Vma1p was successfully detected in most cells (**Figure 3.9B**), indicating that there was no fundamental flaw in the protocol. I concluded that even though the Ynl321w-HA protein was expressed from a multicopy vector, it was possible that its expression was too low to be detectable in most cells.

As an alternative approach towards the detection of Ynl321w by fluorescence microscopy, I constructed a version of Ynl321w C-terminally tagged with the citrine variant of the yellow fluorescent protein (YFP), which has an excellent signal/noise ratio when expressed in yeast (Sheff and Thorn, 2004)**.** Diploid yeast strains that were transformed with the high copy 211YNL44 plasmid (and consequently overexpressed the fusion protein) were examined using epifluorescence microscopy. As shown in **Figure 3.9C**, control cells that did not express the fusion protein showed a low level of diffuse background autofluorescence, which was detectable using the sensitive equipment used.

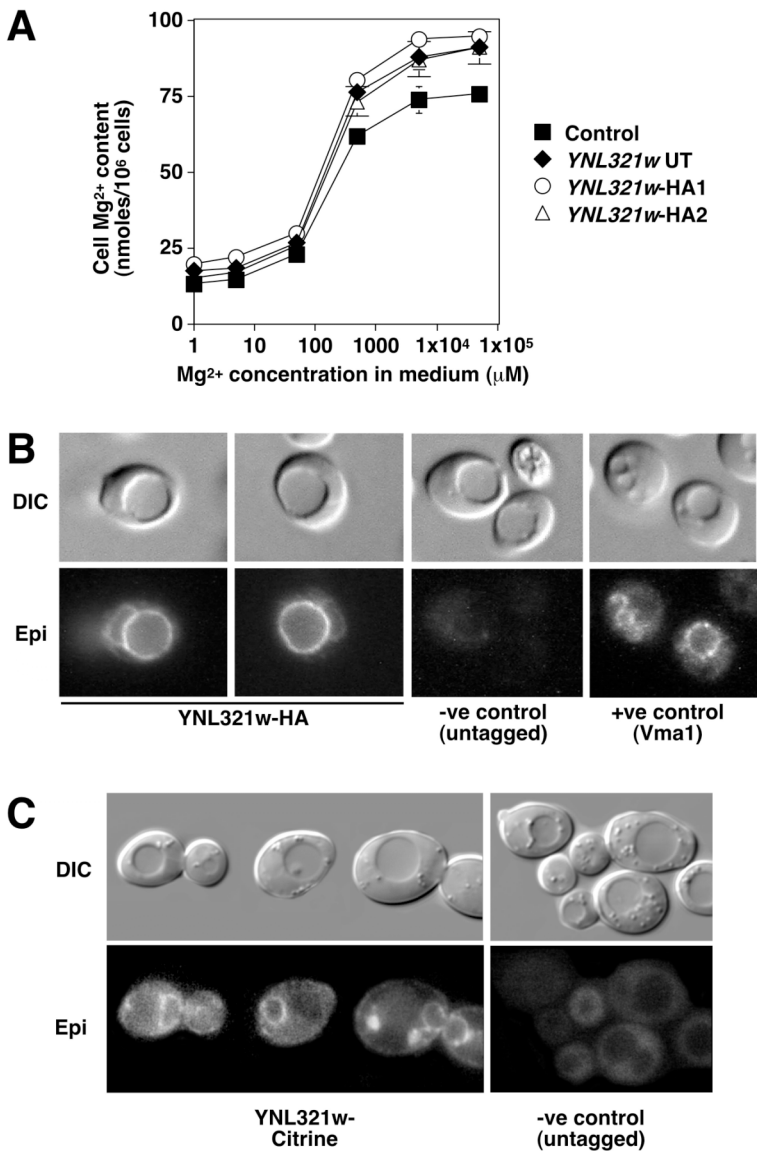

Figure 3.9 Localization of Ynl321w by epifluorescence microscopy. **A**. Mg^{2+} content of DY1457 cells transformed with pFL44YNL (Ynl321w UT), pFL44YNLHA (*YNL321w-HA,* two replicate strains) or a control vector (pFL44-S) were grown in synthetic medium containing the indicated concentration of Mg. Error bars represent the standard deviation of two independent experiments. **B**. Immunofluorescence microscopy of DY1457 cells expressing YNL321w-HA (pFL44YNLHA plasmid), negative control cells transformed with pFL44-S, and negative control cells stained with antibodies to the vacuolar membrane protein Vma1. These cells are examples of the small number of cells that stained brightly: unstained cells, which made up the bulk of the preparation, are not shown. **C**. A *YNL321w*-citrine fusion protein was overexpressed in diploid yeast (BY4743) transformed with 211YNL44. Cells representative of typical observations are shown. Negative control cells (untagged) were transformed with pFL44YNL.

Cells expressing YFP-Ynl321w however showed a brighter signal, with a pattern characteristic of an ER membrane protein. Signal was observed as a ring structure surrounding an organelle located at one pole of the diploid cell, and also occasionally as thread-like structures below the cell periphery. Dividing cells showed signal at the bud neck, again indicating an ER/nuclear location. Unlike the results observed with immunofluorescence, almost all cells examined showed a similar pattern of fluorescence.

3.8.2 Cell fractionation

3.8.2.1 Detection of epitope-tagged Ynl321w by immunoblotting

To examine Ynl321w location using an independent method, I wanted to perform cell fractionation experiments. Prior to these experiments, I performed Western blotting analysis to determine if the expression of the epitope-tagged Ynl321w protein (Ynl321w-HA) could be detected via this method. When Ynl321w-HA was expressed from a single-copy vector, no expression was detected on Western blots of total protein extracts. However, when Ynl321w-HA was overexpressed from a 2μ vector, the protein was detectable (data not shown). The protein was seen as two bands: one had an apparent molecular weight of approximately 100 kDa, which was similar to its predicted molecular weight of 102.5 kDa. The other had a substantially lower mobility, and was too large to be estimated due to the resolution limit of the PAGE system used. The low-mobility band may represent a portion of Ynl321w crosslinked to itself or other proteins, via a bond resistant to the standard concentrations of reducing agent and detergent used in SDS-PAGE. This suggestion is supported by a reduction in the abundance of this band when the SDS concentration in the gel-loading buffer was increased (data not shown). These observations indicated that although Ynl321w-HA needed to be overexpressed, the protein could be detected via Western blotting, which enabled me to perform cell fractionation experiments to determine its location in yeast.

3.8.2.2 Sucrose gradient cell fractionation

To separate yeast organelles based on their buoyant density, I used a sucrose gradient cell fractionation technique, as described in **Chapter 2.12.4**. A strain overexpressing Ynl321w-HA was grown in synthetic medium, and an organelle fraction

was obtained via cell lysis and differential centrifugation. The organelles were loaded on a 20% to 60% sucrose gradient and subjected to ultracentrifugation. One ml fractions were collected drip-wise after puncturing the bottom of the tube. Samples of each gradient fraction, a sample of the original organelle suspension, and a negative control (total protein extracted from a strain expressing untagged *YNL321w*) were separated by SDS-PAGE and blotted to nitrocellulose membranes. To determine which organelles co-fractionated with the Ynl321w-HA protein, I probed the blots with primary antibodies for known organelle-associated marker proteins, and detected Ynl321w-HA using an anti-HA antibody.

The results of a typical experiment (**Figure 3.10A**) are shown. Effective separation of the different organelles was obtained, and the lighter organelles (the

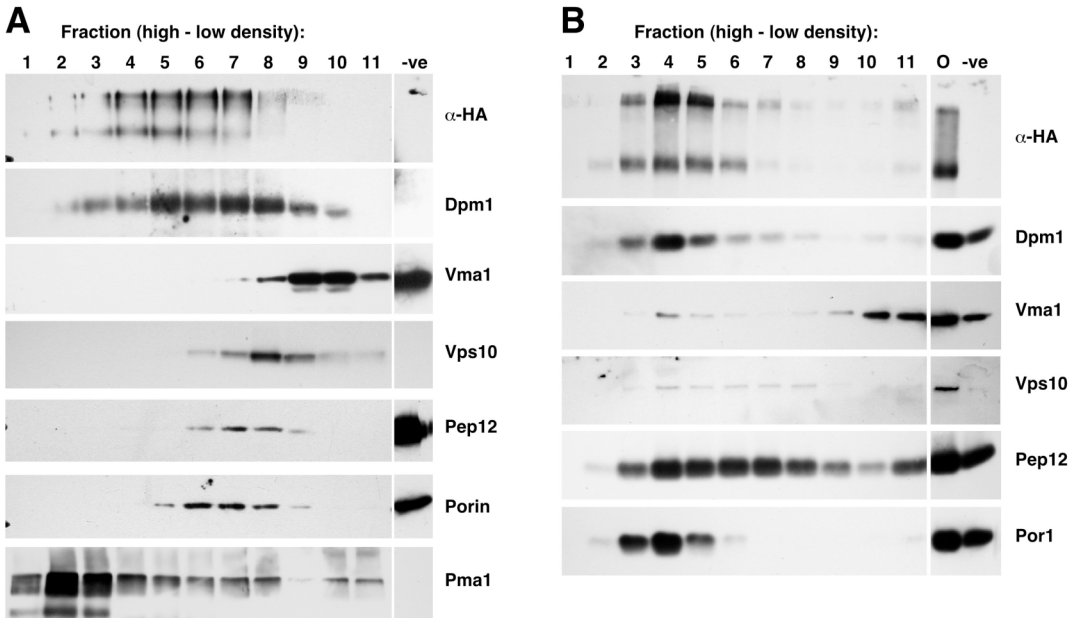

Figure 3.10 Localization of Ynl321w-HA by cell fractionation. Organelles isolated from DY1457/pFL44YNLHA were separated by sucrose gradient fractionation in buffer without (**A**) or with (**B**) Mg^{2+} and protein content analyzed with Western blotting. Primary antibodies for marker proteins were α–HA (Ynl321w-HA), α-Vma1 (vacuole), α-Dpm1 (ER), α-Pep12 (early endosome), α-Vps10 (Golgi), α-Vma1 (plasma membrane) and α-Por1 (mitochondria). Control samples included the unfractionated organelle mixture (lane O, in B) and total protein extracted from DY1457/pFL44YNL (untagged -ve control, in A and B).

vacuole and prevacuolar compartment) were located at the top of the gradient as expected. The Ynl321w-HA protein was again detected as two bands, with the lower band corresponding to the expected molecular weight of the protein. Both bands were absent from protein extracted from the control (untagged) strain. The pattern of distribution of Ynl321w-HA in the fractions was most similar to Dpm1 (an ER protein) and Por1 (a mitochondrial protein). In particular, the epitope-tagged protein was not observed in the light fractions (10 and 11), as would be expected if this protein accumulated in the vacuole membrane. In addition, there was very little overlap between the fractions containing Ynl321w and those containing the plasma membrane marker Pma1 and the Golgi marker Vps10p. Ynl321w was found in fraction 7, where it co-localized with a large portion of the pre-vacuolar marker Pep12: however, in general these markers were widely separated in the gradient. Because of the overlap of the Dpm1 and Por1 markers, I could not discriminate between ER and mitochondrial locations based on this experiment. Other fractionation experiments that I performed using the same technique gave similar results for these markers: the similar density of the two organelles makes it very difficult to separate them using a cell fractionation technique based on differences in buoyant density.

One method suggested to identify ER-localized proteins is to perform cell fractionation in the presence and absence of Mg^{2+} ions (Roberg et al., 1997). The rationale behind this approach is that the removal of Mg^{2+} from the organelle suspensions results in the dissociation of ribosomes from the rough ER, reducing the buoyant density of these membranes. Thus, proteins associated with the ER should shift position in Mg^{2+}-containing vs. Mg^{2+}-free density gradients, while other organelles will retain their

original density and position. However, when I performed experiments to compare Mg^{2+}-free and Mg^{2+}-containing gradients, this technique did not provide any addition information: a shift in the density of the ER compartment was observed in the presence of Mg^{2+}, but the density of some other organelles (including the mitochondria) was also shifted. Thus, the ER and mitochondrial compartments were still co-localized in the presence of Mg^{2+} ions (**Figure 3.10B**). The several published reports of the use of this technique to demonstrate an "ER" location did not consider the possibility of a mitochondrial location for the protein of interest, because in their experiments the distribution of mitochondria in the gradients was not determined (Roberg et al., 1997).

In summary, these results are consistent with an ER location for Ynl321w, which may explain the effect of the *ynl321w* mutation on intracellular Ca^{2+} content: a reduction of the Ca^{2+} content of the ER might result in reduced Ca^{2+} efflux and increased Ca^{2+} content, as has been observed for other mutations that block the supply of divalent cations to the secretory pathway (e.g. *pmr1*, see **Chapter 1.6**). Thus, the majority of this evidence supports a model whereby Ynl321w is required for the removal of Ca^{2+} from the cell via the secretory pathway, in a similar manner to its closest analog in yeast, the Pmr1 protein (Vashist et al., 2002). To reflect this conclusion, Ynl321w was assigned the name Ecx1 (for ER calcium exchanger).

I considered the possibility that the observed location of Ecx1 was a consequence of the overexpression of this protein, and did not reflect its predominant location when expressed at a normal level. Due to the low expression of the protein from the native promoter, this issue may be very difficult to resolve: however, the relatively low expression observed even with a high copy vector may also indicate that overexpression

artifacts are unlikely in this particular case. Although I have not ruled out the possibility of obtaining further localization data (see **Chapter 4.4**), obtaining independent phenotypic evidence for a role of Ecx1p in ER function may be the best strategy to confirm a function of Ecx1p in this compartment.

3.9 pH sensitivity of *ecx1* mutants

CaCA proteins are involved in transporting cations against an electrochemical gradient in exchange for protons entering the cytosol, and this proton transport would be expected to lower the cytosolic pH to some degree. Thus, cation exchangers may also play a role in the regulation of cytosolic or organelle pH: their roles in cation transport may even be of secondary importance to this role. This concept may be one way to explain the apparent redundancy of ER Ca^{2+} transporters that I have identified. Previous work has identified another transporter, Cod1, that supplies Ca^{2+} to the ER compartment, and the Pmr1 protein may also contribute to this supply (Cronin et al., 2002). As an exchanger, Ecx1 could play a role in ER pH homeostasis, a function that could not be performed by a primary ATPase pump such as Cod1p or Pmr1p.

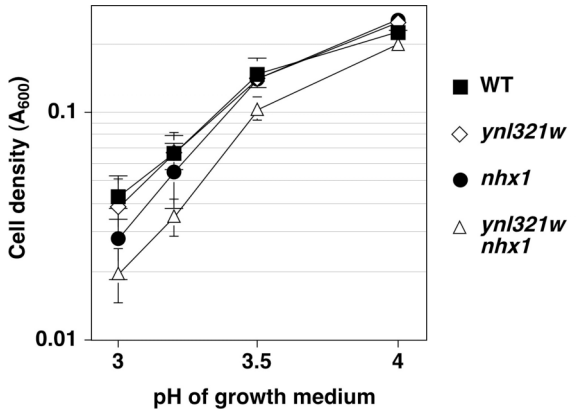

Figure 3.11 pH tolerance of *ecx1* (*ynl321w*) and *nhx1* mutant strains. Low pH phosphate-buffered medium adjusted to the indicated pH was inoculated with cells of the indicated genotypes (DY1457, WX1, AJF02, and AJF16) to give an initial cell density of 0.01. After 16 hrs growth, A_{600} was determined. Data points indicate the mean of three experiments: error bars represent 95% confidence limits.

The yeast proteins Nhx1p and Nha1p appear to fall into this category: as discussed in **Chapter 1**, these proteins resemble mammalian Na^+/H^+ exchangers, but they appear to play a

role in the regulation of organelle and cytosolic pH. Recently, Nhx1p was shown to be an endosomal Na^+/H^+ exchanger, involved in the intracellular sequestration of Na^+ and the regulation of luminal pH in the secretory pathway. Consistent with this function, the *nhx1* mutation was reported to confer sensitivity to low pH (Brett et al., 2005), and was also associated with the secretion of the vacuolar protein carboxypeptidase Y (CpY), indicating a disruption of normal protein targeting mechanisms. This effect could be due to perturbed pH homeostasis within the secretory pathway, or a disruption in the supply of essential Na^+ ions to the lumen of the compartment defined by Nhx1p (the late endosome or PVC).

To investigate if Ecx1p also plays a role in the regulation of cytosolic or organelle pH, I constructed a set of *ecx1*, *nhx1* and double mutant strains, then tested sensitivity to low pH (3-4) by growth in liquid medium, prepared using a method suitable for expression of the pH sensitivity of *nhx1* single mutant strains (Brett et al., 2005). In my experiments, both single mutants showed only a mild pH sensitivity, which was not significantly different from the WT (**Figure 3.11**). However, the double mutant showed a significant increase in sensitivity from WT at the 95% confidence level. These results were not consistent with previous reports of the effect of the *nhx1* mutation, in which this mutation had a much stronger effect in isolation (Brett et al., 2005). I used the exact conditions and media described in this work, but despite several experiments, I could not repeat the published observations. Other workers have also encountered difficulty reproducing this phenotype of *nhx1* (K. Hirshi, personal communication). Nevertheless, the observation that an effect of the *nhx1* mutation on tolerance was observed in combination with *ecx1* suggests that both proteins do have a role to play in pH

homeostasis. The implications of this observation will be discussed further in **Chapter 4.**

3.10 Summary and discussion

The purpose of this work was to identify candidate genes encoding putative active transport systems for magnesium ions, and to determine their role (if any) in magnesium homeostasis. I identified several genes as putative transporters, including *Per1* and *YNL321w*. These proteins were chosen for study on the basis of such criteria as their possession of multiple putative transmembrane domains, previous and novel observations of mutant phenotypes suggesting a function in magnesium homeostasis, or membership in a family of transporters known to play diverse roles in ion homeostasis. In general however, my analysis of these genes did not provide strong evidence for a role of any of these proteins in Mg homeostasis. However, I did identify a novel and important role for one protein, Ynl321w, in calcium homeostasis. My findings are summarized below.

3.10.1 The Per1 protein

Per1 was originally identified in a screen for genes that altered ion homeostasis: the *per1* mutation suppressed the manganese-sensitive phenotype of a mutant strain (Paidhungat and Garrett, 1998). These studies also revealed an interesting phenotype of *per1* mutants, a relatively specific sensitivity to high magnesium concentrations. A recent large-scale study of protein location revealed that Per1 was associated with the ER membrane (Fujita et al., 2006), suggesting the involvement of Per1 in ER function. Additional evidence for this view came from studies showing that *per1* mutation showed a synthetic interaction with the *ire1* and *hac1* mutations, which inactivate genes required for the induction of the unfolded protein response (UPR) (Ng et al., 2000). The UPR is induced by the accumulation of unfolded proteins in the ER lumen, which occurs as a

result of defective protein processing (Rutkowski and Kaufman, 2004). These observations suggest *per1* mutants have a defect in ER function, and must induce the UPR in order to compensate for this defect.

Because the above observations implicated Per1 in ER function and Mg^{2+} homeostasis, I hypothesized that Per1 might play a role in magnesium transport into this compartment. By this model, the loss of Per1 function would result in a higher cytosolic magnesium concentration (due to reduced efflux into the secretory pathway), possibly resulting in magnesium sensitivity. In addition, the loss of Per1 function might deprive the ER of this essential cation, resulting in an increased level of unfolded proteins, and the consequent induction of the UPR.

The above model predicted that overexpression and mutation of *PER1* would result in measurable changes in various parameters of Mg^{2+} homeostasis, including Mg^{2+} accumulation, ability to grow in deficient conditions, and Mg^{2+} sensitivity under different media conditions. For example, if the primary role of Per1 was to supply Mg^{2+} to the ER, I expected that the overexpression of this protein might result in a reduction in cellular Mg^{2+} accumulation, just as the effect of ER and Golgi calcium transporters is to reduce cellular calcium accumulation (as a consequence of efflux via the secretory pathway). Conversely, the inactivation of Per1 might result in higher Mg^{2+} accumulation by the mutant, as Mg^{2+} that might normally be lost from the cell is instead sequestered in intracellular compartments.

However, my results did not support this model. When the Per1 mutant was grown over a range of Mg^{2+} concentrations, this strain showed a large and significant decrease in Mg^{2+} content. This observation may indicate a potential role for Per1 in Mg^{2+}

sequestration into an internal compartment within the cell. However, if this alternative model was correct, I expected that the overexpression of Per1 would increase cellular Mg^{2+} content: my studies show this is not the case, as overexpression had no significant effect. Thus it appears that Per1 does not show the phenotypic effects expected of a protein that sequesters Mg^{2+} in the ER (or vacuole) compartment.

During this work I learned from another research group that the *per1* mutation reduced the accumulation of several other ions in addition to Mg^{2+} (personal communication, R. Schweyen). This effect suggests that Per1p might be required for some general aspect of ion homeostasis, for example by contributing to the integrity of the cell membrane. Such a function would fit with the location of Per1 in the ER, which is a site of lipid biosynthesis. Another essential process that may be defective in *per1* mutants is the addition of glycophosphatidylinositol (GPI) anchors to yeast proteins during transit through the ER. GPI is a complex glycolipid that acts as a membrane anchor point for many cell-surface glycoproteins (Ferguson, 1999; Ikezawa, 2002). Consistent with this observation, *per1* mutants showed defective processing of the GPI-linked cell wall protein Gas1, but did not show altered processing of Cpy, which is glycosylated in the ER but not GPI-anchored (Ng et al., 2000). Finally, recently published work confirmed a defect in GPI anchor synthesis in *per1*, and suggested that Per1 represents the GPI-phospholipase A_2 enzyme of the GPI-anchor remodeling pathway (Fujita et al., 2006), as this step in the synthesis pathway was blocked in a *per1* mutant.

Given these observations supporting a biosynthetic role for Per1p in lipid metabolism and protein processing, it is unclear why the *per1* mutant displays relatively Mg^{2+}-specific phenotypes, such as sensitivity to this cation. One possible explanation is

that these phenotypes reflect a toxic effect of Mg when combined with a general defect in cell integrity or cell wall strength. GPI anchoring of proteins is thought to enable the delivery of proteins to their final sites in the cell wall, by ensuring their temporary tight association with the surface of the plasma membrane. Cells lacking important GPI-linked cell wall proteins (e.g. Gas1) are hypersensitive to agents that disrupt the cell wall, such as calcofluor white (Ram et al., 1995). *per1* mutants also show a cell wall defect and consequent calcofluor sensitivity (Fujita et al., 2006). If high concentrations of Mg had the effect of somehow disrupting the structure of the cell wall, or preventing certain biochemical reactions from occurring within it, *per1* mutants might show a Mg^{2+} sensitivity as a consequence of their existing defect in cell wall function. This model implies that Mg^{2+} has some special properties not shared by other divalent cations that do not affect the growth of *per1* (or other cell wall mutants), but what these properties might be is unclear.

3.10.2 Putative cation transporters of the CaCA superfamily

The CaCA superfamily of proteins includes transporters with a range of substrates, including Ca^{2+}, Mn^{2+}, Cd^{2+}, and various monovalent cations. One member of this family from *Arabidopsis* (AtMHX1) has previously been implicated in Mg^{2+} transport, although the evidence presented to support this function was very inconclusive. However, given this diversity of substrates and functions for CaCA members, it seemed possible that uncharacterized members of this superfamily could potentially mediate active transport of Mg^{2+} ions. In addition, studies of Mg^{2+} transport by the yeast endosomal vesicles have shown that this cation is accumulated in the vacuole via a Mg^{2+}/H^{+} exchange mechanism (Borrelly et al., 2001), which is consistent with the

involvement of a member of the CaCA family. Thus, using a candidate gene approach to this question was an appropriate strategy to identify this transport system.

I was however, unsuccessful at identifying a CaCA-family Mg^{2+} transport system in yeast, as my results did not provide evidence for a large effect on Mg^{2+} homeostasis of deleting any of the three genes examined. There was no effect of the deletions on Mg^{2+} sensitivity, either alone or when combined. Thus, the three genes do not appear to have any redundant function in Mg^{2+} homeostasis. However, it is still possible that one of the three genes is redundant with some other yeast transport system.

When I looked directly at another measure of Mg^{2+} homeostasis, Mg^{2+} accumulation by cells, I also did not see any major effects of the three CaCA genes. Only the overexpression of Ynl321w had any significant effect on Mg^{2+} accumulation, and this effect was relatively small and highly variable: many replications of the experiments were required to be sure that it was statistically significant. In contrast, deletion of *YNL321w* did not affect Mg^{2+} accumulation, even at high Mg^{2+} concentrations where vacuolar storage should be most obvious. Thus, this evidence does not support a major role for Ynl321w in Mg^{2+} homeostasis.

Since my work did not provide strong evidence for Ynl321w function in Mg^{2+} homeostasis, I looked for evidence for other Ynl321w functions. The *ynl321w* mutant showed a weak calcium-sensitive phenotype, and overexpression of this gene gave a slight (although not significant) increase in calcium accumulation. These observations, and its membership with Vcx1 of the CAX subgroup of the CaCA superfamily, motivated me to search for a possible role of Ynl321w in calcium homeostasis. I reasoned that because of the redundancy of calcium homeostasis mechanisms in yeast, combining the

ynl321w mutation with mutations in other known Ca^{2+} transporters might amplify the effect of this gene on simple parameters of calcium homeostasis, such as tolerance and accumulation. These experiments did in fact provide evidence for a role of Ynl321w in calcium homeostasis. Combining *ynl321w* with mutations inactivating the vacuolar calcium transporters Vcx1p and Pmc1p accentuated the calcium sensitive phenotype, consistent with all three of these proteins contributing to the removal of calcium from the cytosol. In particular, combining *ynl321w* with the *pmc1* mutation, which inactivates the major primary ATPase pump in the vacuole, gave rise to a strong synthetic sensitivity phenotype. The significance of this effect is made clear when comparing the effect of combining the effect of the most well characterized calcium exchanger in yeast, Vcx1, with the effect of Ynl321w: combining the *vcx1* and *pmc1* mutations reduced calcium tolerance to approximately the same level as combining the *ynl321w* and *pmc1* mutations. This result indicates that Ynl321w is as important to calcium homeostasis as Vcx1: given the large number of genetic studies performed on yeast calcium transport, this was a very surprising result. Combining mutations of all three genes led to a very strong calcium sensitivity phenotype, completely preventing growth on medium with 600 mM calcium (the lowest concentration tested, data not shown). Thus, it appears that Ynl321w plays a relatively important role in calcium homeostasis.

3.10.3 Model for Ynl321w function

The apparently similar effect of *ynl321w* and *vcx1* mutations on tolerance led me to compare their effects on calcium accumulation: surprisingly, I found that in contrast to *vcx1*, the *ynl321w* mutation was associated with higher calcium accumulation in cells grown in a medium with a high calcium concentration (400 mM). This finding indicates

that Ynl321w and Vcx1 proteins perform different functions in the cell, and that Ynl321w is unlikely to participate in calcium sequestration in the vacuole. In contrast, this protein may act to efflux calcium from the cytosol to the outside of the cell. Efflux systems located in the plasma membrane (the mammalian Na^+/Ca^{2+} exchangers like Ncx1) or secretory pathway (*e.g*. the yeast Pmr1 protein) are known to perform a similar function. The ER location determined for Ynl321w is consistent with a role in the efflux of Ca^{2+} ions into the lumen of the ER compartment (leading to its eventual release from the cell via exocytosis). This location might also explain the synthetic calcium sensitivity phenotype of mutations in the three transporters studied. If all three proteins contribute to the depletion of cytosolic calcium by sequestration in the vacuole or the secretory pathway, eliminating all three would be predicted to significantly increase the cytosolic Ca^{2+} concentration and consequently, enhance calcium toxicity.

In summary, I propose that Ynl321w represents a novel and important calcium/proton exchanger that is most likely located in the secretory pathway, where it serves to efflux excess calcium from the yeast cell. The specific physiological role of Ynl321w is currently unclear: for example, it may primarily play a role in maintaining the cytosolic calcium concentration at an ideal level, or it may function to deliver calcium to an internal compartment to support the functions of enzymes within that space. This model is useful because it allows us to make many testable predictions, providing ideas for many different experiments. Some of these predictions and experiments will be discussed in more detail in **Chapter4**.

Chapter 4 Conclusions

4.1 Strategy for identification of a Mg^{2+}/H^+ exchanger

The goal of my experiments was to identify a novel a Mg^{2+}/H^+ exchanger in yeast. This goal was pursued using a candidate gene approach, rather than a genetic screen: several uncharacterized genes were selected for analysis, based on a variety of criteria. These criteria were: a) genes with previously described mutant phenotypes suggesting a role in Mg^{2+} homeostasis (e.g. Mg^{2+} sensitivity), b) genes that encoded apparent membrane proteins (possessing multiple hydrophobic regions with characteristics of transmembrane domains), and c) genes that encoded proteins related to known divalent cation transporters.

The first candidate identified, *PER1*, was selected because the *per1* mutation was previously described to specifically reduce Mg^{2+} tolerance (Paidhungat and Garrett, 1998), and there was good evidence that Per1 was an integral membrane protein (Paidhungat and Garrett, 1998). However, during this work, a different research group identified Per1 as an ER-localized enzyme involved in the processing of GPI-anchors prior to their addition to proteins in the ER (Fujita et al., 2006). The *per1* mutation had a variety of phenotypes consistent with this role, including inducing a dependence on the function of the unfolded protein response (UPR) (Fujita et al., 2006). Thus it appears that Mg^{2+} sensitivity can arise as a consequence of a variety of physiological defects, and not simply a consequence of altered Mg^{2+} homeostasis. For example, mutation of vacuolar ATPase subunits can produce sensitivity to excess Mg^{2+} ions (presumably because of an inability to sequester Mg^{2+} in the vacuole), but the inactivation of proteins that do not mediate Mg^{2+} transport can have similar effects (the *nhx1* mutation, which inactivates an

endosomal Na^+/H^+ exchanger, also reduces Mg^{2+} tolerance, as do mutations in the *pmr1* Ca^{2+}-ATPase [R. Gardner, personal communication]. Any future strategies to isolate Mg^{2+} transporters in yeast via the identification of Mg^{2+}-sensitive mutants will need to take this limitation into account. However, it is possible that the genes identified using such a screen could be further analyzed using an overexpression strategy. A transporter that was genuinely involved in the regulation of Mg^{2+} storage would reasonably be expected to have an effect on Mg^{2+} content when overexpressed. I found that the overexpression of *PER1* had no such effect on the Mg^{2+} content of yeast, which is consistent with this gene having only an indirect effect on Mg^{2+} tolerance.

4.2 CaCA genes and Mg^{2+} homeostasis.

The second group of candidate Mg^{2+} transporter genes selected for my experiments was related to known divalent cation transporters. Since Mg^{2+} is a positively charged ion, removal of Mg^{2+} from the cytosol (and efflux from the cell or intracellular storage) is expected to require energy input. The CaCA superfamily is a group of proteins that mediate transport of other positively charged divalent ions. Three of these proteins were present in the yeast genome, and had not been characterized when this work began. These proteins were good candidates for the Mg^{2+}/H^+ exchange system that has been described in the yeast secretory pathway and vacuole (Borrelly et al., 2001). I systematically examined these three proteins to determine if they affected Mg homeostasis.

If a putative divalent cation/H^+ exchanger were to be involved in the transport of Mg^{2+}, one might expect to see Mg^{2+} related phenotypes, such as sensitivity or tolerance to Mg^{2+}, and a change in metal ion content when the protein is overexpressed or deleted.

The effect of a putative cation/H^+ exchanger on cation content would depend on its cellular location. For example, if the transporter was responsible for sequestration in a storage compartment like the vacuole, overexpression might result in a significant increase in total cellular content of that particular ion which it transports, as has been observed for other vacuolar cation transport systems [e.g., Zrc1p, (MacDiarmid et al., 2000)]. If the transporter mediated efflux from the cell, via the plasma membrane or secretory pathway, one would expect to observe an increase in ion content if the gene is deleted, and a decrease if the gene is overexpressed. In addition, since a cation/proton exchanger would most likely remove cations from the cytosol, one would most likely observe a sensitivity phenotype upon deletion of the gene, and resistance upon overexpression: as a consequence of overexpression, metals would be removed from the cytosol before they could accumulate to toxic levels.

To test if any of the uncharacterized CaCA genes had effects on Mg content or tolerance when overexpressed, I cloned the entire gene into a high copy vector, which resulted in moderate overexpression of the gene. My experiments showed that one of the three genes, *ECX1*, produced an increase in Mg^{2+} content when it was overexpressed, and other two CaCA genes had no effect. This initial promising result, which suggested a role for *ECX1* in Mg^{2+} homeostasis, was not supported by subsequent experiments however. In particular, deletion of *ECX1* did not affect Mg content or tolerance, even when the strain was grown in medium with a very high concentration of Mg^{2+}. This observation is not consistent with an essential role for *ECX1* in sequestration of Mg^{2+} in the vacuole, or the efflux of Mg^{2+} from the cell.

Since I was not successful in identifying a gene that encoded the vacuolar

Mg^{2+}/H^+ exchanger using a candidate gene approach, it might have been worthwhile to do a genetic screen for proteins that suppress the Mg^{2+} sensitivity of mutants with vacuolar Mg^{2+} storage defects, such as *vma1*. Mutants lacking V-H^+-ATPase activity are unable to accumulate Mg^{2+} in the vacuole, and are sensitive to high Mg^{2+} concentrations (R. Gardner, personal communication). This screen could be performed by using an overexpression library (a library of genomic fragments in a high-copy vector) to overexpress genes at random, then select for transformed cells that are resistant to high Mg^{2+} concentrations, but not to other toxic cations such as Na^+ (which *vma1* mutants are also sensitive to). The reasoning behind this screen would be that that the small amount of residual transport activity seen in these mutants might have been increased by transporter overexpression, leading to increased vacuolar Mg^{2+} storage and tolerance.

4.3 Role of *ECX1* in calcium homeostasis

Studies of the effect of *ECX1* on cation content and sensitivity when overexpressed or deleted provided evidence that Ecx1 is involved in Ca^{2+} homeostasis. Mutation of this gene induced a minor sensitivity to high Ca^{2+} concentrations, which was enhanced by combining the *ecx1* mutation with inactivating mutations in other Ca^{2+} transporters (*vcx1* and *pmc1*) that are required for Ca^{2+} sequestration in the vacuole. It is possible that this sensitivity to Ca^{2+} is the result of a reduced ability to remove Ca^{2+} from the cytosol into the secretory pathway. In addition, the *ecx1* mutation increased calcium accumulation by yeast, both in isolation and when combined with the other two mutations. These observations suggest that *ECX1* is involved in Ca^{2+} efflux from the cell, which is consistent with its membership in the CaCA family of efflux systems.

If *ECX1* is involved in Ca^{2+} efflux or sequestration, I would expect Ca^{2+} content

to be altered when this gene is overexpressed. However, although a slight increase in Ca^{2+} content was observed in these experiments, it was not significant **(Figure 3.6B)**. However, the maximum Ca^{2+} concentration used in these experiments was quite low, and a more significant effect might have been observed if the cells were grown at higher concentrations. Further experiments need to be performed to address this possibility. In addition, in order to more extensively test for effects of *ECX1* overexpression and deletion on yeast physiology, it would have been worthwhile to determine the content of a range of other elements. This experiment could have been done using AAS, but at the time of these experiments I only had the ability to measure Mg^{2+}, Ca^{2+}, and Na^{+} content using this method. An alternative way to determine the levels of many elements in one sample is by the use of inductively coupled plasma mass spectrometry (ICP-MS). This method can measure the concentrations of up to 75 elements at once, and is now routinely used to determine the composition of the yeast "ionome" in different strains (Eide et al., 2005).

4.4 Subcellular location of Ecx1

There are two basic ways in which efflux of Ca^{2+} from the cell could be mediated by the Ecx1 protein. First, Ecx1 may perform a similar function to Pmr1 (Vashist et al., 2002), a P-type ATPase that transports Ca^{2+} and Mn^{2+} into the Golgi (and eventually, releases the ion to the external environment). If Ecx1 transports Ca^{2+} into the ER or Golgi, it could then enter the secretory pathway and eventually be extruded from the cell via exocytosis. However, an alternative model is that Ecx1 is a plasma membrane protein that directly effluxes Ca^{2+} ions from the cytosol to the external environment. To discriminate between these two models for Ecx1 function, I determined its location using

two independent techniques, epifluorescent microscopy of cells expressing YFP-tagged Ecx1, and cell fractionation with an epitope-tagged version. Microscopy of the YFP-tagged version of Ecx1 provided clear evidence for an intracellular location (the ER/nuclear membrane), and did not reveal any strong signal at the plasma membrane. While the results of cell fractionation studies were not definitive, they confirmed that Ecx1 could be located in the ER or mitochondria. The YFP-tagged Ecx1 was clearly not located in the mitochondrial compartment however, as the distinctive morphology of this compartment in yeast (thread-like bodies distributed throughout the cell) was not observed. Hence the results of the two techniques point towards an ER-membrane location for the Ecx1 protein.

One drawback of the above studies was that the very low expression of the Ecx1 protein made it impossible to detect by Western blotting or microscopy of tagged versions. Ecx1 expression had to be increased significantly (by the use of multicopy yeast vectors) in order to perform the localization studies. Since it is formally possible that the protein may be mislocalized when overexpressed, this was not an ideal solution. If detection of normal expression of Ecx1 is required, one strategy may be to try and increase the signal without increasing the protein level. Although the version of Ecx1 that was used had three HA tags, addition of more repeats of this epitope could potentially increase the sensitivity of detection in Western blotting experiments. However, it must be determined whether these tagged versions of the protein are functional. I obtained evidence that the HA tagged version of the protein is functional by its magnesium-related phenotype when overexpressed. Both the tagged and WT versions of Ecx1 produced an increase in Mg^{2+} accumulation when overexpressed (the only known phenotype of Ecx1

when these experiments were performed). Better evidence that the modified versions are functional could be obtained via complementation of the Ca^{2+} related phenotypes of *ecx1* mutants. For example, expression of these versions should complement the Ca^{2+}-sensitive phenotype of the *ecx1 pmc1* mutant (**Figure 3.8**).

In summary, I found evidence that the Ecx1 protein was involved in regulating cytosolic Ca^{2+} concentration in concert with other Ca^{2+} transporters, such as Vcx1 and Pmc1. The location of Ecx1 and the mutant phenotype of higher Ca^{2+} content suggested that this protein was involved in mediating Ca^{2+} efflux via the secretory pathway. This model for Ecx1 function is summarized in **Figure 4.1**.

4.5 Predictions of the model for Ecx1 function

4.5.1 Possible role of Ecx1 in the ER/secretory pathway

Prior to these experiments, the only proteins known to be involved in the transport of Ca^{2+} into the secretory pathway were Pmr1p and Spf1p/Cod1p (a related P-type ATPase) (Cronin et al., 2002; Vashist et al., 2002)**.** As discussed previously, Pmr1p is a P-type ATPase localized to the medial-Golgi, which performs high-affinity Ca^{2+} and Mn^{2+} transport required for entry of these cations into the Golgi compartment (and possibly the ER) (Durr et al., 1998)**.** Spf1p (Cod1p) is a protein that partially overlaps in function with Pmr1, but is localized to the ER membrane. Mutation of *pmr1* increases Ca^{2+} content of yeast cells as a consequence of decreased efflux (Cronin et al., 2002). The strong effect of the *ecx1* mutation on Ca^{2+} content of yeast suggests that it overlaps in function with Pmr1, and contributes significantly to Ca^{2+} secretion from yeast. The Ca^{2+}-sensitivity of the mutant indicates that this process may be important for the maintenance of cytosolic Ca^{2+} homeostasis. The potential overlap in the function of Ecx1 and the P-

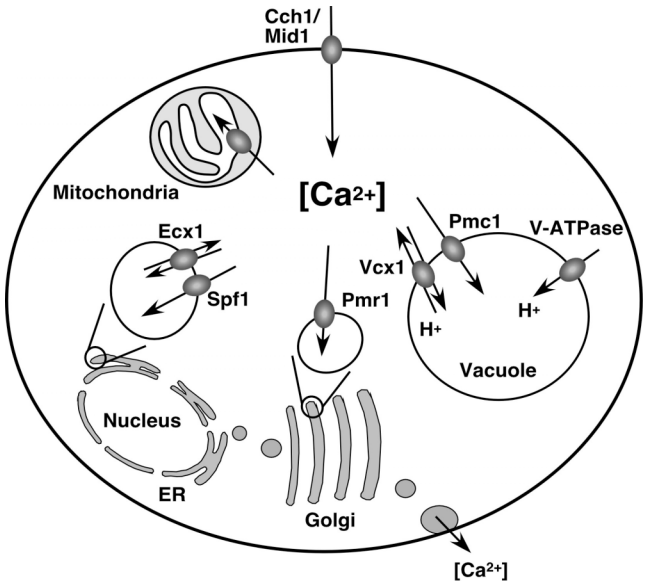

Figure 4.1 Model for Ecx1 function. This figure provides an overview of the transporters known to be required for Ca^{2+} homeostasis in yeast. Cytosolic Ca^{2+} concentration ($[Ca^{2+}]$) must be maintained at a low level to allow signal transduction. Loss of this regulation results in Ca^{2+} sensitivity due to a higher resting cytosolic Ca^{2+} concentration. Entry of Ca^{2+} to the cell is mediated by the Cch1/Mid1 heteromeric Ca^{2+} channel. Removal of excess Ca^{2+} from the cytosol is achieved in part via sequestration in the vacuole, which is mediated by Vcx1 and Pmc1. This process adds to the Ca^{2+} content of the cell by increasing vacuolar stores. Pmr1p, Spf1p and Pmc1p are high affinity, low capacity systems responsible for maintaining very low levels of cytosolic Ca^{2+}. Pmr1p is a P-type ATPase that transports Ca^{2+} and Mn^{2+} to the Golgi, while Spf1p is a homologous Ca^{2+} transporter localized to the ER. In contrast to vacuolar storage, removal of Ca^{2+} to the ER and secretory pathway via Pmr1 and Spf1 ultimately leads to the loss of Ca^{2+} from the cell via secretory vesicle exocytosis. This model suggests that Ecx1 is also involved in the export of Ca^{2+} via the ER and secretory pathway, based on the observation that Ca^{2+} content increased when the protein was inactivated. The model shows that Ca^{2+} is transported into the ER via Ecx1, and moves into the Golgi via vesicular trafficking. From that location, Ca^{2+} can be secreted via vesicles that fuse with the cell membrane, releasing their contents to the external environment.

type ATPases suggests several experiments that could be performed to determine the contribution of Ecx1 to homeostasis. First, it may be possible to test for an effect of *ecx1* mutation on metal sensitivity. Previous studies have shown that both *pmr1* and *spf1* single mutants are sensitive to excess Ca^{2+} (Cronin et al., 2002). The same study showed that combining the *pmr1* and *spf1* mutations resulted in an even greater sensitivity. Although the *spf1* single mutant did not display an increase in intracellular Ca^{2+} content, the *pmr1* mutant did, and there was a synergistic increase in Ca^{2+} content in a *pmr1* and *spf1* double mutant. Similar results may be observed if the *ecx1* deletion was combined with the *pmr1* and *spf1* markers. If so, this interaction would support a role for Ecx1 in the efflux of cytosolic Ca^{2+} via the secretory pathway.

If Ecx1 does in fact remove Ca^{2+} from the cytosol, I would expect to see not just an increase in total intracellular Ca^{2+}, but also an increase in cytosolic Ca^{2+} concentration in the deletion mutant (especially under conditions of Ca^{2+} toxicity). One way to test this prediction might be to directly measure the cytosolic Ca^{2+} concentration using AAS, after all organelles are removed from a cell suspension via centrifugation. However, this method may not give accurate results. For example, organelles may be damaged in the fractionation process, releasing their contents; or all of the organelles may not be removed from the suspension. A better way to determine cytosolic Ca^{2+} concentration might be to use the Ca^{2+} chelating fluorescent dye Fura-2 (O'Connor and Silver, 2007). Fura-2 binds Ca^{2+} ions, which alters the fluorescent properties of the dye. The relative fluorescence intensity of the dye at particular wavelengths thus depends on the concentration of Ca^{2+}. Fura-2 has been shown to be an effective method to directly measure the cytosolic Ca^{2+} concentration in yeast (Iida et al., 1990). However, the use of fluorescent indicators is technically difficult and must be carefully controlled to avoid artifactual results. Another problem with these compounds is that they may accumulate within organelles such as the vacuole in yeast (MacDiarmid et al., 2000)**,** and report incorrect cytosolic concentrations as a result. To avoid these problems, Ca^{2+}-sensitive fluorescent reporters have been developed based on proteins that can be expressed in specific cellular compartments (*e.g.* the cytosol). These include the luminescent protein Aequorin (Chiesa et al., 2001)**,** which produces light emission upon binding Ca^{2+}, and the ratiometric fluorescent indicator Cameleon (Miyawaki et al., 1997)**,** which directly binds Ca^{2+} and alters its conformation, causing an increase in the intensity of fluorescence resonant energy transfer (FRET) between two different fluorescent proteins. Both

Aequorin (Kellermayer et al., 2003) and Cameleon (Facanha et al., 2002) have been used to measure cytosolic Ca^{2+} in yeast, and either might be suitable to study the effect of Ecx1.

Another more indirect, but widely used method to measure changes in cytosolic Ca^{2+} utilizes Ca^{2+}-sensitive reporter genes. An increased abundance of cytosolic Ca^{2+} triggers an increase in the activity of the calmodulin cytosolic Ca^{2+}-sensor, and a consequent induction of genes regulated by this pathway (via the Tcn1/Crz1 transcription factor) (Stathopoulos and Cyert, 1997). β-galactosidase reporter genes are available which measure Tcn1 activity in yeast (Stathopoulos and Cyert, 1997), and the expression of these is altered in other Ca^{2+}-transporter mutants (Muller et al., 2001), and induced under conditions that increase cytosolic Ca^{2+} [*e.g.* (Viladevall et al., 2004)]. Alterations in the expression of such a reporter gene in an *ecx1* mutant would provide good evidence for a role of Ecx1 in maintaining cytosolic Ca^{2+} homeostasis.

If the *ecx1* mutation has no apparent effect on Ca^{2+} sensitivity of *pmr1* and *spf1* strains, or on steady-state cytosolic Ca^{2+} concentration as measured by reporters, this does not necessarily indicate that this protein plays no role in the regulation of cytosolic Ca^{2+}. It is also possible that Ecx1 has a more specialized role in quickly removing Ca^{2+} from the cytosol under conditions of rapid influx. CaCA proteins differ from P-type ATPases in having a high capacity but a relatively low affinity for their substrates. Thus, CaCA proteins can transport particular cations to their destination relatively fast, but cannot contribute to fine regulation of cytoplasmic concentration. ATPases in contrast can contribute to more stringent control of cytosolic concentrations of their substrates. For this reason, it is possible that an effect of the *ecx1* mutation on cytosolic Ca^{2+} might only

be seen under conditions in which cells receive a "pulse" of external Ca^{2+}, which results in a rapid elevation of cytosolic concentration. This increase could trigger an increase in Ecx1 activity sufficient to help rapidly clear the cytosol of Ca^{2+}. When the cytosolic concentration dropped to a low enough level, Ecx1 would be unable to reduce it further: Pmr1 and Spf1 would then contribute to further reducing the concentration to the normal low level. This hypothesis could be tested by using a Ca^{2+}-sensitive reporter gene or fluorescent reporter to measure dynamic changes in cytosolic Ca^{2+} in various mutants exposed to a Ca^{2+}-pulse.

4.5.2 Other models for Ecx1 function

It is believed that Ca^{2+} transport into the secretory pathway via Pmr1 and Spf1 not only maintains cytosolic Ca^{2+} homeostasis, but also supplies the secretory pathway with Ca^{2+} to support essential biological functions. Both Ca^{2+} and Mn^{2+} are required for proper processing of proteins through the secretory pathway (Durr et al., 1998). Ca^{2+} is required for sorting, and Mn^{2+} is required for glycosylation (Durr et al., 1998). In addition, ER Ca^{2+} is involved in protein folding, ER-associated protein degradation (ERAD), ER-resident protein retention, and protein targeting to organelles (Booth and Koch, 1989; Durr et al., 1998; Lodish and Kong, 1990; Sambrook, 1990; Wileman et al., 1991). Pmr1p/Spf1 and Ecx1p may all contribute to the maintenance of proper calcium levels in the secretory pathway. When ER function is impaired, unfolded proteins build up in the lumen, with potentially harmful effects for the cell. For this reason, yeast has a signaling pathway that turns on a set of genes in response to defective ER function. This pathway consists of two components, the integral ER membrane protein Ire1, and the transcriptional activator Hac1 (Cox and Walter, 1996). The Ire1 protein has a cytosolic

domain with a specific RNA-splicing activity, which is activated by unfolded proteins in the ER lumen. The precursor of the *HAC1* mRNA has an intron that must be removed by Ire1 to allow the translation of *Hac1* and its function in activating gene expression. For this reason, mutation of either component of this pathway prevents the induction of UPR-regulated genes. Several workers have shown that non-lethal mutations in genes which are required for some aspect of ER function are synthetic lethal, or show synthetic slow-growth phenotypes when combined with the *ire1* or *hac1* mutations. This is because when important of ER functions are inhibited by mutation, the UPR becomes essential for normal cell function. One such study showed that the *spf1* and *hac1* mutations are synthetically lethal (Ando and Suzuki, 2005) probably because Spf1 is essential for supplying ER Ca^{2+}. To determine if the *ecx1* mutation affects ER function, similar experiments could be performed: for example, an *ecx1 hac1* double mutant might exhibit synthetic lethality (or slow growth) phenotypes, providing support for this model. An *ecx1 ire1* double mutant would likewise be expected to show this phenotype. If the mutations are not synthetically lethal, growth sensitivity studies could be performed to try and identify a subtler growth defect. For example, the growth rate of the double mutant may be reduced at high temperature (37°), or it may be sensitive to an excess or deficiency of Ca^{2+} in the medium.

4.6 Expression and regulation of Ecx1

As yet, it is not clear if or how Ecx1 expression and activity is regulated. Many Ca^{2+} transporters in yeast are regulated according to the cytosolic Ca^{2+} concentration. This concentration is directly sensed by the cytosolic protein Calcineurin, which transmits this signal to a transcriptional activator called Tcn1/Crz1 (Matheos et al., 1997;

Stathopoulos and Cyert, 1997). Genes regulated transcriptionally by Tcn1 include *PMR1* and *PMC1*, both of which encode transporters required for Ca^{2+} efflux and tolerance (Matheos et al., 1997; Stathopoulos and Cyert, 1997; Yoshimoto et al., 2002). These genes possess regulatory sequences that are bound by Tcn1 in order to activate transcription. To determine if Ca^{2+} concentrations have an effect on *ECX1* transcription, I could perform Northern analysis of total RNA from cells grown in media of varying Ca^{2+} concentration. However, the *ECX1* promoter region (like *VCX1*) does not possess any consensus sites for Tcn1 regulation (data not shown), and publicly available data from microarray experiments indicate that induction of *ECX1* mRNA does not occur in response to Ca^{2+} treatment (Yoshimoto et al., 2002). However, it is possible that *ECX1* shows translational or post-translational Ca^{2+}-dependent expression, and that this feature might partly explain the low level of expression that was observed under normal conditions. To test if increased Ca^{2+} levels increased the level of Ecx1 present in cells, Western analysis could be performed with cells grown over a range of Ca^{2+} concentrations. Performing these experiments may provide evidence supporting a role for Ecx1 in Ca^{2+} homeostasis.

4.7 Structural features of the Ecx1 protein

One question raised by this work is why Ecx1 affects Ca^{2+} content, while the related proteins Ydl206wp and Yjr106wp had no effect. Ecx1 possesses a novel conserved motif (Pfam PF03733.3) that is not shared with other CaCA family members, but is found in a small family of prokaryotic proteins of unknown function. This motif is located at position 238-301 in the protein sequence, within a relatively hydrophobic region of the protein **(Figure 3.4).** As yet it is still unclear what function this motif may

perform, but its hydrophobicity suggests that it forms a transmembrane domain. This motif may also play a role in determining the ER location of the protein, as the related Vcx1 protein, which accumulates in the vacuole membrane, does not have an equivalent domain. Other possible roles for this domain include participation in the regulation of Ecx1 activity. The CAX1 protein from *Arabidopsis thaliana* has an N-terminal domain that is dispensable for function, but inhibits CAX1 activity (Pittman and Hirschi, 2001). Deletion of this domain is required for the protein to function when expressed in heterologous systems such as yeast. It is believed that the N-terminal domain interacts with another *Arabidopsis* protein in order to regulate CAX1 activity (Cheng and Hirschi, 2003). Function of the N-terminal domain could be tested by making deletions of the coding region, then expressing the protein in WT stains and an *ecx1* mutant to determine if any of the Ecx1 phenotypes (for example, Ca^{2+} accumulation) were altered.

4.8 Role of Ecx1 in pH regulation

In addition to its role in Ca^{2+} homeostasis, my work also seems to indicate that Ecx1 plays some role in pH regulation. Nhx1 is an endosomal Na^{+}/H^{+} exchanger that is thought to be involved in regulating endosomal pH. Studies of *nhx1* null mutants have demonstrated a sensitivity to low pH (Brett et al., 2005), along with a defect in vacuolar protein sorting. Proteins destined for vacuoles in yeast must first enter the ER and then be delivered to the Golgi and pre-endosome (Bryant et al., 1998). The authors reasoned that the *nhx1* mutation reduced the flow of protons from the endosomal compartment to the cytosol, altering the ability of this compartment to sort proteins correctly. This pH-sensitivity phenotype was also seen in the *nhx1* single mutant in my hands, although I did not observe as high of a sensitivity as previously reported. Likewise, in my experiments,

the *ecx1* mutant AJF02 also demonstrated a slight sensitivity to low pH. When the *ecx1* and *nhx1* mutations were combined, the double mutant exhibited an enhanced sensitivity to pH (greater than the sensitivity conferred by either single mutant allele). This synergistic interaction suggests that Ecx1 could also possibly have a role in controlling the pH of the ER lumen by removing protons, thus making it more alkaline. This sensitivity to low pH is also consistent with the model proposing that Ecx1 is a Ca^{2+}/H^{+} exchanger.

4.9 Recent publications on *ECX1*

After this work was completed, an independent analysis of *ECX1* function was reported (Cagnac et al., 2007). In contrast to my results, the authors concluded that *ECX1* did not affect Ca^{2+} homeostasis. Instead, they presented evidence that the *ecx1* mutation eliminated a Na^{+}/H^{+} exchange activity from the vacuolar membrane. Data was presented showing that in vacuolar membranes from WT strains, Na^{+} ions dissipated the proton gradient generated by the V-ATPase, but that in *ecx1* mutants this activity was absent. In addition, the authors presented evidence that *ecx1* strains were sensitive to the antibiotic hygromycin, which is though to be more toxic to strains with disrupted pH homeostasis. However, their results revealed only a very minor sensitivity to Na^{+} associated with *ecx1* mutation, and only in a very Na^{+}-sensitive genetic background. In addition, while they also presented evidence that GFP-tagged Ecx1 was located in the ER membrane (rather than the vacuole), they did not present any evidence showing complementation of the mutant phenotype by their tagged versions of Ecx1. Clearly, more work needs to be done to unequivocally establish a function for the Ecx1 protein in yeast, and to resolve these conflicting observations.

4.10 Conclusion

The initial aim of this study (to identify a novel Mg^{2+}/H^{+} vacuolar exchanger in yeast) was not achieved. However, I have apparently identified a protein that is involved in the transport of Ca^{2+} to the ER lumen. Future work to more clearly identify the physiological role of this protein is required to understand the role that Ecx1 and related proteins play in secretory pathway function and overall yeast physiology.

References

Altura, B.M. and Altura, B.T. (1996) Role of magnesium in patho-physiological processes and the clinical utility of magnesium ion selective electrodes. *Scand J Clin Lab Invest Suppl*, **224**, 211-234.

Ando, A. and Suzuki, C. (2005) Cooperative function of the CHD5-like protein Mdm39p with a P-type ATPase Spf1p in the maintenance of ER homeostasis in *Saccharomyces cerevisiae*. *Mol Genet Genomics*, **273**, 497-506.

Banuelos, M.A., Sychrova, H., Bleykasten-Grosshans, C., Souciet, J.L. and Potier, S. (1998) The Nha1 antiporter of *Saccharomyces cerevisiae* mediates sodium and potassium efflux. *Microbiology*, **144 (Pt 10)**, 2749-2758.

Barbagallo, M., Dominguez, L.J., Galioto, A., Ferlisi, A., Cani, C., Malfa, L., Pineo, A., Busardo, A. and Paolisso, G. (2003) Role of magnesium in insulin action, diabetes and cardio-metabolic syndrome X. *Mol. Aspects Med.*, **24**, 39-52.

Bonneaud, N., Ozier-Kalogeropoulos, O., Li, G.Y., Labouesse, M., Minvielle-Sebastia, L. and Lacroute, F. (1991) A family of low and high copy replicative, integrative and single-stranded *S. cerevisiae*/*E. coli* shuttle vectors. *Yeast*, **7**, 609-615.

Booth, C. and Koch, G.L. (1989) Perturbation of cellular calcium induces secretion of luminal ER proteins. *Cell*, **59**, 729-737.

Borrelly, G., Boyer, J.C., Touraine, B., Szponarski, W., Rambier, M. and Gibrat, R. (2001) The yeast mutant *vps5*Δ affected in the recycling of Golgi membrane proteins displays an enhanced vacuolar Mg^{2+}/H^{+} exchange activity. *Proc. Natl. Acad. Sci. USA*, **98**, 9660-9665.

Brett, C.L., Tukaye, D.N., Mukherjee, S. and Rao, R. (2005) The yeast endosomal $Na^{+}K^{+}/H^{+}$ exchanger Nhx1 regulates cellular pH to control vesicle trafficking. *Mol Biol Cell*, **16**, 1396-1405.

Bryant, N.J., Piper, R.C., Gerrard, S.R. and Stevens, T.H. (1998) Traffic into the prevacuolar/endosomal compartment of *Saccharomyces cerevisiae*: a *VPS45*-dependent intracellular route and a *VPS45*-independent, endocytic route. *Eur J Cell Biol*, **76**, 43-52.

Cagnac, O., Leterrier, M., Yeager, M. and Blumwald, E. (2007) Identification and characterization of Vnx1p, a novel type of vacuolar monovalent cation/H^{+} antiporter of *Saccharomyces cerevisiae*. *J Biol Chem*, **282**, 24284-24293.

Cai, X. and Lytton, J. (2004) Molecular cloning of a sixth member of the K^{+}-dependent Na^{+}/Ca^{2+} exchanger gene family, NCKX6. *J Biol Chem*, **279**, 5867-5876.

Cheng, N.H. and Hirschi, K.D. (2003) Cloning and characterization of CXIP1, a novel PICOT domain-containing *Arabidopsis* protein that associates with CAX1. *J Biol Chem*, **278**, 6503-6509.

Chiesa, A., Rapizzi, E., Tosello, V., Pinton, P., de Virgilio, M., Fogarty, K.E. and Rizzuto, R. (2001) Recombinant aequorin and green fluorescent protein as valuable tools in the study of cell signalling. *Biochem J*, **355**, 1-12.

Conklin, D.S., Kung, C. and Culbertson, M.R. (1993) The *COT2* gene is required for glucose-dependent divalent cation transport in *Saccharomyces cerevisiae*. *Mol. Cell. Biol.*, **13**, 2041-2049.

Cox, J.S. and Walter, P. (1996) A novel mechanism for regulating activity of a transcription factor that controls the unfolded protein response. *Cell*, **87**, 391-404.

Cronin, S.R., Rao, R. and Hampton, R.Y. (2002) Cod1p/Spf1p is a P-type ATPase involved in ER function and Ca^{2+} homeostasis. *J. Cell. Biol.*, **157**, 1017-1028.

Cunningham, K.W. and Fink, G.R. (1994) Calcineurin-dependent growth control in *Saccharomyces cerevisiae* mutants lacking *PMC1*, a homolog of plasma membrane Ca^{2+} ATPases. *J Cell Biol*, **124**, 351-363.

Cunningham, K.W. and Fink, G.R. (1996) Calcineurin inhibits *VCX1*-dependent H^+/Ca^{2+} exchange and induces Ca^{2+} ATPases in *Saccharomyces cerevisiae*. *Mol. Cell. Biol.*, **16**, 2226-2237.

Da Costa, B.M., Cornish, K. and Keasling, J.D. (2007) Manipulation of intracellular magnesium levels in Saccharomyces cerevisiae with deletion of magnesium transporters. *App. Microbiol. Biotechnol.*

Dancis, A., Haile, D., Yuan, D.S. and Klausner, R.D. (1994) The *Saccharomyces cerevisiae* copper transport protein (Ctr1p). *J. Biol. Chem.*, **41**, 25660-25667.

Delhaize, E. and Ryan, P.R. (1995) Aluminium toxicity in plants. *Plant Physiol*, **107**, 115-121.

Durr, G., Strayle, J., Plemper, R., Elbs, S., Klee, S.K., Catty, P., Wolf, D.H. and Rudolph, H.K. (1998) The medial-Golgi ion pump Pmr1 supplies the yeast secretory pathway with Ca^{2+} and Mn^{2+} required for glycosylation, sorting, and endoplasmic reticulum-associated protein degradation. *Mol Biol Cell*, **9**, 1149-1162.

Eide, D.J., Clark, S., Nair, T.M., Gehl, M., Gribskov, M., Guerinot, M.L. and Harper, J.F. (2005) Characterization of the yeast ionome: a genome-wide analysis of nutrient mineral and trace element homeostasis in *Saccharomyces cerevisiae*. *Genome Biol*, **6**, R77.

Facanha, A.L., Appelgren, H., Tabish, M., Okorokov, L. and Ekwall, K. (2002) The endoplasmic reticulum cation P-type ATPase Cta4p is required for control of cell shape and microtubule dynamics. *J Cell Biol*, **157**, 1029-1039.

Ferguson, M.A. (1999) The structure, biosynthesis and functions of glycosylphosphatidylinositol anchors, and the contributions of trypanosome research. *J. Cell Sci.*, **112 (Pt 17)**, 2799-2809.

Ferreira, A., Rivera, A. and Romero, J.R. (2004) Na^+/Mg^{2+} exchange is functionally coupled to the insulin receptor. *J Cell Physiol*, **199**, 434-440.

Fischer, M., Schnell, N., Chattaway, J., Davies, P., Dixon, G. and Sanders, D. (1997) The *Saccharomyces cerevisiae CCH1* gene is involved in calcium influx and mating. *FEBS Lett*, **419**, 259-262.

Fuhrmann, G.-F. and Rothstein, A. (1968) The transport of Zn^{2+}, Co^{2+} and Ni^{2+} into yeast cells. *Biochim. Biophys. Acta*, **163**, 325-330.

Fujita, M., Umemura, M., Yoko-o, T. and Jigami, Y. (2006) *PER1* is required for GPI-phospholipase A2 activity and involved in lipid remodeling of GPI-anchored proteins. *Mol Biol Cell*, **17**, 5253-5264.

Garcia-del Portillo, F., Foster, J.W., Maguire, M.E. and Finlay, B.B. (1992) Characterization of the micro-environment of *Salmonella typhimurium*-containing vacuoles within MDCK epithelial cells. *Mol Microbiol*, **6**, 3289-3297.

Gardner, R.C. (2003) Genes for magnesium transport. *Curr. Opin. Plant. Biol.*, **6**, 263-267.

Gibson, M.M., Bagga, D.A., Miller, C.G. and Maguire, M.E. (1991) Magnesium transport in *Salmonella typhimurium*: the influence of new mutations conferring Co^{2+} resistance on the CorA Mg^{2+} transport system. *Mol. Microbiol.*, **5**, 2753-2762.

Gonzalez-Serratos, H. and Rasgado-Flores, H. (1990) Extracellular magnesium-dependent sodium efflux in squid giant axons. *Am J Physiol*, **259**, C541-548.

Graschopf, A., Stadler, J.A., Hoellerer, M.K., Eder, S., Sieghardt, M., Kohlwein, S.D. and Schweyen, R.J. (2001) The yeast plasma membrane protein Alr1 controls Mg^{2+} homeostasis and is subject to Mg^{2+}-dependent control of its synthesis and degradation. *J. Biol. Chem.*, **276**, 16216-16222.

Gregan, J., Bui, D.M., Pillich, R., Fink, M., Zsurka, G. and Schweyen, R.J. (2001a) The mitochondrial inner membrane protein Lpe10p, a homologue of Mrs2p, is essential for magnesium homeostasis and group II intron splicing in yeast. *Mol. Gen. Genet.*, **264**, 773-781.

Gregan, J., Kolisek, M. and Schweyen, R.J. (2001b) Mitochondrial Mg^{2+} homeostasis is critical for group II intron splicing *in vivo*. *Genes Dev.*, **15**, 2229-2237.

Gums, J.G. (2004) Magnesium in cardiovascular and other disorders. *Am. J. Health Syst. Pharm.*, **61**, 1569-1576.

Hanikenne, M., Kramer, U., Demoulin, V. and Baurain, D. (2005) A comparative inventory of metal transporters in the green alga *Chlamydomonas reinhardtii* and the red alga *Cyanidioschizon merolae*. *Plant Physiol*, **137**, 428-446.

Hattori, M., Tanaka, Y., Fukai, S., Ishitani, R. and Nureki, O. (2007) Crystal structure of the MgtE Mg^{2+} transporter. *Nature*, **448**, 1072-1075.

Hermans, C. and Verbruggen, N. (2005) Physiological characterization of Mg^{2+} deficiency in *Arabidopsis thaliana*. *J Exp Bot*.

Heus, H.A. and Pardi, A. (1991) Nuclear magnetic resonance studies of the hammerhead ribozyme domain. Secondary structure formation and magnesium ion dependence. *J Mol Biol*, **217**, 113-124.

Hmiel, S.P., Snavely, M.D., Miller, C.G. and Maguire, M.E. (1986) Magnesium transport in Salmonella typhimurium: characterization of magnesium influx and cloning of a transport gene. *J Bacteriol*, **168**, 1444-1450.

Hua, S.B., Qiu, M., Chan, E., Zhu, L. and Luo, Y. (1997) Minimum length of sequence homology required for *in vivo* cloning by homologous recombination in yeast. *Plasmid*, **38**, 91-96.

Huh, W.K., Falvo, J.V., Gerke, L.C., Carroll, A.S., Howson, R.W., Weissman, J.S. and O'Shea, E.K. (2003) Global analysis of protein localization in budding yeast. *Nature*, **425**, 686-691.

Iida, H., Nakamura, H., Ono, T., Okumura, M.S. and Anraku, Y. (1994) *MID1*, a novel *Saccharomyces cerevisiae* gene encoding a plasma membrane protein, is required for Ca^{2+} influx and mating. *Mol Cell Biol*, **14**, 8259-8271.

Iida, H., Yagawa, Y. and Anraku, Y. (1990) Essential role for induced Ca^{2+} influx followed by $[Ca^{2+}]i$ rise in maintaining viability of yeast cells late in the mating pheromone response pathway. A study of $[Ca^{2+}]i$ in single *Saccharomyces cerevisiae* cells with imaging of fura-2. *J Biol Chem*, **265**, 13391-13399.

Ikari, A., Nakajima, K., Suketa, Y., Harada, H. and Takagi, K. (2003) Arachidonic acid-activated Na^{+}-dependent Mg^{2+} efflux in rat renal epithelial cells. *Biochim Biophys Acta*, **1618**, 1-7.

Ikezawa, H. (2002) Glycosylphosphatidylinositol (GPI)-anchored proteins. *Biol. Pharm. Bull.*, **25**, 409-417.

Kawano, Y., Matsuoka, H., Takishita, S. and Omae, T. (1998) Effects of magnesium supplementation in hypertensive patients: assessment by office, home, and ambulatory blood pressures. *Hypertension*, **32**, 260-265.

Kellermayer, R., Aiello, D.P., Miseta, A. and Bedwell, D.M. (2003) Extracellular Ca^{2+} sensing contributes to excess Ca^{2+} accumulation and vacuolar fragmentation in a *pmr1Δ* mutant of *S. cerevisiae*. *J Cell Sci*, **116**, 1637-1646.

Kelly, D.E., Lamb, D.C. and Kelly, S.L. (2001) Genome-wide generation of yeast gene deletion strains. *Comparative and Functional Genomics*, **2**, 236-242.

Kimura, M. (2007) Overview of Magnesium Nutrition. In Nishizawa, Y., Morii, M. and Durlach, J. (eds.), *New Perspectives in Magnesium Research: Nutrition and Research*. Springer-Verlag, London, Vol. 1, pp. 69-93.

Kochian, L.V. (1995) Cellular mechanisms of aluminium toxicity and resistance in plants. *Ann. Rev. Plant. Physiol. Plant Mol. Biol.*, **46**, 237-260.

Kolisek, M., Zsurka, G., Samaj, J., Weghuber, J., Schweyen, R.J. and Schweigel, M. (2003) Mrs2p is an essential component of the major electrophoretic Mg^{2+} influx system in mitochondria. *EMBO J.*, **22**, 1235-1244.

Liu, G., Martin, D., Gardner, R. and Ryan, P. (2002) Large Mg^{2+}-dependent currents are associated with the increased expression of *ALR1* in *Saccharomyces cerevisiae*. *FEMS Microbiol. Lett.*, **213**, 231.

Lodish, H.F. and Kong, N. (1990) Perturbation of cellular calcium blocks exit of secretory proteins from the rough endoplasmic reticulum. *J Biol Chem*, **265**, 10893-10899.

Ma, H., Kunes, S., Schatz, P.J. and Botstein, D. (1987) Plasmid construction by homologous recombination in yeast. *Gene*, **58**, 201-216.

MacDiarmid, C.W., Gaither, L.A. and Eide, D. (2000) Zinc transporters that regulate vacuolar zinc storage in *Saccharomyces cerevisiae*. *EMBO J.*, **19**, 2845-2855.

MacDiarmid, C.W. and Gardner, R.C. (1998) Overexpression of the *Saccharomyces cerevisiae* magnesium transport system confers resistance to aluminum ion. *J. Biol. Chem.*, **273**, 1727-1732.

MacDiarmid, C.W., Milanick, M.A. and Eide, D.J. (2002) Biochemical properties of vacuolar zinc transport systems of *Saccharomyces cerevisiae*. *J. Biol. Chem.*, **277**, 39187-39194.

MacDiarmid, C.W., Milanick, M.A. and Eide, D.J. (2003) Induction of the *ZRC1* metal tolerance gene in zinc-limited yeast confers resistance to zinc shock. *J. Biol. Chem.*, **278**, 15065-15072.

Marchi, V., Sorin, A., Wei, Y. and Rao, R. (1999) Induction of vacuolar Ca^{2+}-ATPase and H^{+}/Ca^{2+} exchange activity in yeast mutants lacking *Pmr1*, the Golgi Ca^{2+}-ATPase. *FEBS Lett*, **454**, 181-186.

Maser, P., Thomine, S., Schroeder, J.I., Ward, J.M., Hirschi, K., Sze, H., Talke, I.N., Amtmann, A., Maathuis, F.J., Sanders, D., Harper, J.F., Tchieu, J., Gribskov, M., Persans, M.W., Salt, D.E., Kim, S.A. and Guerinot, M.L. (2001) Phylogenetic relationships within cation transporter families of *Arabidopsis*. *Plant Physiol.*, **126**, 1646-1667.

Matheos, D.P., Kingsbury, T.J., Ahsan, U.S. and Cunningham, K.W. (1997) Tcn1p/Crz1p, a calcineurin-dependent transcription factor that differentially regulates gene expression in *Saccharomyces cerevisiae*. *Genes Dev*, **11**, 3445-3458.

McGuigan, J.A., Elder, H.Y., Gunzel, D. and Schlue, W.R. (2002) Magnesium Homeostasis in Heart: A Critical Reappraisal. *J Clin Basic Cardiol*, **5**, 5-22.

Meij, I.C., van den Heuvel, L.P. and Knoers, N.V. (2002) Genetic disorders of magnesium homeostasis. *Biometals*, **15**, 297-307.

Millart, H., Durlach, V. and Durlach, J. (1995) Red blood cell magnesium concentrations: analytical problems and significance. *Magnes Res*, **8**, 65-76.

Miseta, A., Kellermayer, R., Aiello, D.P., Fu, L. and Bedwell, D.M. (1999) The vacuolar Ca^{2+}/H^{+} exchanger Vcx1p/Hum1p tightly controls cytosolic Ca^{2+} levels in *S. cerevisiae*. *FEBS Lett.*, **451**, 132-136.

Miyawaki, A., Llopis, J., Heim, R., McCaffery, J.M., Adams, J.A., Ikura, M. and Tsien, R.Y. (1997) Fluorescent indicators for Ca^{2+} based on green fluorescent proteins and calmodulin. *Nature*, **388**, 882-887.

Muller, E.M., Locke, E.G. and Cunningham, K.W. (2001) Differential regulation of two Ca^{2+} influx systems by pheromone signaling in *Saccharomyces cerevisiae*. *Genetics*, **159**, 1527-1538.

Nass, R., Cunningham, K.W. and Rao, R. (1997) Intracellular sequestration of sodium by a novel Na^{+}/H^{+} exchanger in yeast is enhanced by mutations in the plasma membrane H^{+}-ATPase. Insights into mechanisms of sodium tolerance. *J Biol Chem*, **272**, 26145-26152.

Nelson, N. (1999) Metal ion transporters and homeostasis. *EMBO J*, **18**, 4361-4371.

Ng, D.T., Spear, E.D. and Walter, P. (2000) The unfolded protein response regulates multiple aspects of secretory and membrane protein biogenesis and endoplasmic reticulum quality control. *J. Cell. Biol.*, **150**, 77-88.

Nicoll, D.A., Longoni, S. and Philipson, K.D. (1990) Molecular cloning and functional expression of the cardiac sarcolemmal Na^{+}-Ca^{2+} exchanger. *Science*, **250**, 562-565.

O'Connor, N. and Silver, R.B. (2007) Ratio imaging: practical considerations for measuring intracellular Ca^{2+} and pH in living cells. *Methods Cell Biol*, **81**, 415-433.

Okorokov, L.A., Lichko, L.P., Kadomtseva, V.M., Kholodenko, V.P., Titovsky, V.T. and Kulaev, I.S. (1977) Energy-dependent transport of manganese into yeast cells and distribution of accumulated ions. *Eur J Biochem*, **75**, 373-377.

Paidhungat, M. and Garrett, S. (1998) Cdcl and the vacuole coordinately regulate Mn^{2+} homeostasis in the yeast *Saccharomyces cerevisiae*. *Genetics*, **148**, 1787-1798.

Perego, P. and Howell, S.B. (1997) Molecular mechanisms controlling sensitivity to toxic metal ions in yeast. *Toxicol Appl Pharmacol*, **147**, 312-318.

Perez-Vazquez, V., Saavedra-Molina, A. and Uribe, S. (2003) In *Saccharomyces cerevisiae*, cations control the fate of the energy derived from oxidative metabolism through the opening and closing of the yeast mitochondrial unselective channel. *J. Bioenerg. Biomembr.*, **35**, 231-241.

Persson, B.L., Lagerstedt, J.O., Pratt, J.R., Pattison-Granberg, J., Lundh, K., Shokrollahzadeh, S. and Lundh, F. (2003) Regulation of phosphate acquisition in *Saccharomyces cerevisiae*. *Curr Genet*, **43**, 225-244.

Philipson, K.D. and Nicoll, D.A. (2000) Sodium-calcium exchange: a molecular perspective. *Annu Rev Physiol*, **62**, 111-133.

Philipson, K.D., Nicoll, D.A., Ottolia, M., Quednau, B.D., Reuter, H., John, S. and Qiu, Z. (2002) The Na^+/Ca^{2+} exchange molecule: an overview. *Ann N Y Acad Sci*, **976**, 1-10.

Picado, M.J., de la Sierra, A., Aguilera, M.T., Coca, A. and Urbano-Marquez, A. (1994) Increased activity of the Mg^{2+}/Na^+ exchanger in red blood cells from essential hypertensive patients. *Hypertension*, **23**, 987-991.

Pittman, J.K. and Hirschi, K.D. (2001) Regulation of CAX1, an *Arabidopsis* Ca^{2+}/H^+ antiporter. Identification of an N-terminal autoinhibitory domain. *Plant Physiol*, **127**, 1020-1029.

Pluthero, F.G. (1993) Rapid purification of high-activity Taq DNA polymerase. *Nucleic Acids Res*, **21**, 4850-4851.

Pozos, T.C., Sekler, I. and Cyert, M.S. (1996) The product of *HUM1*, a novel yeast gene, is required for vacuolar Ca^{2+}/H^+ exchange and is related to mammalian Na^+/Ca^{2+} exchangers. *Mol. Cell. Biol.*, **16**, 3730-3741.

Ram, A.F., Brekelmans, S.S., Oehlen, L.J. and Klis, F.M. (1995) Identification of two cell cycle regulated genes affecting the β 1,3-glucan content of cell walls in *Saccharomyces cerevisiae*. *FEBS Lett*, **358**, 165-170.

Riek, R.P., Handschumacher, M.D., Sung, S.S., Tan, M., Glynias, M.J., Schluchter, M.D., Novotny, J. and Graham, R.M. (1995) Evolutionary conservation of both the

hydrophilic and hydrophobic nature of transmembrane residues. *J Theor Biol*, **172**, 245-258.

Roberg, K.J., Rowley, N. and Kaiser, C.A. (1997) Physiological regulation of membrane protein sorting late in the secretory pathway of *Saccharomyces cerevisiae*. *J Cell Biol*, **137**, 1469-1482.

Rude, R.K. (2000) Minerials-magnesium. In Stipanuk, M.H. (ed.), *Biochemical and Physical Basis of Human Nutrition*. Saunders, Orlando, FL, pp. 671-685.

Rutkowski, D.T. and Kaufman, R.J. (2004) A trip to the ER: coping with stress. *Trends. Cell. Biol.*, **14**, 20-28.

Sahni, J., Nelson, B. and Scharenberg, A.M. (2007) SLC41A2 encodes a plasma-membrane Mg^{2+} transporter. *Biochem J*, **401**, 505-513.

Sambrook, J., Fritsch, E.F. and Maniatis, T. (1989) *Molecular Cloning: A Laboratory Manual*. Cold Spring Harbor Laboratory Press, Cold Spring Harbor, N.Y.

Sambrook, J.F. (1990) The involvement of calcium in transport of secretory proteins from the endoplasmic reticulum. *Cell*, **61**, 197-199.

Schiestl, R.H. and Gietz, R.D. (1989) High efficiency transformation of intact yeast cells using single stranded nucleic acids as a carrier. *Curr. Genet.*, **16**, 339-346.

Schindl, R., Weghuber, J., Romanin, C. and Schweyen, R.J. (2007) Mrs2p forms a high conductance Mg^{2+} selective channel in mitochondria. *Biophys J*.

Sheff, M.A. and Thorn, K.S. (2004) Optimized cassettes for fluorescent protein tagging in *Saccharomyces cerevisiae*. *Yeast*, **21**, 661-670.

Shigaki, T. and Hirschi, K.D. (2006) Diverse functions and molecular properties emerging for CAX cation/H^+ exchangers in plants. *Plant Biol (Stuttg)*, **8**, 419-429.

Smith, R.L. and Maguire, M.E. (1995) Distribution of the CorA Mg^{2+} transport system in gram-negative bacteria. *J. Bact.*, **177**, 1638-1640.

Snavely, M.D., Florer, J.B., Miller, C.G. and Maguire, M.E. (1989) Magnesium transport in *Salmonella typhimurium*: $^{28}Mg^{2+}$ transport by the CorA, MgtA, and MgtB systems. *J Bacteriol*, **171**, 4761-4766.

Sreedhara, A. and Cowan, J.A. (2002) Structural and catalytic roles for divalent magnesium in nucleic acid biochemistry. *Biometals*, **15**, 211-223.

Stark, M.J. (1987) Multicopy expression vectors carrying the *Lac* repressor gene for regulated high-level expression of genes in *Escherichia coli*. *Gene*, **51**, 255-267.

Stathopoulos, A.M. and Cyert, M.S. (1997) Calcineurin acts through the *CRZ1/TCN1*-encoded transcription factor to regulate gene expression in yeast. *Genes Dev*, **11**, 3432-3444.

Steinmetz, L.M., Scharfe, C., Deutschbauer, A.M., Mokranjac, D., Herman, Z.S., Jones, T., Chu, A.M., Giaever, G., Prokisch, H., Oefner, P.J. and Davis, R.W. (2002) Systematic screen for human disease genes in yeast. *Nat. Genet.*, **31**, 400-404.

Tahara, H. and Nishizawa, Y. (2007) [Hypomagnesemia and hypoparathyroidism]. *Clin Calcium*, **17**, 1200-1204.

Tang, C.Y., Bezanilla, F. and Papazian, D.M. (2000) Extracellular Mg^{2+} modulates slow gating transitions and the opening of *Drosophila* ether-a-Go-Go potassium channels. *J. Gen. Physiol.*, **115**, 319-338.

Tao, T., Grulich, P.F., Kucharski, L.M., Smith, R.L. and Maguire, M.E. (1998) Magnesium transport in Salmonella typhimurium: biphasic magnesium and time dependence of the transcription of the mgtA and mgtCB loci. *Microbiology*, **144**, 655-664.

Thompson, J.D., Gibson, T.J., Plewniak, F., Jeanmougin, F. and Higgins, D.G. (1997) The CLUSTALX windows interface: flexible strategies for multiple sequence alignment aided by quality analysis tools. *Nucleic Acids Res*, **25**, 4876-4882.

Tong, G.M. and Rude, R.K. (2005) Magnesium deficiency in critical illness. *J. Intensive Care Med.*, **20**, 3-17.

Vashist, S., Frank, C.G., Jakob, C.A. and Ng, D.T. (2002) Two distinctly localized P-type ATPases collaborate to maintain organelle homeostasis required for glycoprotein processing and quality control. *Mol. Biol. Cell*, **13**, 3955-3966.

Viladevall, L., Serrano, R., Ruiz, A., Domenech, G., Giraldo, J., Barcelo, A. and Arino, J. (2004) Characterization of the calcium-mediated response to alkaline stress in *Saccharomyces cerevisiae*. *J Biol Chem*, **279**, 43614-43624.

Wachek, M., Aichinger, M.C., Stadler, J.A., Schweyen, R.J. and Graschopf, A. (2006) Oligomerization of the Mg^{2+}-transport proteins Alr1p and Alr2p in yeast plasma membrane. *FEBS J*, **273**, 4236-4249.

Wei, S.K., Quigley, J.F., Hanlon, S.U., O'Rourke, B. and Haigney, M.C. (2002) Cytosolic free magnesium modulates Na^{+}/Ca^{2+} exchange currents in pig myocytes. *Cardiovasc. Res.*, **53**, 334-340.

Wileman, T., Kane, L.P., Carson, G.R. and Terhorst, C. (1991) Depletion of cellular calcium accelerates protein degradation in the endoplasmic reticulum. *J Biol Chem*, **266**, 4500-4507.

Winzeler, E.A., Shoemaker, D.D., Astromoff, A., Liang, H., Anderson, K., Andre, B., Bangham, R., Benito, R., Boeke, J.D., Bussey, H., Chu, A.M., Connelly, C., Davis, K., Dietrich, F., Dow, S.W., El Bakkoury, M., Foury, F., Friend, S.H., Gentalen, E., Giaever, G., Hegemann, J.H., Jones, T., Laub, M., Liao, H., Liebundguth, N., Lockhart, D.J., Lucau-Danila, A., Lussier, M., M'Rabet, N., Menard, P., Mittmann, M., Pai, C., Rebischung, C., Revuelta, J.L., Riles, L., Roberts, C.J., Ross-MacDonald, P., Scherens, B., Snyder, M., Sookhai-Mahadeo, S., Storms, R.K., Veronneau, S., Voet, M., Volckaert, G., Ward, T.R., Wysocki, R., Yen, G.S., Yu, K., Zimmermann, K., Philippsen, P., Johnston, M. and Davis, R.W. (1999) Functional characterization of the *S. cerevisiae* genome by gene deletion and parallel analysis. *Science*, **285**, 901-906.

Wisdom, D.M., Geada, M.M. and Singh, J. (1996) Characterization of a sodium-dependent magnesium efflux from magnesium-loaded rat pancreatic acinar cells. *Exp Physiol*, **81**, 367-374.

Wolf, F.I. and Cittadini, A. (2003) Chemistry and biochemistry of magnesium. *Mol. Aspects Med.*, **24**, 3-9.

Wolf, F.I., Torsello, A., Fasanella, S. and Cittadini, A. (2003) Cell physiology of magnesium. *Mol Aspects Med*, **24**, 11-26.

Yoshimoto, H., Saltsman, K., Gasch, A.P., Li, H.X., Ogawa, N., Botstein, D., Brown, P.O. and Cyert, M.S. (2002) Genome-wide analysis of gene expression regulated by the calcineurin/Crz1p signaling pathway in *Saccharomyces cerevisiae*. *J Biol Chem*, **277**, 31079-31088.

Zsurka, G., Gregan, J. and Schweyen, R.J. (2001) The human mitochondrial Mrs2 protein functionally substitutes for its yeast homologue, a candidate magnesium transporter. *Genomics*, **72**, 158-168.